

Aus dem Institut für Physiologische Chemie
Geschäftsführender Direktor: Prof. Dr. Gerhard Schratt Des
Fachbereichs Medizin der Philipps-Universität Marburg

**Regulation of microRNA function in rodent
hippocampal neurons by an alternative Ube3a
transcript**

Kumulative Dissertation

zur

Erlangung des Doktorgrades
der gesamten Naturwissenschaften

(Dr. rer. nat.)

dem

Fachbereich Medizin
der Philipps-Universität Marburg

vorgelegt von

Jeremy Matthias Valluy

aus Clamart, France

Marburg, 2015

Angenommen vom Fachbereich Medizin der Philipps-Universität Marburg am: 6. November 2015

Gedruckt mit Genehmigung des Fachbereichs.

Dekan: Prof. Dr. H. Schäfer

Referent: Prof. Dr. G. Schratt

1. Korreferent: Prof. Dr. B.Schütz

Table of Contents

<i>List of Abbreviations</i>	p.iii
<i>Summary</i>	p.vi
<i>Zusammenfassung</i>	p.viii
1- Introduction.....	p.1
1.1- Post-mitotic Neuronal development.....	p.1
1.2- Ube3a in neuronal development.....	p.2
1.3- Ube3a transcript isoform diversity.....	p.3
1.4- microRNAs (miRNAs) in neuronal development.....	p.4
1.5- Competing endogenous RNA (ceRNA).....	p.5
2- Aims of the thesis.....	p.7
3- Summary of published work.....	p.8
3.1- Expression analysis of Ube3a variants.....	p.8
3.2- Expression analysis of Ube3a protein isoforms.....	p.10
3.3- Functional analysis of Ube3a transcript variants.....	p.11
4- Discussion.....	p.16
4.1- Expression of Ube3a transcript variants during neuronal development.....	p.16
4.2- Functions of Ube3a isoforms in neuronal development.....	p.19
4.3- Mechanism of Ube3a1 function in neuronal development.....	p.21
4.4- Ube3a1 in disease.....	p.23
5- References.....	p.25
6- Reprint of Original Publication.....	p.30
7- Appendix.....	p.58

7.1- Curriculum Vitae.....	p.58
7.2- List of Academic Teachers.....	p.60
7.3- Acknowledgments.....	p.61
7.4- Eine ehrenwörtliche Erklärung.....	p.62

List of Abbreviations

AAV	adeno-associated virus
AG	Arbeitsgruppe
Arc	activity-regulated cytoskeleton-associated protein (Arg3.1)
AS	Angelman syndrome
ASD	autism-spectrum disorders
BDNF	brain-derived neurotrophic factor
CA1	cornu Ammonis 1
cDNA	complementary DNA (deoxyribonucleic acid)
cds	coding sequence
ceRNA	competing endogenous RNA (ribonucleic acid)
circRNA	circular RNA (ribonucleic acid)
CREB1	cAMP responsive element binding protein 1
Dio1	deiodinase, iodothyronine, type I
DIV	days <i>in vitro</i>
DLR	Dual-Luciferase(r) Reporter Assay system (Promega)
DNA	deoxyribonucleic acid
Dr.	Doctor
dUbe3a	drosophila Ube3a (ubiquitin protein ligase E3A)
e.g.	<i>exempli gratia</i> (lat., for the sake of example)
E2	Ubiquitin-conjugating enzymes
E3	Ubiquitin ligase
E6-AP	E6-associated protein
Fig.	figure
FISH	fluorescence in-situ hybridization
GEF	Guanine nucleotide exchange factor
GFAP	glial fibrillary acidic protein
GFP	green fluorescent protein
GFP-Ube3a-FL	GFP-Ube3a-full-length isoform
GFP-Ube3a-S	GFP-Ube3a-short isoform
Gli2	G2-like transcription factor
GW182	glycine-triptophan protein of 182 kDa
HECT	homologous to the E6-AP carboxyl terminus

HEK	Human Embryonic Kidney
iCLIP	individual-nucleotide resolution cross-linking and IP
IP	immunoprecipitation
KCl	Potassium Chloride
ko	knockout gene
Limk1	LIM domain kinase 1
lncRNA	long non-coding RNA
luc	luciferase reporter
m-/p+	maternal-/paternal+
mEPSC	miniature excitatory post-synaptic current
mer	meros (gr., part)
miRISC	microRNA-Induced Silencing Complex
miRNA	microRNA
mM	milliMolar
mRNA	messenger RNA
P	post natal day
PCR	polymerase chain-reaction
pLNA	power LNA (locked nucleic acid)
pre-miR	precursor microRNA
pri-miR	primary microRNA
PTEN	Phosphatase and tensin homolog
Pum2	Pumilio 2
qPCR	quantitative PCR
rAAV	recombinant adeno-associated virus
RACE	rapid amplification of C-terminal ends
RBP	RNA binding proteins
RISC	RNA-induced silencing complex
RNA	ribonucleic acid
RNAi	RNA interference
RNAse	ribonuclease
RNA-seq	RNA sequencing
RNP	ribonucleoproteins
RT-qPCR	reverse transcriptase PCR
shRNA	short hairpin RNA

SI	supplementary information
sup.	supplementary
Tnrc6	trinucleotide repeat containing 6a
Ube3a	Ubiquitin ligase E3A
Ube3a1-cds	Ube3a1-coding sequence only
Ube3a1-fs	Ube3a1-frameshift mutant
Ube3a1-utr	Ube3a1-3'UTR only
Ube3a-ATS	Ube3a-antisense
UCSC	university of California, Santa Cruz (genome browser)
UPS	Ubiquitin-Proteasome system
UTR	untranslated region
wt	wildtype

Summary

The activity-dependent regulation of neuronal maturation is important for the development of neural circuits and cognition. Defects in this process lead to severe neurodevelopmental disorders associated with intellectual disability and autism (Kuczewski et al., 2010).

UBE3A has been previously demonstrated to control important aspects of neuronal maturation. *UBE3A* loss-of-function mutations cause Angelman syndrome (AS) (Kishino et al., 1997), whereas increased *UBE3A* gene dosage has been associated with autism-spectrum disorders (ASD) (Glessner et al., 2009).

The *UBE3A* gene encodes an enzyme with ubiquitin ligase activity which is important for the degradation of neuronal proteins by the ubiquitin proteasome system. However, defects in *UBE3A* enzymatic activity unlikely account for the full spectrum of AS and ASD cases, since rare mutations outside the coding region have been identified (Bird, 2014).

Recently, several alternative Ube3a transcripts have been described that include variable 5' and 3' ends, suggesting complex post-transcriptional regulation of Ube3a expression. In particular, the different 3'UTRs present in Ube3a 3' variants could be used for differential regulation of mRNA localization and translation. However, little was known concerning expression, localization and regulatory functions of the alternative Ube3a transcripts.

In this work, I discovered that the rodent Ube3a1-RNA, which contains a truncated coding sequence and an alternative 3'UTR, has unique functions in neuronal maturation and a gene regulatory function that strongly differs from those of the transcripts that code for the active Ube3a enzyme.

Ube3a1-RNA is specifically increased by elevated neuronal activity and preferentially localizes to neuronal dendrites. Opposite to Ube3a enzyme-coding transcripts, Ubea1 is a negative regulator of dendrite outgrowth in rodent hippocampal neurons both in dissociated neuronal cultures and *in vivo*. In addition, Ube3a1 is necessary for dendritic spine maturation in cultured hippocampal neurons. Surprisingly, I found that the function of Ube3a1-RNA in the context of dendrite outgrowth was coding-independent and could be attributed to the presence of the alternative 3'UTR.

Considering the molecular mechanisms underlying Ube3a1-RNA function, I found that the Ube3a1-RNA 3'UTR is a target of several microRNAs encoded by the miR-379/410 cluster,

including miR-134 that was previously implicated in dendritogenesis and spine maturation. However, Ube3a1-RNA is not regulated by miRNAs in a canonical manner, but rather competes with other miR-379/410 target mRNAs for binding to common miRNAs. Therefore, Ube3a1-RNA can be considered as a competing endogenous RNA (ceRNA) following a hypothesis that was previously put forward in cancer cell lines. (Salmena et al., 2011)

In conclusion, the results from my thesis describe a new gene regulatory mechanism operating in neuronal dendrites with important implications for neuronal maturation, circuit development and neurodevelopmental disorders.

Zusammenfassung

Die aktivitätsabhängige Regulation der neuronalen Reifung ist ein wichtiger Teil der Entwicklung von neuronalen Schaltkreisen und Kognition. Defekte in diesem Prozess führen zu schweren neurologischen Entwicklungsstörungen und Autismus (Kuczewski et al., 2010).

Es wurde bereits gezeigt, dass *UBE3A* wichtige Aspekte der neuronalen Entwicklung kontrolliert. Mutationen, die zum Verlust der Funktion von *UBE3A* führen, verursachen Angelman Syndrom (AS) (Kishino et al., 1997), während erhöhte *UBE3A* Genexpression mit Autismus (ASD) assoziiert ist (Glessner et al., 2009).

Das *UBE3A* Gen kodiert ein Enzym mit Ubiquitin Ligase Aktivität, die für den Abbau neuronaler Proteine durch das Ubiquitin-Proteasome-System wichtig ist. Defekte der enzymatischen Aktivität von *UBE3A* sind jedoch mit geringer Wahrscheinlichkeit die einzige Ube3a-abhängige Ursache von AS oder ASD, da hier seltene Mutationen identifiziert wurden, die außerhalb der kodierenden Region liegen (Bird, 2014).

Mehrere alternative Ube3a Transkripte wurden beschrieben, die unterschiedliche 5' und 3' Enden enthalten, was auf eine komplexe posttranskriptionale Regulation von Ube3a Genexpression hinweist. Insbesondere könnten verschiedene 3'UTRs in Ube3a 3'-Varianten für differenzielle Regulation der Lokalisierung und Translation genutzt werden. Betreffend der Expression, Lokalisierung und regulatorischen Funktion der alternativen Ube3a Transkripte war jedoch wenig bekannt.

In dieser Arbeit, entdeckte ich dass die Ube3a1-RNA, welche eine verkürzte kodierende Sequenz und eine alternative 3'UTR enthält, einzigartige Funktionen in neuronaler Reifung und eine genregulatorische Funktion, die stark von der Funktion der Transkripte die das aktive Ube3a Enzym kodieren abweicht, hat.

Ube3a1-RNA ist spezifisch erhöht durch verstärkte neuronale Aktivität, und lokalisiert bevorzugt in neuronalen Dendriten. Im Gegensatz zu Ube3a enzymkodierenden Transkripten, ist Ube3a1 ein negativer Regulator von Dendritenwachstum in hippocampalen Neuronen des Nagetiers, sowohl in dissoziierten Kulturen als auch *in vivo*. Zusätzlich, ist Ube3a1 nötig für die Reifung von dendritischen Dornfortsätzen. Überraschenderweise habe

ich herausgefunden, dass die Funktion von Ube3a1-RNA im Zusammenhang mit dendritischem Wachstum unabhängig von der kodierenden Funktion ist, und der Gegenwart einer alternativen 3'UTR zugeschrieben werden konnte.

Bezüglich der molekularen Mechanismen die der Ube3a1-RNA Funktion zugrunde liegen, habe ich herausgefunden, dass der Ube3a1 3'UTR ein Ziel mehrerer MikroRNAs des miR379/410 Clusters, inklusive miR-134, die bereits in Dendritenwachstum und in der Reifung von Dornfortsätze impliziert wurde, ist.

Ube3a1-RNA ist jedoch nicht in kanonischer Weise von MikroRNAs reguliert, sondern konkurriert mit anderen miR-379/410 Ziel-RNAs für die Bindung gemeinsamer MikroRNAs.

Deshalb kann man Ube3a1-RNA nach einer Hypothese, die früher für Krebszellen gelegt wurde, als „competing endogenous RNA“ (ceRNA) erachten. (Salmena et al., 2011)

Letztendlich beschreiben die Ergebnisse, die ich aus meiner Doktorarbeit erhalten habe, einen neuen Mechanismus der Genregulation in neuronalen Dendriten mit wichtigen Bedeutungen für neuronale Reifung, Entwicklung von neuronalen Schaltkreisen und neurologische Entwicklungsstörungen.

1- Introduction

1.1- Post-mitotic neuronal development

The mammalian brain, arguably the most complex of all organs, consists of two main cell types, glial cells and neurons. The latter are interconnected within intricate neural networks, which enables them to participate in information processing, perception and motor control. Glial cells support and maintain neuronal circuits.

The post-mitotic development of neurons is a multistep process that takes place in a stereotypic sequential order. After differentiation and migration, neurons sprout neurites, one of which usually gives rise to the single axon, whereas the remaining neurites differentiate into dendrites. The axons are responsible for the output of neurons and project to the dendrites of a target neuron, where the majority of neuronal input takes place. Circuits are formed by the integration of specialized subtypes of neurons, such as excitatory and inhibitory neurons. Certain neurons, such as the excitatory CA1 pyramidal neurons of the hippocampus, develop specialized protrusions on dendrites called dendritic spines, where most of the excitatory synapses form (Metzger, 2010).

Dendrite development itself consists of multiple phases that are regulated by intrinsic mechanisms and environmental cues. In a first elongation phase, dendritic complexity increases due to the growth of preexisting dendrites and the formation of new branches. In a second pruning phase, excessive dendrites are removed whereas others are stabilized. Dendritic spines start to form during the dendritic growth phase, but the majority of spine maturation and pruning takes place after the dendritic tree has reached its final shape (Chen et al., 2014). The mechanisms that coordinate dendrite arborization and spine maturation in time and space are largely unknown.

All steps of dendrite development are subject to regulation by environmental cues, in particular those related to neuronal activity. For example, growth factors released upon activity (e.g. BDNF) promote dendritic arborization and spine maturation (Kuczewski et al., 2010). In the process of pruning, activity has a role in the selection of specific arbors/spines, and thereby contributes to the shaping of neural circuits (Butz et al., 2009).

Gene regulatory mechanisms, both at the transcriptional and post-transcriptional level, contribute in an important way to the control of activity-dependent dendrite development. While transcription affects gene expression on a neuron-wide level, post-transcriptional mechanisms can operate on a local scale, at the level of individual dendrites or spines, thereby allowing a rapid spatiotemporal control in response to local external cues. One such local mechanism is dendritic protein synthesis, which involves the transport of selected mRNAs into the synapto-dendritic compartment followed by their translation at distant sites. While local mRNA translation has well-documented roles in plasticity, (Schratt, 2009) its significance in dendrite development and maturation is less explored.

In vitro neuronal cultures largely recapitulate the different phases of dendrite development *in vivo*, making them a useful model to study the molecular mechanisms underlying activity-dependent growth, branching and pruning of dendrites (Molnár, 2011).

1.2- Ube3a in neuronal development

UBE3A is a gene found on chromosome 15 q11-13 in human, on chromosome 1 in rat and on the proximal region of chromosome 7 in mice. The *UBE3A* gene encodes a highly conserved protein called E6-AP (for E6-Associated Protein) or Ube3a. There is about 99% similarity between the human and mouse Ube3a proteins (Huibregtse et al., 1993).

Ube3a (E6-AP) is a member of the HECT (Homologous to the E6-AP Carboxyl Terminus) domain E3 Ubiquitin ligase family, which transfer ubiquitin from E2 to target proteins and thereby mark them for degradation as part of the ubiquitin proteasome system (UPS). The HECT domain is a 350 residue conserved C-terminal region shared by all members of the family for which Ube3a/E6-AP is the founding member (Scheffner et al., 1993).

Ube3a knockout mouse models have implicated Ube3a in activity-dependent brain development and plasticity. These animals show impaired experience-dependent cortical development (Sato and Stryker, 2010; Yashiro et al., 2009) and excitatory/inhibitory imbalance (Wallace et al., 2012). This is accompanied by abnormal dendritic spine morphology (Dindot et al., 2008) and defects in dendrite

polarization (Miao et al., 2013) in pyramidal neurons. The drosophila homolog of Ube3a, dUbe3a, has also been shown to regulate dendrite branching (Lu et al., 2009). Studies into the molecular mechanisms of Ube3a in brain development have shown that Ube3a/E6-AP regulates protein stability at the synapse, targeting the immediate early-gene Arc (Greer et al., 2010), the Parkinson's disease protein alpha-synuclein, (Mulherkar et al., 2009) and the RhoA GEF Ephexin 5 (Margolis et al., 2010) for degradation.

Ube3a dysfunction has been linked to several neurodevelopmental disorders. Loss-of-function mutations in the human *UBE3A* gene cause Angelman syndrome (AS), a severe neurodevelopmental disorder characterized by intellectual disability, a characteristic behavior profile, physiognomy, ataxia and seizures (Bird, 2014; Kishino et al., 1997; Matsuura et al., 1997; Fang et al., 1999). Ube3a knockout mice develop symptoms resembling human AS (Jana, 2012), such as motor dysfunction, inducible seizures and deficits in context-dependent learning. These mice therefore provide an animal model for the human condition.

Duplications of the *UBE3A* gene are among the most frequent copy number variations associated with autism-spectrum disorders (ASD) (Flashner et al., 2013; Glessner et al., 2009), early-onset neurodevelopmental disorders characterized by impaired social interactions and repetitive stereotypic behaviors (MIM20895; DSM5). These findings suggest that, in contrast to AS, exaggerated Ube3a production contributes to the development of ASD. Intriguingly, autism is associated with a higher risk of epilepsy, suggesting that fine-tuning Ube3a levels could play an important role in the homeostasis of neural circuits (Tuchman and Rapin, 2002). Recently, increased gene dosage of Ube3a has been shown to result in autism traits in a transgenic mouse model (Smith et al., 2011), providing experimental support for a causal link between increased Ube3a levels and the development of ASD.

1.3- Ube3a transcript isoform diversity

The mouse *UBE3A* gene consists of 13 exons (Fig. 1a). As a result of alternative splicing, two different transcript variants (Ube3a2,3) are generated that differ at their 5' terminus due to alternative inclusion of exons 2/3, but contain a common 3'UTR (untranslated region, UTR2). In addition, the alternative usage of a proximal polyadenylation site generates a truncated transcript, Ube3a1, that includes an

alternative 3'UTR (UTR1). Consequently, Ube3a1 is missing exons 12/13, which encode critical amino acid residues within the catalytic centre of Ube3a. Therefore, translation of Ube3a1 is expected to give rise to a catalytically inactive Ube3a protein isoform. The *UBE3A* gene is paternally imprinted in neurons, meaning that only the copy from the maternal allele is transcribed. Repression of paternal transcription is achieved by a long non-coding RNA (Ube3a ATS) that is transcribed from the paternal allele (Runte et al., 2001) in antisense direction. In neurons, expression of paternal Ube3a or the Ube3a ATS is mutually exclusive (Yamasaki et al., 2003; Landers et al., 2005). Interestingly, unsilencing of the paternal Ube3a allele by targeting Ube3a ATS was recently presented as a potential novel therapeutic strategy in AS (Meng et al., 2015).

In human, *UBE3A* was reported to produce three isoforms, encoded by at least five alternative transcripts (Yamamoto et al., 1997). However, in contrast to rodents, these transcript variants are exclusively generated by alternative splicing at the 5' terminus. A truncated Ube3a transcript (Ube3a-005) that terminates after the exon homologous to rodent Ube3a1 exon 11 has been reported in the ENSEMBL database, but not experimentally validated.

In summary, a variety of Ube3a transcripts containing different 3'UTRs are expressed in mammalian neurons, but their specific functions are unknown.

1.4- microRNAs (miRNAs) in neuronal development

MicroRNAs are short (around 22 nucleotides), single-stranded non-coding RNAs with gene regulatory functions that are found in most organisms, including plants, metazoa and viruses. A typical mammalian genome contains several hundred miRNAs gene families, which together account for about 1% of the genome.

The biogenesis of miRNAs is a multistep process (Krol et al., 2010): In mammals, a primary RNA polymerase II transcript (pri-miR) is cleaved by a multiprotein complex known as the microprocessor to a precursor miRNA stem-loop (pre-miRNA). The Ribonuclease (RNase) III enzyme Drosha is one of the main components of the microprocessor. The pre-miRNA is then exported into the cytosol where it undergoes a second cleavage by the highly conserved RNaseIII Dicer. The resulting miRNA duplex is then unwound into single strands which can then be incorporated into Argonaute

proteins, the core components of the miRNA effector complex miRISC (miRNA-containing RNA-induced silencing complex).

MiRISC is guided to target mRNAs via imperfect base pairing between the miRNA and a partially complementary sequence which is mostly located in the 3'UTR of the target mRNA. After target recognition, miRISC exerts its gene regulatory function, which in most cases consists of a combination of translational inhibition and mRNA degradation. In miRISC, GW182 proteins (Tnrc6a-c) are important scaffold proteins allowing for the recruitment of effector proteins (e.g. deadenylation, decapping complexes) which regulate RNA stability and translational silencing (Yao et al., 2013, Pfaff and Meister, 2013). Since each miRNA usually has hundreds of different target mRNAs, they are believed to regulate about one third of the entire transcriptome (Lewis et al., 2005).

MiRNAs play a critical role in different steps of neuronal development, including neurogenesis, neuronal maturation and plasticity (Fineberg et al., 2009; Bicker et al., 2014). In post-mitotic neurons, miRNAs are involved in axon and dendrite development (Schratt, 2009; Siegel et al., 2011). At the synapse, miRNAs play key roles in regulating the local translation of regulators of dendritic spine maturation and plasticity (Schratt, 2009). MiRNAs are necessary for higher cognitive functions and deregulation of their expression and function has been linked to several neurological disorders (Saba and Schratt, 2010; Fiore et al., 2011).

The neuron-enriched miR-134 has been extensively studied in the context of neuronal development and plasticity (Bicker et al., 2014). It was first shown to negatively regulate the maturation of dendritic spines in rat hippocampal neurons by targeting LIM-domain containing protein kinase 1 (Limk1) (Schratt et al., 2006). In addition, miR-134 is required for activity-dependent dendrite outgrowth (Fiore et al., 2009) and homeostatic synaptic scaling by inhibiting Pumilio-2 (Pum2) expression. Mir-134 also regulates cAMP response element-binding protein (CREB) signaling and thus plays a role in plasticity (Gao et al., 2010) and cell survival (Huang et al., 2015).

Mir-134 is embedded within the large, activity-regulated miR379-410 cluster which is part of the imprinted Glk2/Dio1 domain (Seitz et al., 2004). The miR379/410 cluster consists of 39 miRNAs in mice and is involved in nervous system function and liver metabolism (Labiaille et al., 2014).

1.5- Competing endogenous RNA (ceRNA)

Although transcriptional regulation is the most important means of regulating miRNA expression, (Choudhry and Catto, 2011) miRNAs are also subject to elaborate regulation both at the level of their biogenesis and their function (Krol et al., 2010). The activity of mature miRNA can be regulated in several ways, including stability and miRISC function (Krol et al., 2010). More recently, new regulatory RNA molecules called competing endogenous RNAs (ceRNA) were proposed to regulate miRNA activity *in trans*. According to this hypothesis, RNAs that share miRNA binding sites compete for common miRNAs. Thus, changes in the levels of one ceRNA affect the expression of other ceRNAs *in trans* due to alterations in miRNA occupancy.

The ceRNA hypothesis was first presented in 2011, (Salmena et al., 2011) and was subsequently experimentally supported by the finding that expression of the tumor suppressor PTEN can be regulated by the PTEN pseudogene via competition for common miRNAs (Tay et al., 2011). Since then, other cases of ceRNA regulation have been reported, reviewed by Tay, Rinn and Pandolfi in 2014 (Tay et al., 2014). CeRNA function is not limited to pseudogenes, but also applies to other classes of endogenous RNAs, both coding (mRNAs) and non-coding (e.g. long non-coding RNAs (lncRNAs), circular RNAs (circRNAs)).

Most ceRNA interactions observed so far were found in the context of cancer research (Karreth and Pandolfi, 2013), where large fluctuations in gene expression are common (Ala et al., 2013; Yuan et al., 2015). It was suggested that the drastic changes in the levels of one RNA as observed in cancer cells could affect expression of other RNAs sharing miRNA regulation through a modulation of miRNA activity.

In contrast, the physiological relevance of ceRNA crosstalk is still a matter of debate. In 2014, a quantitative study of miR-122 and its targets in hepatocytes suggested that, under physiological conditions, none of the targets of miR-122 varied in expression enough to explain changes in miRNA occupancy of the remaining target pool. Moreover, miR-122 levels were in large excess over target RNAs, with the consequence that even large increases in miRNA target sites, e.g. caused by a strong up-regulation of one of the targets, should be buffered by miRNA complexes that are not engaged with their targets (Denzler et al., 2014).

Shortly thereafter, Bosson et al. used Argonaute iCLIP to assess miRNA binding in living cells, and demonstrated that hierarchical binding of miRNA to high- and low-

affinity targets was an important feature of miRNA regulation in living cells (Bosson et al., 2014). Using single cell reporters, they further showed that the likelihood that specific miRNA targets participate in ceRNA crosstalk depends on miRNA to target RNA ratios. In this scenario, less abundant miRNAs are strongly affected by changes in target RNA levels, in particular by alterations of high-affinity targets. These findings are, further, in agreement with recent conclusions from modeling studies (Yuan et al., 2015).

Taken together, ceRNA regulation appears to be limited to cases in which the spatiotemporal concentrations of miRNAs and target RNAs, as well as the specific miRNA-target RNA affinities, are favorable. However, direct experimental support for ceRNA regulation under physiological conditions is missing in most cellular systems, including post-mitotic neurons.

2- Aims of the thesis

The ubiquitin ligase Ube3a has long been implicated in the regulation of neuronal development and synaptic plasticity, and Ube3a mutations have been associated with neurodevelopmental disorders. While most studies focused on the identification of downstream targets mediating the effects of Ube3a, little is known about how Ube3a activity is regulated. The recent discovery of several Ube3a transcript variants containing different 3'UTRs raises the possibility that post-transcriptional mechanisms, such as mRNA transport, stability or translation, could play a major role in Ube3a regulation.

Therefore, I focused on the following aims during my experimental thesis work:

- *to characterize the spatiotemporal expression of Ube3a 3'UTR transcript variants during hippocampal neuron dendrite development.*
- *to characterize the function of Ube3a 3'UTR transcript variants during dendrite development of hippocampal neurons.*
- *to identify post-transcriptional mechanisms of Ube3a regulation, with a specific focus on the involvement of neuronal miRNAs.*

By pursuing these aims, I intended to increase our knowledge about Ube3a regulation in hippocampal neurons, with implications for the understanding of the mechanisms important in synapse development and neurodevelopmental disorders.

3- Summary of published work

The results of my PhD thesis have been recently published in Valluy et al., 2015. If not otherwise stated, all experiments included in this manuscript have been performed by myself.

3.1- Expression analysis of Ube3a transcript variants

Using primers specific for the two reported rodent Ube3a 3'UTR, UTR1 and UTR2 (see Fig. 1A), we assessed the expression of the two Ube3a 3'UTR variants in primary rat hippocampal cultures by conventional reverse transcriptase polymerase chain reaction (RT-PCR). Thereby, we detected robust expression of both variants in mature, 18 day in vitro (DIV), primary hippocampal neurons. One single band at the expected size was detected, suggesting that the RT-PCR amplification was specific (Fig.1B). To validate Ube3a1 expression further, we used a forward primer located in the common coding sequence in combination with the Ube3a1 reverse primer. This PCR produced a single band at the expected size (Fig.1B; the primers used for this experiment are shown in Fig. 1A). Quantitative real-time PCR (qPCR) performed on the same RNA yielded in both cases a single product. These products were confirmed as Ube3a UTR1 and UTR2, respectively, by sequencing. qPCR further revealed that Ube3a UTR2 (Ube3a2/3) was about fourfold more abundant in hippocampal neurons (DIV18) compared to Ube3a UTR1 (Ube3a1). Whole transcriptome shotgun sequencing (RNA-seq) of RNA further confirmed expression of the Ube3a1 transcript in rat hippocampal neurons (Supplementary Figure 1a and b; UCSC genome browser), although this method, in contrast to qPCR, indicated very low expression of Ube3a UTR1. The reason for the discrepancy between the qPCR and RNA-seq results is currently unknown.

In neurons, the Ube3a gene is imprinted and expressed only from the maternal allele. Imprinting requires Ube3a-ATS, which is transcribed antisense to Ube3a and covers large parts of the Ube3a gene, including UTR1 and 2. Therefore, the observed PCR amplifications could derive, at least partially, from Ube3a-ATS. To investigate this

possibility, we performed strand-specific RT using Ube3a-specific primers, either in sense or antisense direction, to generate cDNA. Next, we evaluated the expression of either strand by qPCR. Significant amplification was only observed with cDNA transcribed with primers in sense direction, suggesting that the vast majority of Ube3a1 originates from the sense strand (supplementary Fig.1c).

To get insight into potential functions of Ube3a variants at different stages of neuronal development, we investigated the expression of the Ube3a 3'UTR variants by qPCR in a time-course experiment from 3-18 DIV in collaboration with Dr.S. Bicker (AG Schratt). We found that both Ube3a1 and Ube3a2/3 progressively increased during this period, suggesting that they could be involved in processes related to dendrite/spine pruning and maturation (supplementary Fig.2).

Neuronal activity was previously shown (Greer et al., 2010) to increase Ube3a expression. To study activity-dependent regulation of the Ube3a transcript variants, I used qPCR to assess Ube3a expression upon neuronal stimulation (RNA kindly supplied by Dr. S. Khudayberdiev, AG Schratt). RNA was obtained from neurons treated with two different stimulation protocols (Fig.1C). First, bath-application of the growth factor Brain-Derived Neurotrophic Factor (BDNF), which is synthesized and released in response to neuronal activity. Second, membrane depolarizing concentrations of KCl, which are used to mimic neuronal firing induced by action potentials.

Whereas the expression of Ube3a2/3 remained unchanged in neurons stimulated with either BDNF or KCl, Ube3a1 expression was increased about twofold above control levels by both stimuli (Fig. 1C). Therefore, Ube3a1 is selectively induced by neural-activity related stimuli, such as BDNF or depolarizing KCl concentrations.

The 3'UTR plays an important role in the localization of many neuronal mRNAs (Andreassi and Riccio, 2009). As the Ube3a protein is found at the synapse (Greer et al., 2010), we asked whether specific dendritic localization of Ube3a 3'UTR variants could be responsible for synaptic Ube3a expression (in collaboration with Dr. S. Bicker, AG Schratt). Preliminary data from quantitative PCR suggested that Ube3a1, but not Ube3a2/3 was enriched in synaptosome preparations obtained from P15 rat forebrains (sup. Fig. 3c and d). In addition, qPCR was performed with RNA obtained from compartmentalized DIV 18 hippocampal cultures. In these cultures, cell bodies are physically separated from processes (axons and dendrites) by a thin porous membrane.

Ube3a1 was enriched in the process compared to the cell body compartment, to a comparable magnitude as the known dendritically localized Arc transcript. (Lyford et al., 1995) In comparison, Ube3a2/3 was mostly found in the cell body compartments (Fig.1D). The enrichment of the Ube3a1 3'UTR in dendritic processes after overexpression in primary hippocampal neurons was confirmed by fluorescence in situ hybridization (FISH) (Fig.1e), which was performed by Dr. S. Bicker.

Taken together, we could confirm the expression of two alternative Ube3a 3'UTR variants in primary neurons. Moreover, we observed differential regulation of Ube3a 3'UTR variants at the level of activity-dependent expression and subcellular localization.

3.2- Expression analysis of Ube3a protein isoforms

To investigate expression of different Ube3a protein isoforms, we first designed plasmids that allow the expression of mouse recombinant Ube3a GFP-fusion proteins that are derived from the different Ube3a 3'UTR variants. We overexpressed these fusion proteins in HEK293 cells and found by Western blotting a robust expression of a truncated protein (GFP-Ube3a-S) encoded by the Ube3a UTR1 containing transcript as well as a full-length protein (GFP-Ube3a-FL) encoded by the Ube3a UTR2 containing transcript (supplementary Fig.4b). In addition, using a commercial antibody raised against a domain common to all Ube3a protein isoforms, we found that HEK293 cells endogenously express Ube3a-FL, but not Ube3a-S (supplementary Fig.4b). Expression of transfected GFP-Ube3a fusion proteins in neurons was confirmed by fluorescence microscopy (dsRed co-transfection was used to visualize cell morphology; supplementary Fig. 4c) and by Western blotting (data not shown). We conclude that both Ube3a 3'UTR variants have coding potential and can be efficiently translated in different cellular systems.

We went on to verify expression of the endogenous Ube3a protein isoforms in the rodent brain using Western blotting. Similar to our results from HEK293 cells, we were unable to detect expression of a truncated Ube3a-S in protein lysates generated either from young rat or mouse forebrain (not shown), P15 rat forebrain synaptosomes (supplementary Fig. 4a), or from DIV 18 cultured rat hippocampal neurons (supplementary Fig. 4c). In contrast, Ube3a-FL was abundantly present in all these lysates (e.g. supplementary figure 4a). Thus, a Ube3a-S protein corresponding to the Ube3a1 RNA is not detectably expressed in rat hippocampal neurons or rodent forebrain.

3.3- Functional analysis of Ube3a transcript variants

Despite the absence of Ube3a-S, our qPCR analysis indicated expression of at least two different Ube3a 3'UTR variants in hippocampal neurons. To investigate the function of these variants in hippocampal dendrite development, we designed shRNAs targeting conserved sequences of the specific 3'UTRs of Ube3a1 and Ube3a2/3. For control purposes, additional shRNAs targeting either a sequence common to all Ube3a transcript variants (Ube3a-cds) or a control shRNA were designed. These shRNAs were cloned in a pSuper vector for transfection and a U6/pAM-GFP-AAV vector for the production of adeno-associated viruses (AAV). To assess shRNA efficiency and specificity, HEK293 cells were co-transfected with GFP-Ube3a fusion proteins and the shRNA expression plasmids (supplemental Fig. 4d). Western blot analysis revealed that each of the shRNAs specifically reduced the expression of the respective recombinant GFP-Ube3a protein. To study the effect of Ube3a shRNAs on endogenous Ube3a-FL protein in rat hippocampal neurons, we infected neurons with rAAV expressing the different Ube3a shRNAs, which resulted in a near complete infection one week after virus application. Using Western blotting, we found that the Ube3a1 shRNA did not affect Ube3a-FL expression, whereas the latter was reduced in the presence of the Ube3a2/3 and Ube3a-cds shRNAs (supplementary fig.4e). Since Ube3a-S is not detectable by Western blotting in neurons, we validated the efficacy of the Ube3a1 shRNA at the RNA level. Therefore, we extracted total RNA of hippocampal neurons infected with the AAV-Ube3a1 or control shRNA and measured the expression of the Ube3a 3'UTR variants by qPCR. We found that infection with the Ube3a1 shRNA virus significantly reduced expression of the Ube3a1 transcript (up to 60%) compared to a control shRNA, without affecting the expression of the other Ube3a transcripts (supplementary figure 4f). Altogether, these experiments demonstrate that the chosen shRNA sequences can specifically and efficiently knockdown the respective Ube3a transcript variants.

We then used the validated shRNAs to investigate the function of individual Ube3a 3'UTR transcript variants during the development of cultured hippocampal neurons. We used co-transfection of a GFP plasmid to monitor neuronal morphology by confocal microscopy and focused on two parameters of dendrite development, dendrite complexity and dendritic spine morphogenesis. The determination of dendrite complexity by Sholl analysis revealed that Ube3a1 knockdown between DIV11-18 led

to a highly significant increase in dendrite complexity of rat hippocampal pyramidal neurons (Fig. 2a and b). Interestingly, transfection of the Ube3a2/3 shRNA had the opposite effect, leading to a significant reduction in dendrite complexity. Further, neurons transfected with the Ube3a-cds shRNA were morphologically indistinguishable from control neurons (Fig.2a and b). These results suggest that Ube3a1 and Ube3a2/3 transcripts have opposite roles in dendrite development and likely operate in independent pathways.

Our results from expression and functional analysis provided first evidence that the Ube3a1 transcript could play a unique role in activity-dependent dendrite development in hippocampal neurons. We therefore decided to study the function and regulatory mechanism of Ube3a1 in further detail. To determine a possible function of Ube3a1 in activity-dependent dendrite development, we used bath application of the activity-induced neurotrophin BDNF in DIV 4-10 hippocampal neurons (Fiore et al., 2009). We found that expression of GFP-Ube3a1 could abolish the dendrite growth-promoting effect of BDNF in these neurons (supplementary fig.5c and d). This result demonstrates that Ube3a1 is not only necessary to restrict dendrite outgrowth in developing neurons, but also sufficient to inhibit activity-induced dendrite growth.

Having found that Ube3a1 negatively regulates activity-dependent dendrite outgrowth, we decided to assess a potential role of Ube3a1 in dendritic spine maturation, which is also subject to regulation by activity (Kuczewski et al., 2010). We transfected rat hippocampal neurons with either a control shRNA or the Ube3a1 shRNA together with GFP and performed high-resolution confocal fluorescence microscopy of the dendritic branches. A quantitative assessment of hundreds of spines from multiple neurons (Fig.2c) revealed that the average spine volume in Ube3a1 knockdown neurons was significantly smaller compared to control cells (Fig.2d), whereas spine density was unchanged (Fig.2f). To investigate whether these morphological changes translated into alterations in excitatory postsynaptic function, patch-clamp electrophysiological recordings of miniature excitatory post-synaptic currents (mEPSCs) were performed on different neurons transfected in the same manner as described for confocal microscopy (in collaboration with Dr. A. Aksoy-Aksel, AG Schratt). In agreement with the morphological data, average mEPSC amplitudes, but not frequencies, were significantly reduced in Ube3a1 knockdown neurons compared to control cells (Fig.2F-

H). This indicates that excitatory postsynaptic function is compromised in the absence of Ube3a1.

In order to ensure that the knockdown of Ube3a1 was indeed responsible for the increased dendrite complexity of cells transfected with the Ube3a1 shRNA, we performed rescue experiments. Towards this end, we co-expressed the Ube3a1 shRNA and an shRNA-resistant recombinant mouse GFP-Ube3a1 (which is 97% identical to the rat homologue). We found that expressing mouse Ube3a1 normalized dendrite complexity in Ube3a1 shRNA expressing cells (Fig.3C), demonstrating that loss of Ube3a1 is indeed responsible for excessive dendrite complexity and ruling out off-target effects of the Ube3a1 shRNA.

Having shown that the Ube3a1 shRNA is specific and that no Ube3a-S protein is expressed, we hypothesized that Ube3a1 function in dendrite regulation could be coding-independent. To address this possibility, we designed several mutant Ube3a1 constructs based on the parental shRNA resistant mouse GFP-Ube3a1. By introducing a frameshift at the start of the putative Ube3a1 coding sequence, we generated a construct (GFP-Ube3a1-fs) that could not be translated into Ube3a-S and therefore allowed us to test a coding-independent function of Ube3a1 RNA (Fig.3A and B, supplemental Fig. 5a). We found that transfection of this construct could completely rescue dendrite complexity in Ube3a1 knockdown neurons (Fig. 3E and F). Thus, expression of the Ube3a1-RNA, but not Ube3a-S protein, is required for the inhibitory function of Ube3a1 in dendrite development. Results obtained with transfection of additional deletion constructs further identified the alternative Ube3a1 3'UTR as the functionally important sequence within Ube3a1-RNA (Fig.3A-F). To obtain more conclusive evidence that the Ube3a1 3'UTR, but not the Ube3a-S protein is involved in the regulation of dendritic complexity, we further used a construct containing the intact GFP-Ube3a1-cds but lacking the 3'UTR (supplementary Fig. 6). Consistent with our previous results, this construct was not able to rescue the Ube3a1 shRNA phenotype. These experiments provide multiple lines of evidence for a coding-independent function of the Ube3a1 RNA in neuronal dendrites.

We further wished to elucidate the mechanism underlying the coding-independent function of the Ube3a1-RNA in the regulation of dendrite outgrowth, focusing on the functionally important 3'UTR. 3'UTRs are preferred binding sites for miRNAs, and we

could identify 31 potential binding sites (based on seed match pairing) for several members of the miR379/410 cluster within the Ube3a1 3'UTR using bioinformatics (Fig.5A). Specifically, one strong candidate site for the one known dendritic member of the miR379/410 cluster, miR-134, could be identified. Therefore, we considered the possibility that miRNAs, especially the miR379/410 cluster, could be involved in the dendrite regulatory function of Ube3a1.

First, we determined the functionality of a selection of putative miRNA binding sites, including the miR-134 binding site, using luciferase reporter gene assays in rat neurons. Thereby, we found that overexpression of three out of four tested miR379/410 miRNAs specifically reduced expression of a Ube3a1-luc reporter (Fig.5B), suggesting that the respective sites are functional in neurons. Focusing on one of the functional miRNAs, miR-134, we found that the repressive effect was indeed mediated by the seed targeting site, since a Ube3a1-luc reporter containing a mutated miR-134 site was unaffected by miR-134 transfection (Fig.5C). Moreover, transfection of an antisense inhibitory miR-134 oligonucleotide (pLNA-134) specifically increased expression of Ube3a1-luc in a seed targeting-site dependent manner (Fig.5D), demonstrating that endogenous miR-134 does target the Ube3a1 3'UTR in neurons.

If miRNAs are responsible for Ube3a1-RNA function, interfering with miRNA production or function in a general manner should abolish the dendrite growth promoting effect of Ube3a1 knockdown. To globally reduce miRNA activity, we performed knockdown of either the microprocessor protein Drosha (Gregory et al., 2004) or the miRNA effector protein Tnrc6c (GW182) (Meister et al., 2005) (Fig.4A and D). We found that knockdown of either of these proteins prevented excessive dendrite growth in the presence of the Ube3a1 shRNA (Fig.4B-C and E-F, respectively). These two independent experiments strongly suggest that miRNAs are involved in the function of Ube3a1.

Among the 39 miRNAs within the miR379/410 cluster, miR134 represented an attractive candidate for mediating functions of Ube3a1, since it had been previously implicated in the regulation of dendritogenesis and spine morphology. However, the neuromorphological phenotypes observed upon miR134 and Ube3a1 inhibition (Schratt et al., 2006; Fig.2a) are inconsistent with repression of Ube3a1 by miR-134, as would be expected for a canonical mode of miRNA-target regulation. Instead, our observations

could be better explained by a competing endogenous RNA (ceRNA, see introduction) function of Ube3a1. According to the ceRNA model, Ube3a1-RNA knockdown (see supplementary fig.4f) would be expected to decrease expression of other miR-134 target mRNAs, since more miR-134 becomes available for their repression. To test this hypothesis we performed luciferase assays in hippocampal neurons using reporter genes that contain the 3'UTRs of three validated miR-134 targets, *Limk1*, *Pum2* and *Creb1* (supplementary fig 8a). We found that knockdown of Ube3a1 significantly reduced expression of *Limk1-luc* and *Creb1-luc* (Fig.5E, supplementary fig. 8b.), and resulted in a reproducible, but non-significant reduction in *Pum2-luc* expression. These results support the idea that Ube3a1-RNA works as a ceRNA for specific miR-134 targets.

We next used infection of rAAV-Ube3a1 shRNA to test if Ube3a1-RNA regulates the expression of miR-134 target proteins in neurons. We infected rat hippocampal neurons at DIV11 with either the rAAV-Ube3a1 shRNA or a control shRNA and prepared protein extracts for western blot analysis at DIV18. We found that, in agreement with the data from luciferase assays, Ube3a1 knockdown led to a significantly reduced expression of *Limk1* and *Pum2* protein. Expression of *Creb1* protein, on the other hand, was not affected by Ube3a1 knockdown, suggesting that regulation of the *Creb1-luc* reporter by Ube3a1-RNA does not recapitulate regulation of the endogenous *Creb1* protein.

The relative abundance of ceRNAs and natural target mRNAs is an important determinant of an effective ceRNA crosstalk (Bosson et al., 2014). We therefore decided to measure copy numbers of *Limk1*, *Pum2* and *Ube3a1* RNAs in hippocampal neurons using absolute quantification qPCR. This method uses standard curves generated with defined amounts of plasmid DNA, which in turn allows the determination of transcript copy numbers within a given amount of total RNA used for the experiment. Based on this method, *Limk1* and *Ube3a1* RNA are expressed at comparable levels in hippocampal neurons at both the whole-cell level and within neuronal processes (which mainly consist of dendrites). In contrast, *Pum2* expression was found to be about one order of magnitude higher (supplementary Fig.9).

Finally, we investigated the relevance of Ube3a1 in neuronal development in mice *in vivo* (in collaboration with M. Wöhr (AG Schwarting, Psychology, Marburg) and M. Lackinger (AG Schrott)). We found that Ube3a1-RNA and miR-134 were induced in

mice raised in social isolation (SI) compared to normal housing conditions. Since SI is a stress paradigm that among other things impairs memory performance (Fig.6A and B), this suggested an involvement of the Ube3a1-miR134 interaction in activity-dependent neural processes related to cognition.

To study the role of Ube3a1-RNA in neuromorphology in the developing mouse hippocampus in living animals, we injected rAAV expressing Ube3a1 or control shRNA into the lateral ventricles of P0 mice before preparing coronal brain slices at P21. We then assessed dendritic complexity of CA1 hippocampal neurons within these slices by confocal fluorescence microscopy. Infected neurons could be imaged due to the expression of GFP encoded by the rAAV construct. Similar to results obtained with *in vitro* cultured neurons (Fig. 2a), CA1 hippocampal neurons that had developed in the living animal displayed an increased dendritic complexity upon Ube3a1 knockdown compared to control neurons (Fig.6.C and D).

Having shown that Ube3a1 regulates dendritogenesis *in vivo*, we wanted to test whether this required the presence of miRNAs expressed from the miR379/410 cluster that contains miR-134. For these experiments, we could use a *miR379-410*^{-/-}(ko) mouse strain deficient for the entire miR379/410 microRNA cluster that was generated by Taconic Artemis and already available in the lab (Fig. 6E). Based on experiments performed in collaboration with M. Lackinger, these mice entirely lack miR-134 and other selected members of the cluster according to qPCR analysis (Fig. 6F). Furthermore, brain organization of these mice is overtly normal (sup. Fig.12). Unlike in wildtype (wt) mice, rAAV mediated knockdown of Ube3a1 had no significant effect on dendrite complexity in miR379/410 ko mice. This indicates that the function of Ube3a1-RNA in regulating dendrite complexity of mouse hippocampal neurons is dependent on the expression of the miR379/410 cluster.

4- Discussion

4.1- Expression of Ube3a transcript variants during neuronal development

Ube3a is an important element in the cellular machinery regulating post-mitotic neuronal maturation (Bird, 2014). Although the existence of several transcript variants

encoding different Ube3a protein isoforms has been known for quite some time, previous studies have almost exclusively focused on Ube3a-FL and its role as E3 ubiquitin ligase (Bird, 2014). Our interest in alternative Ube3a transcripts was driven by our observation that the Ube3a1 RNA (or its human counterpart UBE3A-005) contains a unique 3'UTR which harbors 31 potential binding sites for members of the miR379/410 cluster (Fig.5a). Since Ube3a1-RNA is lacking the two most distal exons, this further suggested that the Ube3a1 encoded truncated protein product (Ube3a-S) could have specific functions.

We obtained evidence for the presence of Ube3a1-RNA in mouse and rat brain, but were unable to detect the respective protein product, Ube3a-S, by Western blotting. To our knowledge, endogenous Ube3a-S has not been reported in the literature, and our findings from qPCR are in agreement with a recent publication wherein Ube3a1-RNA levels were reported to be low compared to Ube3a2/3 (Miao et al., 2013). Nevertheless, it is possible that Ube3a-S is translated in specific cell types or under specific environmental conditions. Since Ube3a-S is lacking catalytic activity, it could perhaps act as a dominant-negative for the catalytically active Ube3a-FL. Our results that GFP-Ube3a-S protein is expressed upon transfection of plasmids containing the intact Ube3a1 open reading frame in both neurons and non-neuronal cells demonstrate that Ube3a1 RNA has coding potential. One possibility why we do not detect an endogenous Ube3a-S is that translation of the endogenous Ube3a1 RNA is strongly inhibited by trans-acting factors, such as miRNAs and RBPs. This is supported by the presence of at least 31 (Fig.5a) miRNA seeds from the miR379/410 cluster targeting sites within the Ube3a1 3'UTR, some of which we could functionally validate (Fig. 5b). Further biochemical experiments should help to identify the full spectrum of gene regulatory factors that interact with the Ube3a1 3'UTR.

Our results concerning endogenous Ube3a1 RNA expression mostly rely on the PCR method, which has several potential pitfalls that should be considered. First, PCR primers could in principle non-specifically amplify another transcript containing similar sequence stretches. Since we used several primer pairs covering different regions of the Ube3a1 3'UTR and verified all resulting PCR amplicons by sequencing, we consider this possibility highly unlikely. In the future, rapid amplification of 5' and 3' C-terminal ends (3' and 5' RACE) could be used to obtain more detailed information about the exact start and end positions of Ube3a1-RNA. In addition, Northern blotting with

probes directed against the unique Ube3a1 3'UTR would provide information on the size and abundance of Ube3a1-related transcripts.

Second, the PCR primers used for the amplification of Ube3a1 are also complementary to the respective antisense transcript and could therefore amplify Ube3a transcripts in antisense direction, such as Ube3a-ATS. However, our results from strand-specific PCR experiments (Sup. Fig.1C) suggest that the vast majority of the transcripts detected with Ube3a1-specific primers are in sense orientation. Also, Ube3a-ATS is localized preferentially in the nucleus (Meng et al., 2013), and therefore unlikely accounts for Ube3a1 3'UTR containing transcripts detected in dendrites. Further, we believe Ube3a-ATS was not significantly affected by the Ube3a1 knockdown, as expression of Ube3a-ATS is reported to be inversely proportional to that of the canonical Ube3a from the paternal allele (Yamasaki et al., 2003). Indeed, in our Ube3a1 knockdown experiments, neither Ube3a2/3 transcript nor Ube3a-FL protein were increased.

In addition to PCR, whole genome shotgun RNA sequencing (RNA-seq) was used to validate expression of the Ube3a1 transcript in rodent brain (Sup. fig.1). This dataset further supported expression of Ube3a1 3'UTR containing transcripts in sense orientation. Interestingly, the abundance of Ube3a1 RNA was much lower based on RNA-seq compared to PCR. The reason for this difference is unclear and could be due to a low coverage of the Ube3a1 3'UTR in RNA-seq experiments because of an unfavorable local nucleotide composition (Zheng et al., 2011).

We found that Ube3a1 and Ube3a2/3 were differentially regulated by neuronal activity. While expression of Ube3a1 was increased by bath-applied BDNF or a depolarizing KCl concentration, Ube3a2/3 was unresponsive to both stimuli. Previously, in experiments that did not distinguish between the isoforms, Ube3a mRNA and protein levels were reported to increase upon KCl, but not BDNF stimulation (Greer et al., 2010). Since Ube3a2/3 is about 4-fold more abundant than Ube3a1 in neurons (Fig.1), the BDNF-dependent increase in Ube3a1 might be masked by the non-responsive Ube3a2/3 in this study which pools together all Ube3a transcripts. However, this cannot explain why we failed to observe KCl-dependent upregulation of Ube3a2/3. An alternative explanation could be the lower KCl concentration we used (16mM compared 55mM).

Furthermore, using a biochemical fractionation method, we found that Ube3a1 RNA, unlike Ube3a2/3, was enriched in dendrites, at a comparable level to known dendrite-enriched transcripts such as Arc (Lyford et al., 1995). Previously, both the Ube3a protein, associated with the 26S proteasome (Tai et al., 2010) and Ube3a RNA (Cajigas et al., 2012) were found in dendrites. It is possible that the Ube3a RNA found in dendrites contained a large proportion of Ube3a1, as the probes used for this study did not differentiate between the Ube3a 3'UTR variants. In addition, dendritic localization of the Ube3a protein could be independent of dendritic Ube3a RNA localization, for example as a cargo of the 26S proteasome. Unfortunately, we were unable to validate dendritic localization of endogenous Ube3a1-RNA by fluorescence in situ hybridization experiments. One possible explanation for this negative result could be that the Ube3a1-RNA is inaccessible for the FISH probe, e.g. due to the association with RNP complexes. In line with this, we observed increased dendritic FISH signal intensity for the transfected Ube3a1 3'UTR upon protease treatment. Further optimization of the FISH protocol will be required to obtain more conclusive evidence for dendritic localization of endogenous Ube3a1-RNA in neurons.

4.2- Functions of Ube3a isoforms in neuronal development

Using a 3'UTR-specific knockdown approach, we found that the two rodent Ube3a 3'UTR variants (Ube3a1, Ube3a2/3) have different roles in neuronal development. Whereas the canonical Ube3a2/3, which gives rise to Ube3a-FL, is necessary for dendrite growth and arborization, we found that Ube3a1 is on the contrary a negative regulator of dendrite complexity (Fig.2A,B). Interestingly, the knockdown of all Ube3a isoforms with an shRNA directed against the common coding sequence had no effect on dendritogenesis, which strongly argues that Ube3a 3'UTR variants work in independent pathways. These results are in agreement with published data. First, no effect on dendrite outgrowth was observed in UBE3A knockout mice, which lack all Ube3a transcript variants (Dindot et al., 2008). Second, Ube3a2 was shown to be necessary for the terminal dendritic arborization of hippocampal neurons in vivo (Miao et al., 2013). Finally, expression of a dominant negative dUbe3a in drosophila, which would be equivalent to a loss-of-function of the Ube3a-FL encoding transcript (Ube3a2/3), decreases dendrite outgrowth in sensory neurons (Lu et al., 2009). In conclusion, Ube3a 3'UTR variants apparently have opposing effects on dendrite growth and work in

parallel pathways, so that simultaneous loss of all transcripts has no net effect on dendrite complexity.

In addition to its role in regulating dendrite outgrowth, we found that Ube3a1 knockdown also reduced dendritic spine volume in cultured hippocampal neurons. Since neurons from Ube3a knockout mice have reduced spine size (Lu et al., 2009), this raises the possibility that Ube3a1 contributes to this phenotype. However, since this phenotype was previously attributed to the loss of the Ube3a-FL protein, the specific contribution of Ube3a2/3 to spine development will have to be determined in future experiments. Intriguingly, we found that loss of Ube3a1 affected spine size, but not density (Fig.2). In contrast, Ube3a was found to be necessary for Ephexin5 inhibition of EphrinB-dependent spine formation (Margolis et al., 2010). Since Ephexin5 degradation requires the proteasome-dependent pathway, spine formation could be specifically regulated by the Ube3a-FL encoding Ube3a2/3. Taken together, it is intriguing to speculate that the different Ube3a transcript variants have specific functions in spine formation and maturation.

Finally, overexpression of Ube3a1 had no effect on dendritic complexity of hippocampal neurons under basal growth conditions (supplementary Fig. 5d), suggesting that Ube3a1 is not sufficient to affect normal dendrite outgrowth. Our results are consistent with previous studies from our laboratory that used miR-134 inhibition in developing neurons. While necessary for activity-driven dendritogenesis and homeostatic downscaling (Fiore et al., 2009), (Fiore et al., 2014), inhibition of miR-134 activity did not affect dendrite outgrowth in cultured neurons under basal growth conditions.

Interestingly, Ube3a1 selectively blocked activity-dependent dendritogenesis in young neurons (Fig.3D) in which network activity is still low due to the low number of synapses, but was ineffective in highly interconnected neurons at later developmental stages. As such, Ube3a1 would function as an activity-sensitive rheostat preventing excessive dendrite outgrowth until a sufficient level of activity is reached. We already obtained two lines of evidence in support of the rheostat model: First, we found that expression of Ube3a1 in comparison to Ube3a2/3 during neuronal development was delayed (Sup. Fig.2). Second, we found that Ube3a1 expression was more sensitive to changes in neuronal activity compared to Ube3a2/3 (Fig.1C). Ube3a1 is a negative

regulator of dendrite growth and a positive regulator of spine maturation, while Ube3a2/3 is a positive regulator of dendrite outgrowth and of synapse formation (Margolis et al., 2010). The net effect of the Ube3a gene on dendrite outgrowth and maturation would therefore first be supportive, until activity stimulates Ube3a1 expression. Then Ube3a1 would counterbalance the Ube3a2/3 support of growth until activity levels are sufficiently high, and promote spine maturation. This model could explain how neurons switch from a dendrite growth phase to a phase of dendrite and spine maturation and provide insight into the activity-dependent coordination of post-mitotic neuronal maturation.

4.3- Mechanism of Ube3a1 function in neuronal development

Using multiple lines of experimentation, we found that the function of Ube3a1 in dendrite development required miRNAs, in particular the miR379/410 cluster, *in vitro* and *in vivo*. Consistently, analysis of the Ube3a1 3'UTR revealed a large number of binding sites for the miR379/410 cluster, including a conserved strong (8-mer) site for miR-134. In comparison, Limk1 harbors a non-canonical, presumably weak binding site for miR-134 (Schratt et al., 2006). Our results suggest that a canonical regulation of Ube3a1 expression by miR-134 is unlikely. Indeed, the phenotypes of Ube3a1 knockdown and miR-134 gain-of-function or inhibition are not consistent with such a model. Further, the lack of expression of the Ube3a-S protein in neurons in basal conditions makes it unlikely that it is responsible for the Ube3a1 knockdown phenotype. We show this explicitly in supplementary figure 6b, where a 3'UTR-lacking Ube3a1 construct failed to rescue the Ube3a1 knockdown phenotype. Therefore, we investigated the possibility that the Ube3a1-miR-134 interaction might represent a ceRNA system that regulates other known miR-134 targets such as Limk1.

Recent *in-silico* modeling approaches of microRNA-target interactions (Yuan et al., 2015), together with quantitative assessments of miRNA-target ratios (Bosson et al., 2014), favored a model whereby miRNAs that have a low miRNA/target ratio are the most likely candidates for ceRNA regulation. MiR-134, like many of the other miR379/410 miRNAs, is expressed at relatively low levels in neurons under basal conditions, making it a good candidate to participate in effective ceRNA crosstalk (S. Khudayberdiev, G. Schratt, unpublished). In addition, the model also makes predictions concerning the effect of ceRNA manipulation on targets with different miRNA affinities.

For instance, depletion of a high-affinity ceRNA would preferentially affect natural targets with low affinities, since these targets become increasingly occupied by miRNAs that are released from the ceRNA. Our data is mainly consistent with this prediction: when using both luciferase reporter assay and western blotting for the endogenous protein, the low-affinity miR-134 target *Limk1* responded very strongly to *Ube3a1* (which contains a high-affinity miR-134 site) knockdown. In contrast, the high-affinity target *Pum2*, which is also considerably more abundant than both *Limk1* and *Ube3a1*, was less affected at the protein level (Sup.fig. 9; Fig.5) and not significantly altered at the reporter gene level by *Ube3a1* knockdown. The results obtained for a third miR-134 target, *CREB1*, were more ambiguous. At the reporter gene level, a *Creb1*-3'UTR construct was strongly downregulated by *Ube3a1* knockdown, suggesting efficient ceRNA crosstalk between *CREB1* and *Ube3a1* (sup. fig. 8b). However, *CREB1* protein levels were not affected by the loss of *Ube3a1* (Fig.5G). This observations could be explained by two mechanisms, which are not mutually exclusive. First, the majority of *CREB1* protein present in neurons is translated from transcripts that contain different 3'UTRs to the one used in our study. Second, *Ube3a1* regulation is restricted to the dendritic compartment (see below) and proteins whose translation is mostly regulated in neuronal cell bodies (such as *CREB1*) are not responsive to *Ube3a1* depletion.

In this study, luciferase assays provided evidence for a regulation of the *Ube3a1* 3'UTR by different miRNAs, and for an interplay between *Ube3a1* and reporters for *Limk1* and *Creb1* (Fig.5). Yet, direct association between miRNAs and *Ube3a1*, which is necessary for ceRNA function according to the current model, was not explored. Biochemical purification techniques could be used to directly test a physical interaction between *Ube3a1* and miRNAs. For example, MiTRAP (Braun et al., 2014), a recently published method that uses bead-associated synthetic RNA to pull down RNA binding factors from protein lysates, could be used in combination with small RNA sequencing to identify miRNAs that interact with *Ube3a1* RNA in neuronal lysates.

Alternatively, the MirTrap (Clontech) method is an improvement upon traditional pull-down approaches and can be used to show a direct interaction between miRNAs and their targets. This technology uses a dominant negative RISC element called MirTrap, which traps the miRNA-associated RISC on target RNAs. An epitope-tag on MirTrap then allows stringent purification of miRNA and target RNAs and their identification by RNA sequencing. This could be especially useful for low abundance transcripts and/or

miRNAs as well as transient interactions between miRNAs and their targets. On the other hand, MirTrap requires efficient transfection of miRNA mimics and the miR-TRAP protein, which is particularly challenging in neurons.

Our observations together with published data led us to a model whereby the Ube3a1 ceRNA could participate in the control of local mRNA translation in dendrites (supplemental Fig. 13). In addition to Ube3a1 (this study), miR-134, Limk1 mRNA (Schratt et al., 2006) and Pum2 mRNA (Vessey et al., 2010) are present in dendrites and known to participate in local translational control. According to this model, dendritically localized Ube3a1 sequesters miR-134 and other miR379-410 members, thereby facilitating the translation of natural dendritic targets, such as Limk1 and Pum2. In the absence of Ube3a1, miR379-410 miRNAs become increasingly available for the repression of Limk1 and Pum2, resulting in dendrite growth and dendritic spine shrinkage.

However, the precise localization of all elements within this ceRNA crosstalk is not known. For example, high resolution FISH could provide information on a possible co-localization of miR-134, Ube3a1 and the other miR-134 targets in neuronal dendrites or within dendritic spines. To directly monitor changes in local translation of miR-134 targets, improved reporter systems which allow to distinguish between pre-existing and newly-synthesized proteins, such as myristoylated GFP (Schratt et al., 2006) or photoconvertible dendra2 reporters could be used. Modifying Ube3a1 levels in the context of these local reporter systems could provide more conclusive evidence about an involvement of Ube3a1 in local translational control in dendrites.

4.4- Ube3a1 in disease

Loss of Ube3a causes AS (Kishino et al., 1997), while excessive dosage is associated with ASD (Smith et al., 2011). While loss-of function of the Ube3a enzymatic activity is sufficient to cause full-spectrum AS, several so-called atypical mutations have also been observed (Bird, 2014). How these mutations lead to Ube3a-related disorders is largely unknown (Smith et al., 2011). Taken together with some of the data obtained in this study, this raises the possibility that Ube3a1 may play a role in AS and/or ASD.

Using AAV delivery of Ube3a1 shRNA into the intact developing mouse brain, we show that Ube3a1 function in regulating dendrite complexity is conserved *in vivo*

(Fig.6). In the future, additional parameters (spine morphology, electrophysiological properties) should be analyzed in the *in vivo* context to obtain a more comprehensive picture of the physiological significance of Ube3a1 in the rodent hippocampus. In addition, the behavioral consequences of Ube3a1 loss-of-function could be addressed with the study of a Ube3a1 knockout mouse line.

Ube3a m-/p+ knockout mice are already available (Jana, 2012). By reintroducing, either with viruses or electroporation, specific Ube3a transcripts, one could determine their function by assessing behavioral or phenotypic changes *in vivo* or in neuronal cultures.

Importantly, a human Ube3a1-like transcript (UBE3A-005) containing an alternative 3'UTR was reported in the ENSEMBL genomic database. This raises the interesting possibility that Ube3a-mediated ceRNA regulation could occur in the human brain. A more detailed characterization of this transcript will be required before more definitive conclusions about conservation can be drawn.

Many cases of Angelman Syndrome are caused by loss of a large genomic region encompassing the entire UBE3A gene (Bird, 2014). In these conditions, UBE3A-005 expression is likely affected, suggesting that deregulated Ube3a-005 expression could contribute to neurological disease. So far, the catalytic function of Ube3a-FL was shown to be mainly responsible for the involvement of UBE3A in Angelman syndrome (Jana, 2012) and it was reported that Angelman syndrome symptoms could be relieved by restoring α CamKII activity (van Woerden et al., 2007) or normal Ube3a expression in model mice (Meng et al., 2015). However, these findings do not rule out the possibility that aberrant expression of Ube3a1-like transcripts also contributes, in particular since only about 11% of AS patients carry UBE3A mutations (Bird, 2014). Further, about 14 % of AS patients carry mutations outside the Ube3a coding region which do not necessarily result in impaired Ube3a-FL expression (Bird, 2014).

Similarly, Ube3a1-like human transcripts could also be involved in cases of autism-spectrum disorders that are characterized by duplications of the UBE3A locus. For example, dendrite complexity is reported to be decreased in some ASD patients (Raymond et al., 1996) or animal models (Penzes et al., 2011), consistent with the dendrite inhibitory activity we observed for Ube3a1 in cultured hippocampal neurons. We therefore believe that our study provides a starting point for the further characterization of the different human Ube3a transcripts, starting with the putative

Ube3a-005, and their potential involvement in neuronal function and disease. In this regard, further screens for mutations in chromosomal regions encompassing Ube3a-005 in AS or ASD patients could provide valuable insights.

5- References

Ala, U., Karreth, F.A., Bosia, C., Pagnani, A., Taulli, R., Léopold, V., Tay, Y., Provero, P., Zecchina, R., and Pandolfi, P.P. (2013). Integrated transcriptional and competitive endogenous RNA networks are cross-regulated in permissive molecular environments. *Proc. Natl. Acad. Sci. U. S. A.* *110*, 7154–7159.

Andreassi, C., and Riccio, A. (2009). To localize or not to localize: mRNA fate is in 3'UTR ends. *Trends Cell Biol.* *19*, 465–474.

Bicker, S., Lackinger, M., Weiß, K., and Schratt, G. (2014). MicroRNA-132, -134, and -138: a microRNA troika rules in neuronal dendrites. *Cell. Mol. Life Sci. CMLS* *71*, 3987–4005.

Bird, L.M. (2014). Angelman syndrome: review of clinical and molecular aspects. *Appl. Clin. Genet.* *7*, 93–104.

Bosson, A.D., Zamudio, J.R., and Sharp, P.A. (2014). Endogenous miRNA and target concentrations determine susceptibility to potential ceRNA competition. *Mol. Cell* *56*, 347–359.

Braun, J., Misiak, D., Busch, B., Krohn, K., and Hüttelmaier, S. (2014). Rapid identification of regulatory microRNAs by miTRAP (miRNA trapping by RNA in vitro affinity purification). *Nucleic Acids Res.* *42*, e66.

Butz, M., Wörgötter, F., and van Ooyen, A. (2009). Activity-dependent structural plasticity. *Brain Res. Rev.* *60*, 287–305.

Cajigas, I.J., Tushev, G., Will, T.J., tom Dieck, S., Fuerst, N., and Schuman, E.M. (2012). The local transcriptome in the synaptic neuropil revealed by deep sequencing and high-resolution imaging. *Neuron* *74*, 453–466.

Chen, C.-C., Lu, J., and Zuo, Y. (2014). Spatiotemporal dynamics of dendritic spines in the living brain. *Front. Neuroanat.* *8*, 28.

Choudhry, H., and Catto, J.W.F. (2011). Epigenetic regulation of microRNA expression in cancer. *Methods Mol. Biol. Clifton NJ* *676*, 165–184.

Denzler, R., Agarwal, V., Stefano, J., Bartel, D.P., and Stoffel, M. (2014). Assessing the ceRNA hypothesis with quantitative measurements of miRNA and target abundance. *Mol. Cell* *54*, 766–776.

Dindot, S.V., Antalffy, B.A., Bhattacharjee, M.B., and Beaudet, A.L. (2008). The Angelman syndrome ubiquitin ligase localizes to the synapse and nucleus, and maternal deficiency results in abnormal dendritic spine morphology. *Hum. Mol. Genet.* *17*, 111–118.

Fang, P., Lev-Lehman, E., Tsai, T.F., Matsuura, T., Benton, C.S., Sutcliffe, J.S., Christian, S.L., Kubota, T., Halley, D.J., Meijers-Heijboer, H., et al. (1999). The spectrum of mutations in UBE3A causing Angelman syndrome. *Hum. Mol. Genet.* *8*, 129–135.

Fineberg, S.K., Kosik, K.S., and Davidson, B.L. (2009). MicroRNAs potentiate neural development. *Neuron* *64*, 303–309.

Fiore, R., Khudayberdiev, S., Christensen, M., Siegel, G., Flavell, S.W., Kim, T.-K., Greenberg, M.E., and Schratt, G. (2009). Mef2-mediated transcription of the miR379-410 cluster regulates activity-dependent dendritogenesis by fine-tuning Pumilio2 protein levels. *EMBO J.* *28*, 697–710.

Fiore, R., Khudayberdiev, S., Saba, R., and Schratt, G. (2011). MicroRNA function in the nervous system. *Prog. Mol. Biol. Transl. Sci.* *102*, 47–100.

Fiore, R., Rajman, M., Schwale, C., Bicker, S., Antoniou, A., Bruehl, C., Draguhn, A., and Schratt, G. (2014). MiR-134-dependent regulation of Pumilio-2 is necessary for homeostatic synaptic depression. *EMBO J.* *33*, 2231–2246.

Flashner, B.M., Russo, M.E., Boileau, J.E., Leong, D.W., and Gallicano, G.I. (2013). Epigenetic factors and autism spectrum disorders. *Neuromolecular Med.* *15*, 339–350.

Gao, J., Wang, W.-Y., Mao, Y.-W., Gräff, J., Guan, J.-S., Pan, L., Mak, G., Kim, D., Su, S.C., and Tsai, L.-H. (2010). A novel pathway regulates memory and plasticity via SIRT1 and miR-134. *Nature* *466*, 1105–1109.

Glessner, J.T., Wang, K., Cai, G., Korvatska, O., Kim, C.E., Wood, S., Zhang, H., Estes, A., Brune, C.W., Bradfield, J.P., et al. (2009). Autism genome-wide copy number variation reveals ubiquitin and neuronal genes. *Nature* *459*, 569–573.

Greer, P.L., Hanayama, R., Bloodgood, B.L., Mardinly, A.R., Lipton, D.M., Flavell, S.W., Kim, T.-K., Griffith, E.C., Waldon, Z., Maehr, R., et al. (2010). The Angelman Syndrome protein Ube3A regulates synapse development by ubiquitinating arc. *Cell* *140*, 704–716.

Gregory, R.I., Yan, K.-P., Amuthan, G., Chendrimada, T., Doratotaj, B., Cooch, N., and Shiekhattar, R. (2004). The Microprocessor complex mediates the genesis of microRNAs. *Nature* *432*, 235–240.

Huang, W., Liu, X., Cao, J., Meng, F., Li, M., Chen, B., and Zhang, J. (2015). miR-134 Regulates Ischemia/Reperfusion Injury-Induced Neuronal Cell Death by Regulating CREB Signaling. *J. Mol. Neurosci.* *MN 55*, 821–829.

Huibregtse, J.M., Scheffner, M., and Howley, P.M. (1993). Cloning and expression of the cDNA for E6-AP, a protein that mediates the interaction of the human papillomavirus E6 oncoprotein with p53. *Mol. Cell. Biol.* *13*, 775–784.

Jana, N.R. (2012). Understanding the pathogenesis of Angelman syndrome through animal models. *Neural Plast.* *2012*, 710943.

Karreth, F.A., and Pandolfi, P.P. (2013). ceRNA cross-talk in cancer: when ce-bling rivalries go awry. *Cancer Discov.* *3*, 1113–1121.

- Kishino, T., Lalonde, M., and Wagstaff, J. (1997). UBE3A/E6-AP mutations cause Angelman syndrome. *Nat. Genet.* *15*, 70–73.
- Krol, J., Loedige, I., and Filipowicz, W. (2010). The widespread regulation of microRNA biogenesis, function and decay. *Nat. Rev. Genet.* *11*, 597–610.
- Kuczewski, N., Porcher, C., and Gaiarsa, J.-L. (2010). Activity-dependent dendritic secretion of brain-derived neurotrophic factor modulates synaptic plasticity. *Eur. J. Neurosci.* *32*, 1239–1244.
- Labialle, S., Marty, V., Bortolin-Cavaillé, M.-L., Hoareau-Osman, M., Pradère, J.-P., Valet, P., Martin, P.G.P., and Cavaillé, J. (2014). The miR-379/miR-410 cluster at the imprinted *Di1-1-Dio3* domain controls neonatal metabolic adaptation. *EMBO J.* *33*, 2216–2230.
- Landers, M., Calciano, M.A., Colosi, D., Glatt-Deeley, H., Wagstaff, J., and Lalonde, M. (2005). Maternal disruption of *Ube3a* leads to increased expression of *Ube3a-ATS* in trans. *Nucleic Acids Res.* *33*, 3976–3984.
- Lewis, B.P., Burge, C.B., and Bartel, D.P. (2005). Conserved seed pairing, often flanked by adenosines, indicates that thousands of human genes are microRNA targets. *Cell* *120*, 15–20.
- Lu, Y., Wang, F., Li, Y., Ferris, J., Lee, J.-A., and Gao, F.-B. (2009). The *Drosophila* homologue of the Angelman syndrome ubiquitin ligase regulates the formation of terminal dendritic branches. *Hum. Mol. Genet.* *18*, 454–462.
- Lyford, G.L., Yamagata, K., Kaufmann, W.E., Barnes, C.A., Sanders, L.K., Copeland, N.G., Gilbert, D.J., Jenkins, N.A., Lanahan, A.A., and Worley, P.F. (1995). *Arc*, a growth factor and activity-regulated gene, encodes a novel cytoskeleton-associated protein that is enriched in neuronal dendrites. *Neuron* *14*, 433–445.
- Margolis, S.S., Salogiannis, J., Lipton, D.M., Mandel-Brehm, C., Wills, Z.P., Mardinly, A.R., Hu, L., Greer, P.L., Bikoff, J.B., Ho, H.-Y.H., et al. (2010). EphB-mediated degradation of the RhoA GEF Ephexin5 relieves a developmental brake on excitatory synapse formation. *Cell* *143*, 442–455.
- Matsuura, T., Sutcliffe, J.S., Fang, P., Galjaard, R.J., Jiang, Y.H., Benton, C.S., Rommens, J.M., and Beaudet, A.L. (1997). De novo truncating mutations in E6-AP ubiquitin-protein ligase gene (*UBE3A*) in Angelman syndrome. *Nat. Genet.* *15*, 74–77.
- Meister, G., Landthaler, M., Peters, L., Chen, P.Y., Urlaub, H., Lührmann, R., and Tuschl, T. (2005). Identification of novel argonaute-associated proteins. *Curr. Biol.* *15*, 2149–2155.
- Meng, L., Person, R.E., Huang, W., Zhu, P.J., Costa-Mattioli, M., and Beaudet, A.L. (2013). Truncation of *Ube3a-ATS* unsilences paternal *Ube3a* and ameliorates behavioral defects in the Angelman syndrome mouse model. *PLoS Genet.* *9*, e1004039.
- Meng, L., Ward, A.J., Chun, S., Bennett, C.F., Beaudet, A.L., and Rigo, F. (2015). Towards a therapy for Angelman syndrome by targeting a long non-coding RNA. *Nature* *518*, 409–412.
- Metzger, F. (2010). Molecular and cellular control of dendrite maturation during brain development. *Curr. Mol. Pharmacol.* *3*, 1–11.

- Miao, S., Chen, R., Ye, J., Tan, G.-H., Li, S., Zhang, J., Jiang, Y., and Xiong, Z.-Q. (2013). The Angelman syndrome protein Ube3a is required for polarized dendrite morphogenesis in pyramidal neurons. *J. Neurosci. Off. J. Soc. Neurosci.* *33*, 327–333.
- Molnár, E. (2011). Long-term potentiation in cultured hippocampal neurons. *Semin. Cell Dev. Biol.* *22*, 506–513.
- Mulherkar, S.A., Sharma, J., and Jana, N.R. (2009). The ubiquitin ligase E6-AP promotes degradation of alpha-synuclein. *J. Neurochem.* *110*, 1955–1964.
- Penzes, P., Cahill, M.E., Jones, K.A., VanLeeuwen, J.-E., and Woolfrey, K.M. (2011). Dendritic spine pathology in neuropsychiatric disorders. *Nat. Neurosci.* *14*, 285–293.
- Pfaff, J., and Meister, G. (2013). Argonaute and GW182 proteins: an effective alliance in gene silencing. *Biochem. Soc. Trans.* *41*, 855–860.
- Raymond, G.V., Bauman, M.L., and Kemper, T.L. (1996). Hippocampus in autism: a Golgi analysis. *Acta Neuropathol. (Berl.)* *91*, 117–119.
- Runte, M., Hüttenhofer, A., Gross, S., Kiefmann, M., Horsthemke, B., and Buiting, K. (2001). The IC-SNURF-SNRPN transcript serves as a host for multiple small nucleolar RNA species and as an antisense RNA for UBE3A. *Hum. Mol. Genet.* *10*, 2687–2700.
- Saba, R., and Schratt, G.M. (2010). MicroRNAs in neuronal development, function and dysfunction. *Brain Res.* *1338*, 3–13.
- Salmena, L., Poliseno, L., Tay, Y., Kats, L., and Pandolfi, P.P. (2011). A ceRNA hypothesis: the Rosetta Stone of a hidden RNA language? *Cell* *146*, 353–358.
- Sato, M., and Stryker, M.P. (2010). Genomic imprinting of experience-dependent cortical plasticity by the ubiquitin ligase gene Ube3a. *Proc. Natl. Acad. Sci. U. S. A.* *107*, 5611–5616.
- Scheffner, M., Huibregtse, J.M., Vierstra, R.D., and Howley, P.M. (1993). The HPV-16 E6 and E6-AP complex functions as a ubiquitin-protein ligase in the ubiquitination of p53. *Cell* *75*, 495–505.
- Schratt, G. (2009). microRNAs at the synapse. *Nat. Rev. Neurosci.* *10*, 842–849.
- Schratt, G.M., Tuebing, F., Nigh, E.A., Kane, C.G., Sabatini, M.E., Kiebler, M., and Greenberg, M.E. (2006). A brain-specific microRNA regulates dendritic spine development. *Nature* *439*, 283–289.
- Seitz, H., Royo, H., Bortolin, M.-L., Lin, S.-P., Ferguson-Smith, A.C., and Cavallé, J. (2004). A large imprinted microRNA gene cluster at the mouse Dlk1-Gtl2 domain. *Genome Res.* *14*, 1741–1748.
- Siegel, G., Saba, R., and Schratt, G. (2011). microRNAs in neurons: manifold regulatory roles at the synapse. *Curr. Opin. Genet. Dev.* *21*, 491–497.
- Smith, S.E.P., Zhou, Y.-D., Zhang, G., Jin, Z., Stoppel, D.C., and Anderson, M.P. (2011). Increased gene dosage of Ube3a results in autism traits and decreased glutamate synaptic transmission in mice. *Sci. Transl. Med.* *3*, 103ra97.

- Tai, H.-C., Besche, H., Goldberg, A.L., and Schuman, E.M. (2010). Characterization of the Brain 26S Proteasome and its Interacting Proteins. *Front. Mol. Neurosci.* 3.
- Tay, Y., Kats, L., Salmena, L., Weiss, D., Tan, S.M., Ala, U., Karreth, F., Poliseno, L., Provero, P., Di Cunto, F., et al. (2011). Coding-independent regulation of the tumor suppressor PTEN by competing endogenous mRNAs. *Cell* 147, 344–357.
- Tay, Y., Rinn, J., and Pandolfi, P.P. (2014). The multilayered complexity of ceRNA crosstalk and competition. *Nature* 505, 344–352.
- Tuchman, R., and Rapin, I. (2002). Epilepsy in autism. *Lancet Neurol.* 1, 352–358.
- Vessey, J.P., Schoderboeck, L., Gingl, E., Luzi, E., Riefler, J., Di Leva, F., Karra, D., Thomas, S., Kiebler, M.A., and Macchi, P. (2010). Mammalian Pumilio 2 regulates dendrite morphogenesis and synaptic function. *Proc. Natl. Acad. Sci. U. S. A.* 107, 3222–3227.
- Wallace, M.L., Burette, A.C., Weinberg, R.J., and Philpot, B.D. (2012). Maternal loss of Ube3a produces an excitatory/inhibitory imbalance through neuron type-specific synaptic defects. *Neuron* 74, 793–800.
- Van Woerden, G.M., Harris, K.D., Hojjati, M.R., Gustin, R.M., Qiu, S., de Avila Freire, R., Jiang, Y., Elgersma, Y., and Weeber, E.J. (2007). Rescue of neurological deficits in a mouse model for Angelman syndrome by reduction of alphaCaMKII inhibitory phosphorylation. *Nat. Neurosci.* 10, 280–282.
- Yamamoto, Y., Huibregtse, J.M., and Howley, P.M. (1997). The human E6-AP gene (UBE3A) encodes three potential protein isoforms generated by differential splicing. *Genomics* 41, 263–266.
- Yamasaki, K., Joh, K., Ohta, T., Masuzaki, H., Ishimaru, T., Mukai, T., Niikawa, N., Ogawa, M., Wagstaff, J., and Kishino, T. (2003). Neurons but not glial cells show reciprocal imprinting of sense and antisense transcripts of Ube3a. *Hum. Mol. Genet.* 12, 837–847.
- Yao, B., Li, S., and Chan, E.K.L. (2013). Function of GW182 and GW bodies in siRNA and miRNA pathways. *Adv. Exp. Med. Biol.* 768, 71–96.
- Yashiro, K., Riday, T.T., Condon, K.H., Roberts, A.C., Bernardo, D.R., Prakash, R., Weinberg, R.J., Ehlers, M.D., and Philpot, B.D. (2009). Ube3a is required for experience-dependent maturation of the neocortex. *Nat. Neurosci.* 12, 777–783.
- Yuan, Y., Liu, B., Xie, P., Zhang, M.Q., Li, Y., Xie, Z., and Wang, X. (2015). Model-guided quantitative analysis of microRNA-mediated regulation on competing endogenous RNAs using a synthetic gene circuit. *Proc. Natl. Acad. Sci. U. S. A.*
- Zheng, W., Chung, L.M., and Zhao, H. (2011). Bias detection and correction in RNA-Sequencing data. *BMC Bioinformatics* 12, 290.

6- Reprint of Original publication

"A coding-independent function of an alternative Ube3a transcript during neuronal development. "

Nature Neuroscience, 2015, ISSN: 1097-6256

Valluy J, Bicker S, Aksoy-Aksel A, Lackinger M, Sumer S, Fiore R, Wüst T, Seffer D, Metge F, Dieterich C, Wöhr M, Schwarting R, Schratt G.

Including Supplementary information and tables.

A coding-independent function of an alternative Ube3a transcript during neuronal development

Jeremy Valluy¹, Silvia Bicker¹, Ayla Aksoy-Aksel¹, Martin Lackinger¹, Simon Sumer¹, Roberto Fiore¹, Tatjana Wüst^{2,5}, Dominik Seffer³, Franziska Metge⁴, Christoph Dieterich⁴, Markus Wöhr³, Rainer Schwarting³ & Gerhard Schratt¹

The E3 ubiquitin ligase Ube3a is an important regulator of activity-dependent synapse development and plasticity. *Ube3a* mutations cause Angelman syndrome and have been associated with autism spectrum disorders (ASD). However, the biological significance of alternative Ube3a transcripts generated in mammalian neurons remains unknown. We report here that Ube3a1 RNA, a transcript that encodes a truncated Ube3a protein lacking catalytic activity, prevents exuberant dendrite growth and promotes spine maturation in rat hippocampal neurons. Surprisingly, Ube3a1 RNA function was independent of its coding sequence but instead required a unique 3' untranslated region and an intact microRNA pathway. Ube3a1 RNA knockdown increased activity of the plasticity-regulating miR-134, suggesting that Ube3a1 RNA acts as a dendritic competing endogenous RNA. Accordingly, the dendrite-growth-promoting effect of Ube3a1 RNA knockdown *in vivo* is abolished in mice lacking miR-134. Taken together, our results define a noncoding function of an alternative Ube3a transcript in dendritic protein synthesis, with potential implications for Angelman syndrome and ASD.

The experience-dependent development of neural circuits is essential for higher cognitive functions, and defects lead to severe neurodevelopmental disorders, including ASD¹. The ubiquitin E3 ligase Ube3a is crucial to mammalian neural circuit development. Whereas loss of *UBE3A* is the leading cause for the neurodevelopmental disorder Angelman syndrome, *UBE3A* duplications are among the most frequent copy number variations associated with ASD^{2–4}. *Ube3a* knockout mice, an animal model of Angelman syndrome, display cognitive impairments and defects in hippocampal long-term potentiation², impaired experience-dependent cortical development^{5,6} and excitatory/inhibitory imbalance⁷. This is accompanied by abnormal dendritic spine morphology⁸ and defects in dendrite polarization⁹ in pyramidal neurons.

Ube3a promotes the degradation of synaptic proteins, including Arc and ephexin 5 (refs. 10,11), thereby reducing AMPA receptor internalization and stabilizing excitatory synaptic contacts. Alternative Ube3a transcripts containing different 5' leader exons and 3' UTRs are generated by alternative splicing and/or polyadenylation in rodents and human. However, little is known regarding the function and regulation of these transcripts.

microRNAs are an extensive class of small noncoding RNAs that act as important post-transcriptional regulators of gene expression in neurons¹². miRNAs primarily bind to the 3' UTR of target mRNAs by imperfect complementary base pairing, thereby inducing translational silencing. Specific miRNAs that regulate several aspects of activity-dependent neuronal development have been identified^{13,14}. Among

the best studied examples is miR-134, which is embedded in a large mammalian-specific miRNA cluster (miR379–410) encoded by the imprinted *Meg3–Dio1* domain¹⁵. miR-134 is a negative regulator of dendritic spine size and is required, together with other miR379–410 members, for activity-dependent dendritogenesis in rat hippocampal neurons^{16,17}. In mice, silencing miR-134 rescues LTP and memory impairments caused by *Sirt1* deficiency and suppresses kainate-induced epileptic seizures^{18,19}. miR-134 exerts its function by locally regulating the translation of dendritic target mRNAs, including *Limk1* and *Pum2* (refs. 16,17). miR-134 itself is subject to activity-dependent regulation at the level of transcription and dendritic localization^{16,20}. Whether miRNAs are involved in the regulation of alternative Ube3a transcripts is unknown.

RESULTS

Expression of alternative Ube3a transcripts in hippocampal neurons

In mouse, three alternative Ube3a transcripts are known (Ube3a1 (NM_173010), Ube3a2 (NM_011668) and Ube3a3 (NM_001033962), generated by alternative splicing and/or polyadenylation (Fig. 1a and Supplementary Fig. 1a)^{9,21,22}. Ube3a2/3 transcripts, which encode full-length, catalytically active Ube3a proteins (Ube3a-FL; NP_035798 and NP_001029134), contain a common 3' UTR but different 5' leader exons as a result of alternative promoter usage and splicing. In contrast, in Ube3a1 an alternative polyadenylation signal is used (Fig. 1a and Supplementary Table 1). The resulting transcript therefore contains

¹Institute of Physiological Chemistry, Biochemical-Pharmacological Center Marburg, Philipps University Marburg, Marburg, Germany. ²Interdisciplinary Center for Neurosciences, SFB488 Junior Group, University Heidelberg, Heidelberg, Germany. ³Behavioral Neuroscience, Experimental and Biological Psychology, Philipps-University Marburg, Marburg, Germany. ⁴Max Planck Institute for Biology of Ageing, Computational RNA Biology Lab, Cologne, Germany. ⁵Present address: Sanquin Blood Supply, Amsterdam, the Netherlands. Correspondence should be addressed to G.S. (schratt@staff.uni-marburg.de).

Received 23 January; accepted 12 March; published online 13 April 2015; doi:10.1038/nn.3996

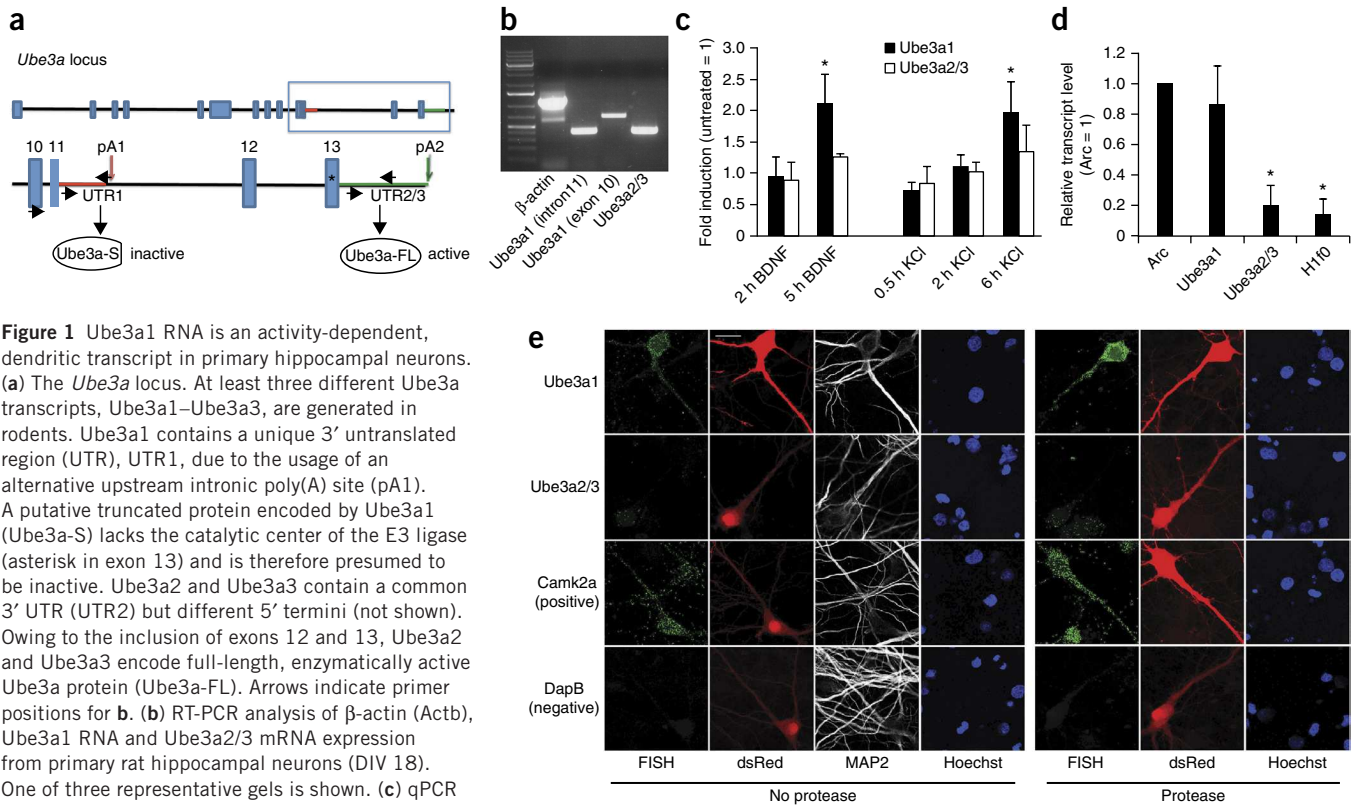


Figure 1 Ube3a1 RNA is an activity-dependent, dendritic transcript in primary hippocampal neurons. (a) The *Ube3a* locus. At least three different Ube3a transcripts, Ube3a1–Ube3a3, are generated in rodents. Ube3a1 contains a unique 3′ untranslated region (UTR), UTR1, due to the usage of an alternative upstream intronic poly(A) site (pA1). A putative truncated protein encoded by Ube3a1 (Ube3a-S) lacks the catalytic center of the E3 ligase (asterisk in exon 13) and is therefore presumed to be inactive. Ube3a2 and Ube3a3 contain a common 3′ UTR (UTR2) but different 5′ termini (not shown). Owing to the inclusion of exons 12 and 13, Ube3a2 and Ube3a3 encode full-length, enzymatically active Ube3a protein (Ube3a-FL). Arrows indicate primer positions for **b**. (b) RT-PCR analysis of β-actin (Actb), Ube3a1 RNA and Ube3a2/3 mRNA expression from primary rat hippocampal neurons (DIV 18). One of three representative gels is shown. (c) qPCR analysis of Ube3a1 RNA and Ube3a2/3 mRNA expression from rat cortical neurons (DIV 4) treated for the indicated time with BDNF (50 ng/ml) or KCl (55 mM). Values are presented as fold induction ± s.d. compared to that in unstimulated cells. *N* = 3 independent experiments. **P* = 0.047 (BDNF); **P* = 0.031 (KCl) (*t*-test, compared to unstimulated cells). (d) qPCR analysis of indicated transcripts from compartmentalized hippocampal neuron cultures (DIV 19). Values are presented as fold enrichment ± s.d. of RNA in processes compared to RNA in cell body compartment. Expression of the dendritic Arc mRNA was set to 1. Histone H1 (H1f0) is a non-dendritic control RNA. *N* = 3 independent experiments. **P* = 0.016 (Ube3a2/3); **P* = 0.010 (H1f0) (*t*-test, compared to Ube3a1). (e) FISH analysis of Ube3a1 RNA–overexpressing hippocampal neuron cultures (DIV 19) using probe sets against the indicated RNAs. Neurons were co-transfected with dsRed to identify transfected cells. MAP2 counterstain was used to visualize neuronal dendrites. Hoechst staining was used to assess nuclear integrity. In the right panels, neurons were treated with protease before proceeding to FISH. MAP2 was not preserved in protease-treated neurons. Representative images from a total of three independent hybridizations. Scale bar, 20 μm.

a unique 3′ UTR and encodes a truncated Ube3a protein lacking catalytic activity (Ube3a-S; NP_766598)²³. Furthermore, a human UBE3A transcript (UBE3A-005; ENST00000604860) was reported in which, as in Ube3a1 of rodents, a unique 3′ UTR is included as a result of the usage of an alternative polyadenylation signal in intron 11. Little is known regarding the function of Ube3a1 RNA in neurons.

We were able to detect robust expression of both Ube3a1 and Ube3a2/3 transcripts in rat hippocampal neurons by conventional reverse transcriptase (RT)-PCR (Fig. 1b). Analysis of RNA sequencing data further confirmed expression of the rat Ube3a1 3′ UTR in neurons (Supplementary Fig. 1b). An antisense transcript (Ube3a-ATS) overlaps the Ube3a1 3′ UTR²⁴. However, results from strand-specific quantitative PCR (qPCR) demonstrated that most Ube3a1 3′ UTR-containing transcripts were in the sense orientation (Supplementary Fig. 1c). qPCR further showed developmentally regulated expression of both Ube3a 3′ UTR variants and the dendritic *Limk1* mRNA (Supplementary Fig. 2).

Neuronal activity was previously shown to induce transcription from the *Ube3a* locus^{10,25}. We therefore measured expression of the Ube3a 3′ UTR variants after bath application to neurons of BDNF, a neurotrophin that is released upon elevated neuronal activity, or membrane-depolarizing KCl concentrations. We found that both BDNF and KCl significantly induced Ube3a1 RNA expression at 5–6 h after stimulation (Fig. 1c). In contrast, the Ube3a2/3 mRNA was

not significantly altered by either treatment. Our results suggest that Ube3a1 RNA is specifically regulated by neuronal activity, suggesting a function in activity-dependent neuronal development.

The 3′ UTR often harbors sequence elements necessary for mRNA localization²⁶. We therefore interrogated subcellular localization of the different Ube3a 3′ UTR variants in neurons, using a compartmentalized culture system²⁰. To rule out any contribution of glial processes, we blocked glial cell proliferation with 5-fluoro-2′-deoxyuridine (Supplementary Fig. 3a). We found that Ube3a1 RNA, but not Ube3a2/3 mRNA, was enriched in the dendritic compartment of glia-depleted neuronal cultures to a similar degree as the dendritic Arc mRNA (Fig. 1d)^{17,27}. Whereas the amount of Ube3a1 RNA was about 40% that of Ube3a2/3 mRNA in cell bodies, it was almost three times more abundant in neuronal processes (Supplementary Fig. 3b). Ube3a1 RNA was also enriched in postnatal day (P) 15 synaptosomes as compared to whole forebrain as assessed by RT-PCR (Supplementary Fig. 3c,d). Moreover, using high-resolution fluorescence *in situ* hybridization (FISH), we observed that a Ube3a1 3′ UTR-containing transcript localized to dendrites when transfected into hippocampal neurons (Fig. 1e). The signal was specific, as no dendritic signal was observed when probe sets directed against the Ube3a2/3 3′ UTR were used. The dendritic Camk2a and the bacterial DapB RNA served as positive and negative control, respectively. The dendritic signal of Ube3a1 was enhanced when neurons were treated

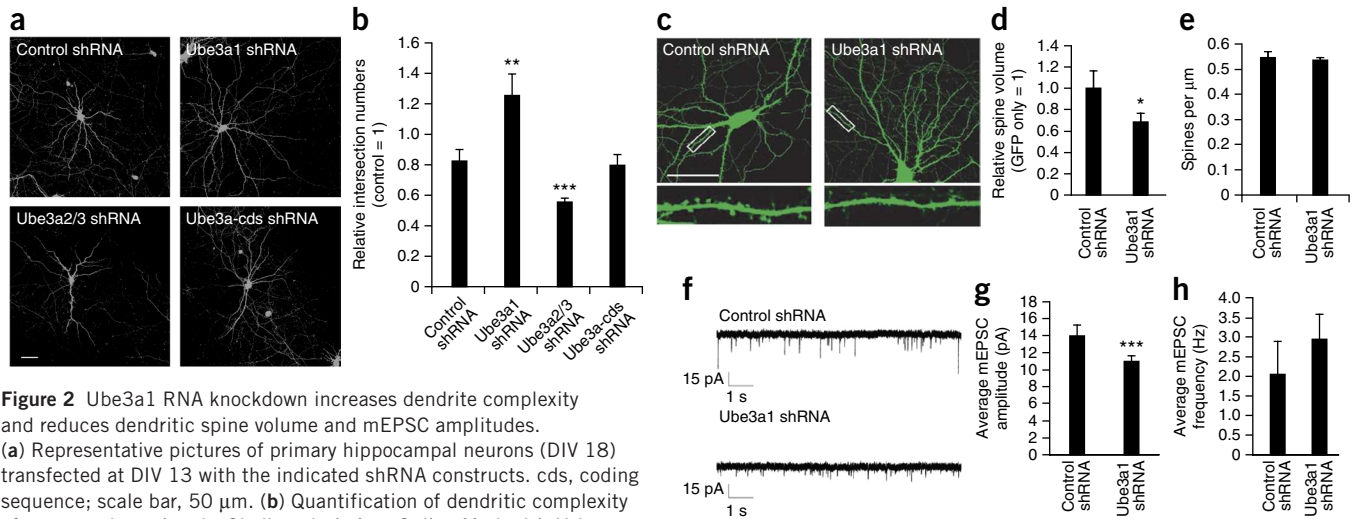


Figure 2 Ube3a1 RNA knockdown increases dendrite complexity and reduces dendritic spine volume and mEPSC amplitudes.

(a) Representative pictures of primary hippocampal neurons (DIV 18) transfected at DIV 13 with the indicated shRNA constructs. cds, coding sequence; scale bar, 50 μ m. (b) Quantification of dendritic complexity of neurons shown in **a** by Sholl analysis (see Online Methods). Values are intersection numbers relative to a GFP-only-transfected control \pm s.d. $N = 3$ independent experiments (ANOVA $P < 0.001$); ** $P < 0.01$, *** $P < 0.001$ (*post hoc t*-test). (c) Representative pictures of primary hippocampal neurons (DIV 18) that had been transfected with eGFP and control shRNA (left) or Ube3a1 shRNA (right). Bottom, insets at higher magnification illustrate reduced average spine volume in Ube3a1 shRNA-transfected cells. Scale bar, 50 μ m. (d) Quantification of average spine volume. Values are presented relative to those in GFP-only transfected neurons. $N = 3$ independent experiments. * $P = 0.026$. (e) Quantification of average spine density. $N = 3$ independent experiments. (f) Representative mEPSC traces from DIV 18–21 hippocampal neurons transfected with the indicated shRNAs. (g) Average mEPSC amplitudes \pm s.e.m. *** $P < 0.001$ (Student's *t*-test). (h) Average mEPSC frequency \pm s.e.m. ($n = 3$ independent experiments; control shRNA: 15 neurons; Ube3a1 shRNA: 12 neurons).

with protease before hybridization (Fig. 1e), indicating that a fraction of Ube3a1 RNA could be masked by proteins. Taken together, our results suggest that the unique Ube3a1 3' UTR confers localization to the synapto-dendritic compartment.

We next explored the expression of Ube3a protein isoforms in developing rat neurons *in vitro* and rat brain *in vivo*. Whereas Ube3a2 and Ube3a3 mRNAs encode two proteins of highly similar size (96 and 94 kDa, respectively, commonly referred to as Ube3a-FL), Ube3a1 RNA is expected to encode a truncated protein (Ube3a-S, 84 kDa). Using a mouse monoclonal antibody that recognizes all Ube3a isoforms (amino acids 501–712 in mouse), we detected a single band, corresponding to Ube3a-FL, by western blotting using protein extracts either from biochemical fractionation of P15 rat brain (Supplementary Fig. 4a) or primary hippocampal neurons (Supplementary Fig. 4e). In contrast, we could not detect a band at the expected size of Ube3a-S, strongly suggesting that Ube3a-S is not detectably expressed in neurons at the time of synapse development. This lack of expression is not due to an intrinsic incapacity of the Ube3a1 RNA to be translated, as a plasmid encoding an eGFP-Ube3a1 fusion protein gave rise to a protein of the expected size when transfected into human embryonic kidney 293 (HEK293) cells (Supplementary Fig. 4b). Moreover, eGFP-Ube3a1 is expressed when transfected into mature primary neurons (Supplementary Fig. 4c). We conclude that Ube3a1 RNA, despite its coding potential, is not efficiently translated into Ube3a-S in neurons during synaptic development.

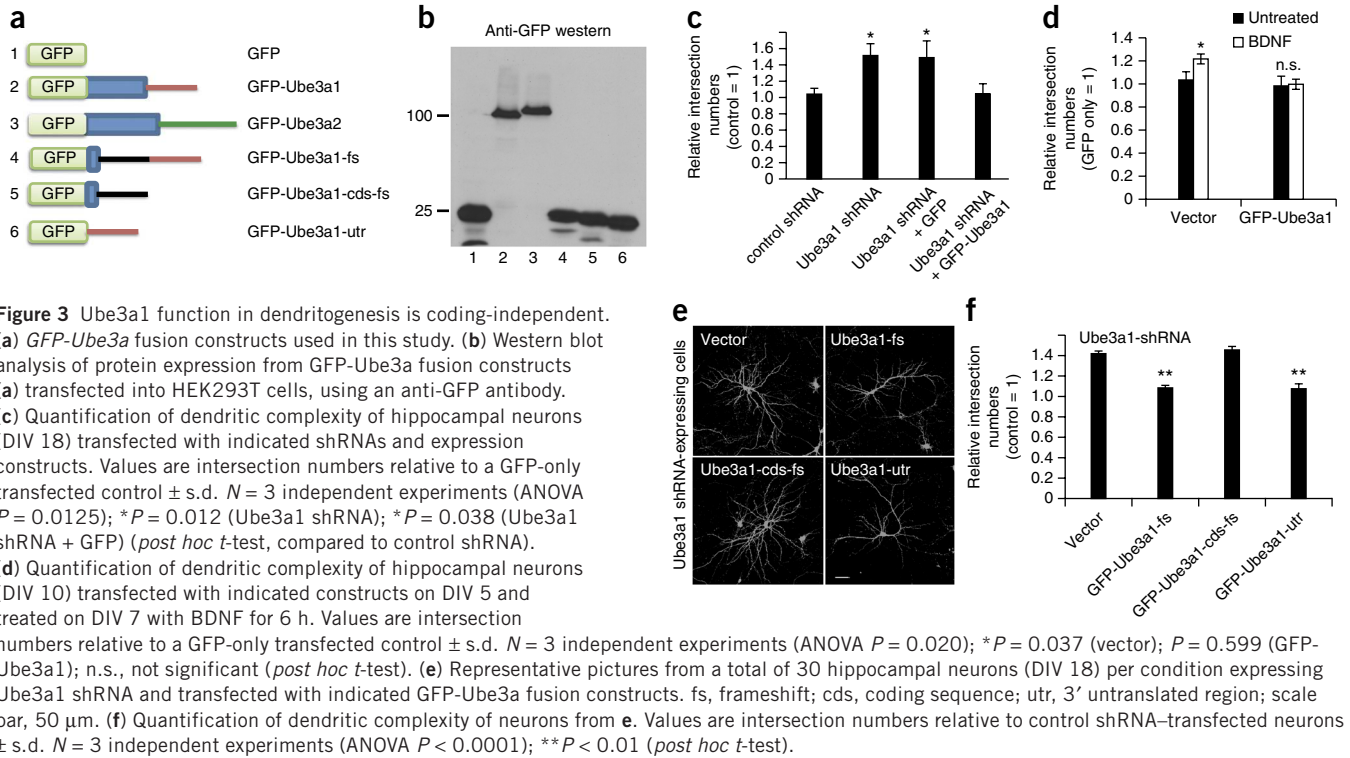
Ube3a1 RNA regulates dendrite complexity and spine morphogenesis

Mammalian Ube3a has been previously implicated in the regulation of dendrite and spine development in neurons^{5,8,9}, but the contribution of the Ube3a 3' UTR variants to these phenotypes is unclear. To address this issue, we designed short hairpin RNAs specifically targeting either the Ube3a1 3' UTR, the Ube3a2/3 3' UTR or the common Ube3a coding sequence. We confirmed the specificity of the shRNAs by knockdown of the respective recombinant Ube3a proteins

in HEK293 cells (Supplementary Fig. 4d). In addition, recombinant adeno-associated virus (rAAV)-mediated expression of Ube3a2/3 and Ube3a coding sequence shRNAs specifically reduced endogenous Ube3a-FL in rat hippocampal neurons, whereas Ube3a1 shRNA, as expected, had no effect on Ube3a-FL (Supplementary Fig. 4e). We confirmed specific knockdown of the endogenous Ube3a1 transcript in these neurons relative to a control shRNA that was designed to target a sequence not present in the rat transcriptome by qPCR (Supplementary Fig. 4f).

We first tested the effect of knockdown of specific Ube3a 3' UTR variants on dendritogenesis in mature primary rat hippocampal neurons (days *in vitro* (DIV) 13–18). Surprisingly, knockdown of Ube3a1 RNA, which is not detectably translated into protein, led to a significant increase in dendritic complexity of primary hippocampal neurons compared to control conditions, as assessed by Sholl analysis (see Online Methods) (Fig. 2a,b). In contrast, knockdown of Ube3a2/3 mRNA significantly reduced dendritic complexity (Fig. 2a,b). Knockdown of all three Ube3a isoforms by the Ube3a coding sequence-targeting shRNA did not significantly alter dendritic complexity (Fig. 2a,b), in agreement with results from Ube3a knockout neurons⁸. Together, our results demonstrate that Ube3a1 RNA is a negative regulator of dendritogenesis in mature hippocampal neurons. They further indicate that Ube3a 3' UTR variants have distinct roles in the regulation of dendritogenesis and likely work in independent pathways, in agreement with their different regulation by neuronal activity and subcellular localization (Fig. 1c–e).

In addition to dendritogenesis, Ube3a has a well-documented role in the regulation of excitatory synapses^{2,6,10}. Specific knockdown of Ube3a1 RNA led to a significant reduction in the average size, but not density, of dendritic spines as compared to those in control conditions (Fig. 2c–e). Consistent with the observed effects on spines, Ube3a1 RNA knockdown reduced the average amplitude, but not frequency, of miniature excitatory postsynaptic currents (mEPSCs) as determined by patch-clamp electrophysiology recordings (Fig. 2f–h). Taken together, our results demonstrate that Ube3a1 RNA works as



a rheostat during the development of hippocampal pyramidal neurons, concomitantly preventing excessive dendritic growth and promoting spine maturation.

Ube3a1 function is coding-independent

Since Ube3a1 knockdown robustly affected neuronal morphogenesis in the absence of a corresponding Ube3a-S protein, we hypothesized that Ube3a1 function might be independent of protein expression. To test this hypothesis, we designed a rescue experiment whereby we introduced different shRNA-resistant Ube3a1 mutants, either protein-coding or non-coding, and screened for their ability to block the induction of dendritic complexity caused by Ube3a1 RNA knockdown (Fig. 3a).

All Ube3a mutants were expressed to a similar degree (Fig. 3b and Supplementary Fig. 5a). Expression of an shRNA-resistant GFP-Ube3a1 RNA encompassing the 5' UTR, the coding region and the 3' UTR fully rescued the increased dendritic complexity caused by Ube3a1 RNA knockdown (Fig. 3c and Supplementary Fig. 5b). This result confirms that the Ube3a1 shRNA phenotype is caused by the lack of Ube3a1 RNA. Expression of GFP-Ube3a1 in immature hippocampal neurons (DIV 4–10) that express little endogenous Ube3a1 RNA also completely abolished increased dendritic complexity caused by BDNF treatment (Fig. 3d and Supplementary Fig. 5c), whereas GFP-Ube3a1 or GFP-Ube3a2 alone had no effect on dendritic complexity (Supplementary Fig. 5d). In conclusion, our results

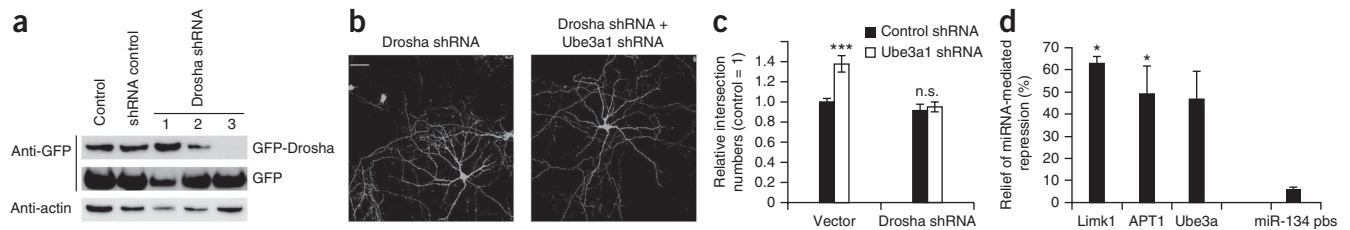
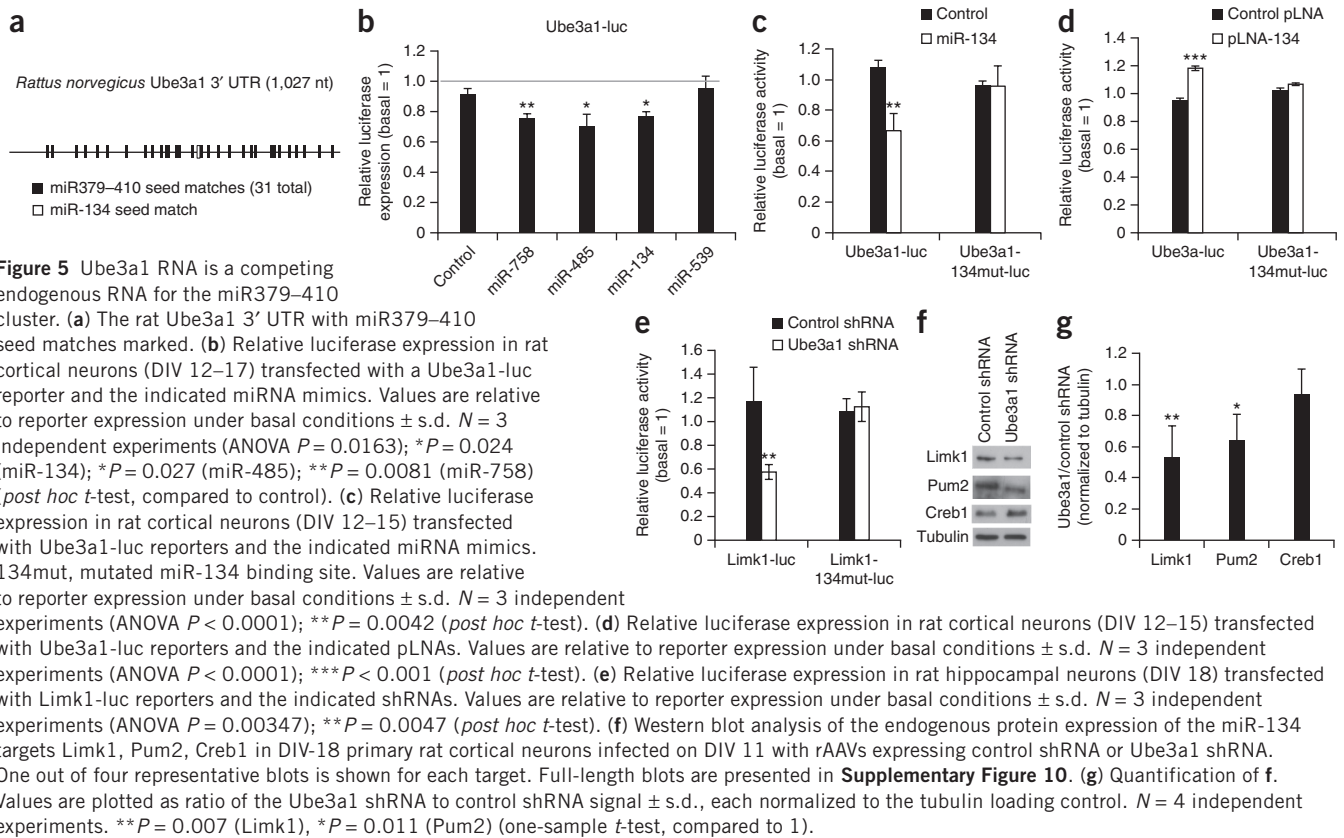


Figure 4 Ube3a1 function in dendritogenesis requires an intact microRNA pathway. (a) HEK293 cells were co-transfected with GFP-Drosha and the indicated shRNA constructs. Western blotting was performed with anti-GFP to detect GFP-Drosha expression and anti-actin as a loading control. Full-length blots are presented in Supplementary Figure 7. (b) Representative images of hippocampal neurons co-transfected with Drosha shRNA and either control (left) or Ube3a1 (right) shRNA. Scale bar, 50 μ m. (c–f) Quantification of dendritic complexity of neurons transfected with indicated shRNA constructs (c, e, f) and luciferase assay (d). Values in c, e, f are intersection numbers relative to GFP-only transfected neurons \pm s.d. $N = 3$ independent experiments (ANOVA $P = 0.000362$ (c), $P = 0.0140$ (e), $P < 0.0001$ (f)); $***P < 0.001$ (c, vector); $P = 0.558$ (c, Drosha shRNA); $*P = 0.014$ (e, vector); $P = 0.113$ (e, Tnrc6c shRNA); $***P < 0.001$ (f); n.s., not significant (*post hoc t*-test). (d) Luciferase assay in primary cortical neurons co-transfected with the indicated firefly reporter constructs (Limk1, APT1 (also known as Lypla1), Ube3a and miR-134 perfect binding site (pbs)), Tnrc6c siRNA and miRNA mimics (miR-134 for Limk1, Ube3a and miR-134 pbs; miR-138 for APT1). Values are presented as percentage relief of miRNA-mediated repression. $N = 3$ independent experiments. $*P = 0.012$ (Limk1); $*P = 0.028$ (APT1) (*t*-test).



demonstrate that Ube3a1 is necessary and sufficient to confine dendritic complexity during activity-dependent neuronal development.

We went on to test the ability of shRNA-resistant Ube3a1 mutants that lack protein coding potential in our dendritogenesis assay. Ube3a1 RNA containing a frameshift mutation (Ube3a1-fs) was as effective in rescuing the dendrite phenotype caused by Ube3a1 knockdown as the wild-type construct, strongly suggesting that Ube3a1 function in dendritogenesis is independent of the expression of a Ube3a1 protein (**Fig. 3e,f**). In further support, expression of the Ube3a1 3' UTR alone was sufficient to rescue the increased dendritic complexity caused by Ube3a1 RNA knockdown, whereas expression of the Ube3a1 coding sequence both with or without a frameshift mutation (Ube3a1-cds-fs or Ube3a1-cds, respectively) had no effect (**Fig. 3e,f** and **Supplementary Fig. 6**). Together, these results suggest a function of the Ube3a1 RNA in the regulation of dendritic complexity and map this function to the unique Ube3a1 3' UTR.

Ube3a1 function requires an intact miRNA pathway

3' UTRs are preferred target sequences for miRNAs, an extensive class of small noncoding RNAs with important functions in post-transcriptional gene regulation in neurons^{13,14}. Therefore, we decided to test whether intact miRNA-dependent regulation might be required for the inhibitory function of Ube3a1 RNA in dendritogenesis. To perturb miRNA production in neurons globally, we performed knockdown of the RNase III enzyme Droscha, an essential component of the microprocessor complex²⁸. We confirmed specific knockdown of Droscha by western blotting (**Fig. 4a** and **Supplementary Fig. 7**). Knockdown of Droscha completely abolished increased dendritic complexity caused by Ube3a1 RNA knockdown, suggesting that Ube3a1 function depends on miRNA expression (**Fig. 4b,c**). We further assessed Ube3a1 function in the context of knockdown of

the mammalian GW182 homolog Tnrc6c, a core component of the miRNA-induced silencing complex (miRISC)²⁹. miRNA reporter assays demonstrated efficient relief of miRNA-dependent, but not short interfering RNA-dependent, repression by the Tnrc6c shRNA (**Fig. 4d**), confirming that knockdown of Tnrc6c specifically impairs miRNA function. Similarly to Droscha knockdown, Ube3a1 RNA knockdown was ineffective in increasing dendritic complexity in the presence of a Tnrc6c shRNA (**Fig. 4e**). Tnrc6c knockdown did not interfere with the ability of a Ube3a2/3 mRNA-specific shRNA to reduce dendritic complexity, demonstrating that Tnrc6c knockdown does not generally perturb shRNA function (**Fig. 4f**). Taken together, two independent lines of evidence suggest that Ube3a1 function in neuronal development requires an intact miRNA pathway.

Ube3a1 RNA is a competing endogenous RNA for targets of the miR379–410 cluster

We next sought to identify the specific miRNAs involved in Ube3a1-regulated dendritic complexity. The miR379–410 cluster is the largest known miRNA cluster in the mammalian genome¹⁵ and contains several miRNAs involved in activity-dependent dendritogenesis¹⁶, making it a suitable candidate effector of Ube3a1 RNA. We therefore cloned the rat Ube3a1 3' UTR from P15 brain cDNA (GenBank accession code [KP742805](#)) and screened it for seed matches potentially targeted by miRNAs of the miR379–410 cluster. Strikingly, in its 1,027-nucleotide-long 3' UTR region, rat Ube3a1 RNA harbors a total of 31 seed matches for 21 mature miRNA sequences derived from 19 miRNA genes located in the miR379–410 cluster (**Fig. 5a** and **Supplementary Table 2**). The miRNAs corresponding to most (29) of these seed matches are expressed in rat hippocampal neurons, as judged by small RNA sequencing (**Supplementary Table 2**). The corresponding 3' UTR of the mouse Ube3a1/human UBE3A-005 transcript

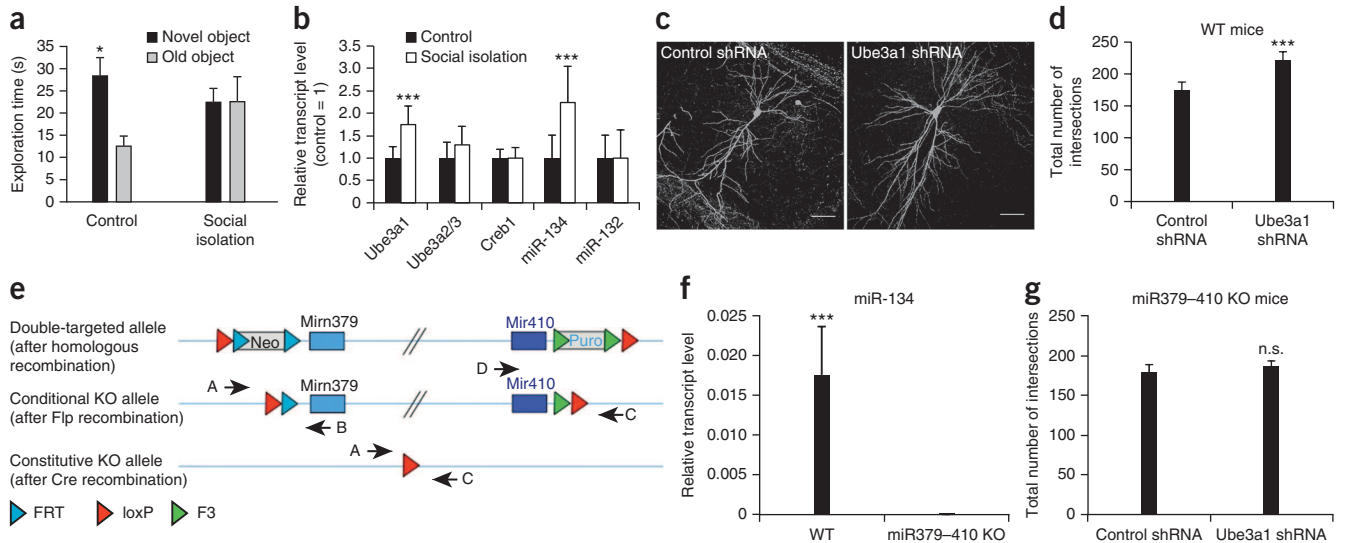


Figure 6 Ube3a1 function *in vivo* depends on miR379–410 miRNAs. **(a)** Cognitive impairment in socially isolated rats. Values represent average time that juvenile rats housed either under standard cage conditions (control, $n = 17$ animals) or in isolation for 4 weeks (social isolation, $n = 16$ animals) spent with a novel or familiar (old) object \pm s.d. * $P = 0.042$ (t -test). **(b)** qPCR analysis of Ube3a1 RNA, Ube3a2/3 RNA, Creb1 mRNA, miR-132 and miR-134 from a subset of hippocampi of rats used in **a** (control, $n = 11$ animals; social isolation, $n = 12$ animals). Values represent average transcript levels \pm s.d. relative to U6 small nuclear RNA (Rnu6). Average values from control conditions were set to 1 for each transcript after normalization. *** $P < 0.001$ (t -test). **(c)** Representative mouse hippocampal CA1 neurons imaged from P21 mouse coronal brain slices after P0 injection of rAAV expressing GFP-control shRNA (targeting a sequence not present in the mouse transcriptome) or GFP-Ube3a1 shRNA. Scale bars, 50 μ m. **(d)** Quantification of dendritic complexity of neurons from **c**. The average number of total intersections \pm s.d. is shown. WT, wild type. $n = 7$ animals (control shRNA) and $n = 9$ animals (Ube3a1 shRNA). *** $P < 0.001$ (t -test). Power ($\alpha = 0.05$) = 1.0. **(e)** Targeting strategy for the mouse *miR379–410* locus. Target sequences of recombinases and the location of primers used for genotyping are indicated. KO, knockout. **(f)** qPCR analysis of mature miR-134 levels relative to U6 snRNA in the cerebellum of 2- to 4-month old wild-type ($n = 7$) and constitutive *miR379–410*^{-/-} (KO) mice ($n = 7$) \pm s.d. *** $P < 0.001$ (t -test). **(g)** Quantification of dendritic complexity of CA1 pyramidal neurons from P21 *miR379–410*^{-/-} mice infected at P0 with rAAV expressing the indicated shRNAs. $n = 7$ animals (control shRNA) and $n = 10$ animals (Ube3a1 shRNA) \pm s.d. n.s. not significant; $P = 0.38$ (t -test). Power ($\alpha = 0.05$) = 0.24.

contains a total of 27/22 seed matches for 19/16 miR379–410 members, 11/9 of which also target the rat Ube3a1 3' UTR (**Supplementary Tables 1 and 3**). Together, these data suggests that regulation of Ube3a1 3' UTRs by miR379–410 might be conserved in mammals.

Initially, we tested whether some of the identified seed sequences are indeed targeted by miR379–410 miRNAs in neurons using a Ube3a1 luciferase reporter gene assay. Three of the four tested miRNA duplexes (miR-134, miR-758 and miR-485) significantly reduced relative luciferase expression of the Ube3a1-luc reporter as compared to that of an empty control reporter, suggesting that the corresponding miRNA seed sites in the Ube3a1 3' UTR are functional (**Fig. 5b**). Since miR-134 has a well-described function in neuronal development and plasticity^{16–18}, we decided to focus on miR-134-dependent regulation of Ube3a1 RNA in our further studies. We found that Ube3a1-134mut-luc, which contains a mutated miR-134 binding site, was not downregulated by miR-134, demonstrating that the inhibitory effect of miR-134 depends on the identified binding site in the Ube3a1 3' UTR (**Fig. 5c**). Sequestration of the endogenous miR-134 by power-locked nucleic acid (pLNA)-modified antisense oligonucleotides (pLNA-134) specifically elevated expression of Ube3a1-luc, but not Ube3a1-134mut-luc, demonstrating that endogenous miR-134 in neurons downregulates Ube3a1-luc expression via the identified binding site (**Fig. 5d**). These results suggest that Ube3a1 RNA is a target of miRNAs originating from the miR379–410 cluster, including miR-134.

Recently, protein-coding mRNAs and non-coding RNAs were shown to sequester miRNAs away from their natural target mRNAs, thereby working as competing endogenous RNAs (ceRNAs)³⁰. Since Ube3a1 RNA knockdown phenocopies miR-134 gain of function with regard to activity-dependent dendritogenesis and spine morphogenesis,

we tested the possibility that Ube3a1 RNA could regulate the known miR-134 target mRNAs *Limk1* (ref. 17), *Pum2* (ref. 16) and *Creb1* (ref. 18) (**Supplementary Fig. 8a**) by a ceRNA mechanism. Consistent with this hypothesis, Ube3a1 RNA knockdown led to a specific reduction in luciferase expression of *Limk1-luc* (**Fig. 5e**) and *Creb1-luc* (**Supplementary Fig. 8b**) constructs, both of which contain a miR-134 binding site. In contrast, Ube3a1 RNA knockdown had no effect on the respective constructs containing mutated miR-134 binding sites (**Fig. 5e** and **Supplementary Fig. 8b**). Absolute quantification qPCR showed that Ube3a1 transcripts were expressed at comparable levels to *Limk1* mRNA in hippocampal neuron cell bodies and dendrites, whereas *Pum2* mRNA expression was about six- to eightfold higher (**Supplementary Fig. 9**). Furthermore, we observed a significant downregulation of the endogenous miR-134 target proteins *Limk1* and *Pum2* upon Ube3a1 knockdown (**Fig. 5f,g** and **Supplementary Fig. 10**). Surprisingly, endogenous *Creb1* protein levels were unaffected by Ube3a1 RNA knockdown (**Fig. 5f,g** and **Supplementary Fig. 10**), suggesting that the bulk of *Creb1* protein is synthesized independently of miR-134. Taken together, these results indicate that Ube3a1 RNA regulates a specific group of dendritic miR-134 targets by fine-tuning miR-134 availability.

Ube3a1 function *in vivo* is abolished in *miR379–410*^{-/-} mice

Finally, we decided to investigate the role of Ube3a1 RNA in the developing rodent brain *in vivo*. *Ube3a* deficiency in the Angelman syndrome mouse model leads to cognitive deficits². We used the juvenile social isolation model of early-life stress, known to cause cognitive deficits in the novel object recognition test³¹, to interrogate a potential contribution of Ube3a 3' UTR variants. Strikingly, juvenile

social isolation, resulting in poor novel object recognition as expected (Fig. 6a), specifically elevated Ube3a1 RNA levels (Fig. 6b) but had no significant effect on Ube3a2/3 ($P = 0.081$) or Creb1 ($P = 0.754$) mRNA expression. The increase in Ube3a1 RNA expression in the hippocampus of socially isolated rats was paralleled by elevated levels of miR-134, but not miR-132 (Fig. 6b). This suggests a specific role of Ube3a1-regulated miR-134 activity in cognitive functions. To determine the function of Ube3a1 RNA during neuronal morphogenesis *in vivo*, we injected rAAV expressing Ube3a1 or control shRNA into the neonatal mouse hippocampus and assessed dendritic complexity of hippocampal pyramidal neurons at P21. As in cultured rat hippocampal neurons, Ube3a1 RNA knockdown significantly increased dendritic complexity of mouse hippocampal CA1 pyramidal neurons compared to that in control conditions *in vivo* (Fig. 6c,d).

To address whether miRNAs originating from the miR379–410 cluster—in particular, miR-134—are required for Ube3a1-regulated dendrite complexity *in vivo*, we generated a mouse model containing a conditional *miR379–410* allele (Fig. 6e and Supplementary Fig. 11a). Homozygous deletion of the *miR379–410* region by crossing the *miR379–410* flox strain to a germline Cre-deleter mouse strain resulted in a complete loss of the expression of miR-134 (Fig. 6f) and other (pre-)miRNAs encoded by the *miR379–410* cluster in the adult brain (Supplementary Fig. 11b and data not shown). *miR379–410*^{-/-} mice were viable and displayed an apparently normal layering of the neocortex and hippocampus (Supplementary Fig. 12). A detailed anatomical and behavioral analysis of these mice will be presented elsewhere. Strikingly, in contrast to knockdown in wild-type mice, Ube3a1 RNA knockdown in P15 *miR379–410*^{-/-} mice failed to induce dendritic complexity in hippocampal CA1 pyramidal neurons (Fig. 6g). This result demonstrates that expression of miRNAs, specifically those expressed from the *miR379–410* cluster, is an important downstream component in Ube3a1 RNA-regulated dendrite complexity.

DISCUSSION

Here we show that an activity-regulated, alternative transcript generated from the rat *Ube3a* locus sequesters miRNAs from the *miR379–410* cluster, thereby regulating local translation of miR379–410 targets in dendrites and activity-dependent neuronal development (Supplementary Fig. 13). This study provides to our knowledge the first example of a neuronal mechanism involving a ceRNA—a protein-coding mRNA that controls the expression of neuronal miRNA targets *in trans*—and adds to the growing list of regulatory mechanisms fine-tuning the local dendritic proteome in response to environmental cues.

A few studies have reported the presence of Ube3a1 RNA in rodents, but to our knowledge a corresponding endogenous truncated Ube3a protein (Ube3a-S) has not been described⁹. In agreement, we were unable to detect Ube3a-S at the expected size in western blotting with neuronal protein lysates. However, we do not rule out the possibility that low levels of the catalytically inactive Ube3a-S could be functionally important—for example, as a dominant negative for Ube3a-FL.

In any case, both a Ube3a1 RNA containing a frameshift mutation and the Ube3a1 3' UTR alone are sufficient to restore dendrite complexity, strongly suggesting that at least part of the function of Ube3a1 RNA during neuronal development is coding-independent. Our data are consistent with Ube3a1 RNA functioning as a ceRNA by competing with miR379–410 miRNAs—in particular, miR-134—for their natural target mRNAs. Noncoding ceRNAs have been identified in human cancer cells (PTENP1, HULC), human and mouse myoblasts (LINCMD1), *Arabidopsis thaliana* (IPS1) and herpesvirus saimiri³⁰. Furthermore, mRNAs are part of ceRNA networks in human cancer³².

Quantitative considerations with regard to cellular miRNA and target abundances raised concerns about the physiological significance of ceRNA crosstalk³³. However, it was subsequently shown that some miRNAs—in particular, those with low miRNA/target ratios—can be effectively regulated by ceRNAs under physiological conditions³⁴. For such miRNAs, depletion of a high-affinity ceRNA leads to increased repression of low-affinity targets that are otherwise not occupied by the miRNA. Our results are in agreement with this model: first, miR-134 (along with other miR379–410 members) is only modestly expressed in neurons, suggesting that the miRNA/target ratio for miR-134 is low. Second, the effect of Ube3a1 RNA knockdown on miR-134 target gene repression is stronger for Limk1, which contains a noncanonical low-affinity target site¹⁷, than for other targets containing perfect seed matches (for example, Pum2, Creb1)^{16,18}.

Our results suggest that Ube3a1 RNA could be involved in the spatiotemporal control of mRNA translation in dendrites. Consistent with this, expression of the dendritic proteins Limk1 and Pum2, but not of the nuclear Creb1, is affected by Ube3a1 RNA knockdown. Ube3a1 RNA and Limk1 mRNA are expressed in dendrites at comparable levels (Supplementary Fig. 9), which might support an effective local ceRNA crosstalk between these RNAs. In comparison, dendritic levels of Pum2 mRNA are almost 1 order of magnitude higher, which, together with the higher affinity for miR-134, could explain why Pum2 expression is less sensitive to alterations in Ube3a1 RNA levels.

The Ube3a1 RNA developmental profile, regulation by neuronal activity and the knockdown phenotype are consistent with a function of Ube3a1 RNA as a rheostat during neuronal maturation. In young neurons, low levels of Ube3a1 RNA and a corresponding high activity of miR379–410 are permissive for dendrite growth while preventing premature spine maturation. Once neuronal activity increases during development, the resulting higher Ube3a1 RNA levels buffer miR379–410 activity, thereby allowing a switch from dendrite growth to spine maturation. In line with this model, we found that ectopic Ube3a1 RNA expression blocked activity-dependent dendritogenesis in young neurons (Fig. 3d) while Ube3a1 knockdown in mature neurons led to exuberant dendrite growth and immature spines (Fig. 2b,d). The general loss of miRNAs caused by Drosha knockdown (Fig. 4c) or the specific inactivation of the miR379–410 cluster (Fig. 6d,g) does not significantly alter dendrite complexity, indicating that alterations in miRNA activity—for example, triggered by Ube3a1 RNA knockdown or neuronal activity—might be required to elicit phenotypic consequences.

Finally, our findings could have important implications concerning the molecular basis of neurodevelopmental disorders. Duplications of chromosomal regions encompassing the *UBE3A* gene are frequently observed in autism⁴. Reduced dendrite complexity is a common feature of neurons from autism patients^{35,36} or ASD animal models³⁷, and it will be interesting to test whether increased levels of Ube3a1 RNA early in development might contribute to this defect. Elevated Ube3a1 RNA levels might further contribute to the defective activity-dependent synaptic pruning that has been observed in ASD mouse models³⁷ and autism patients³⁸. A recent study reported recurrent CNVs associated with autism in the 7q11.23 Williams syndrome region, which comprises, among other genes *LIMK1* (ref. 39), pointing to deregulation of the Ube3a1-Limk1 pathway as feature common in ASD. Neurons from Angelman syndrome model mice display reduced spine size and surface AMPA receptor expression^{8,10}, a phenotype also observed with Ube3a1 RNA deficiency. However, there is a strong correlation between Angelman syndrome-associated mutations and a loss of Ube3a E3 ligase activity, suggesting that deficiency in transcripts encoding Ube3a-FL (for example, Ube3a2/3) is the primary cause

of Angelman syndrome and that Ube3a1 RNA does not play a major role in this disorder²³. Nevertheless, 15–20% of patients with Angelman syndrome do not carry classical mutations, warranting a more detailed inspection of intronic and UTR regions concerning potential mutations. In the future, experiments with induced pluripotent stem cell–derived neurons from Angelman syndrome or ASD patients in combination with *Ube3a* overexpression or knockdown could be a promising strategy for unraveling the contributions of different Ube3a transcripts to phenotypic alterations observed in these devastating disorders.

METHODS

Methods and any associated references are available in the [online version of the paper](#).

Accession codes. GenBank: rat Ube3a1 3' UTR, [KP742805](#).

Note: Any Supplementary Information and Source Data files are available in the online version of the paper.

ACKNOWLEDGMENTS

We acknowledge technical assistance of U. Beck, E. Becker, R. Gondrum, G. Jarosch, H. Kaiser and H. Rippberger. This work was funded by grants from the European Research Council (Starting Grant “Neuromir”), the European Union FP7 (“EpimiRNA”), the Deutsche Forschungsgemeinschaft (DFG) (SFB593, FOR2107: SCHR 1136/3-1) and the Universitätsklinikum Gießen-Marburg to G.S., the DFG (FOR2107) to R.S. (SCHW 559/14-1) and M.W. (WO 1732/4-1) and the Von Behring-Röntgen-Foundation (62-0004) to S.B.

AUTHOR CONTRIBUTIONS

J.V. performed most experiments (dendritogenesis, luciferase assays, western blots, rAAV injections, strand-specific qPCR) and analyzed the data. G.S. designed the study, supervised the project and wrote the manuscript. S.B. performed FISH, compartmentalized culture and synaptosome assays. A.A.-A. performed and analyzed patch-clamp recordings. M.L. and R.F. established and characterized the *miR379-410* knockout colony. S.S. cloned and validated the Droscha shRNA construct. T.W. performed dendritogenesis assays and generated Ube3a constructs. R.S. and M.W. designed and supervised the rat behavioral studies. D.S. performed juvenile social isolation studies in rats. F.M. and C.D. analyzed deep sequencing data.

COMPETING FINANCIAL INTERESTS

The authors declare no competing financial interests.

Reprints and permissions information is available online at <http://www.nature.com/reprints/index.html>.

- Ebert, D.H. & Greenberg, M.E. Activity-dependent neuronal signalling and autism spectrum disorder. *Nature* **493**, 327–337 (2013).
- Jiang, Y.H. *et al.* Mutation of the Angelman ubiquitin ligase in mice causes increased cytoplasmic p53 and deficits of contextual learning and long-term potentiation. *Neuron* **21**, 799–811 (1998).
- Matsuura, T. *et al.* De novo truncating mutations in E6-AP ubiquitin-protein ligase gene (*UBE3A*) in Angelman syndrome. *Nat. Genet.* **15**, 74–77 (1997).
- Glessner, J.T. *et al.* Autism genome-wide copy number variation reveals ubiquitin and neuronal genes. *Nature* **459**, 569–573 (2009).
- Sato, M. & Stryker, M.P. Genomic imprinting of experience-dependent cortical plasticity by the ubiquitin ligase gene Ube3a. *Proc. Natl. Acad. Sci. USA* **107**, 5611–5616 (2010).
- Yashiro, K. *et al.* Ube3a is required for experience-dependent maturation of the neocortex. *Nat. Neurosci.* **12**, 777–783 (2009).
- Wallace, M.L., Burette, A.C., Weinberg, R.J. & Philpot, B.D. Maternal loss of Ube3a produces an excitatory/inhibitory imbalance through neuron type-specific synaptic defects. *Neuron* **74**, 793–800 (2012).
- Dindot, S.V., Antalffy, B.A., Bhattacharjee, M.B. & Beaudet, A.L. The Angelman syndrome ubiquitin ligase localizes to the synapse and nucleus, and maternal deficiency results in abnormal dendritic spine morphology. *Hum. Mol. Genet.* **17**, 111–118 (2008).
- Miao, S. *et al.* The Angelman syndrome protein Ube3a is required for polarized dendrite morphogenesis in pyramidal neurons. *J. Neurosci.* **33**, 327–333 (2013).
- Greer, P.L. *et al.* The Angelman Syndrome protein UBE3A regulates synapse development by ubiquitinating arc. *Cell* **140**, 704–716 (2010).
- Margolis, S.S. *et al.* EphB-mediated degradation of the RhoA GEF Ephexin5 relieves a developmental brake on excitatory synapse formation. *Cell* **143**, 442–455 (2010).
- Filipowicz, W., Bhattacharyya, S.N. & Sonenberg, N. Mechanisms of post-transcriptional regulation by microRNAs: are the answers in sight? *Nat. Rev. Genet.* **9**, 102–114 (2008).
- Schratt, G. microRNAs at the synapse. *Nat. Rev. Neurosci.* **10**, 842–849 (2009).
- McNeill, E. & Van Vactor, D. MicroRNAs shape the neuronal landscape. *Neuron* **75**, 363–379 (2012).
- Seitz, H. *et al.* A large imprinted microRNA gene cluster at the mouse Dlk1-Gtl2 domain. *Genome Res.* **14**, 1741–1748 (2004).
- Fiore, R. *et al.* Mef2-mediated transcription of the miR379–410 cluster regulates activity-dependent dendritogenesis by fine-tuning Pumilio2 protein levels. *EMBO J.* **28**, 697–710 (2009).
- Schratt, G.M. *et al.* A brain-specific microRNA regulates dendritic spine development. *Nature* **439**, 283–289 (2006).
- Gao, J. *et al.* A novel pathway regulates memory and plasticity via SIRT1 and miR-134. *Nature* **466**, 1105–1109 (2010).
- Jimenez-Mateos, E.M. *et al.* Silencing microRNA-134 produces neuroprotective and prolonged seizure-suppressive effects. *Nat. Med.* **18**, 1087–1094 (2012).
- Bicker, S. *et al.* The DEAH-box helicase DHX36 mediates dendritic localization of the neuronal precursor-microRNA-134. *Genes Dev.* **27**, 991–996 (2013).
- Huibregtse, J.M., Scheffner, M., Beaudenon, S. & Howley, P.M. A family of proteins structurally and functionally related to the E6-AP ubiquitin-protein ligase. *Proc. Natl. Acad. Sci. USA* **92**, 2563–2567 (1995).
- Yamamoto, Y., Huibregtse, J.M. & Howley, P.M. The human E6-AP gene (*UBE3A*) encodes three potential protein isoforms generated by differential splicing. *Genomics* **41**, 263–266 (1997).
- Cooper, E.M., Hudson, A.W., Amos, J., Wagstaff, J. & Howley, P.M. Biochemical analysis of Angelman syndrome-associated mutations in the E3 ubiquitin ligase E6-associated protein. *J. Biol. Chem.* **279**, 41208–41217 (2004).
- Landers, M. *et al.* Regulation of the large (approximately 1000 kb) imprinted murine Ube3a antisense transcript by alternative exons upstream of Snurf/Snrpn. *Nucleic Acids Res.* **32**, 3480–3492 (2004).
- Filonova, I., Trotter, J.H., Banko, J.L. & Weeber, E.J. Activity-dependent changes in MAPK activation in the Angelman Syndrome mouse model. *Learn. Mem.* **21**, 98–104 (2014).
- Martin, K.C. & Ephrussi, A. mRNA localization: gene expression in the spatial dimension. *Cell* **136**, 719–730 (2009).
- Steward, O., Wallace, C.S., Lyford, G.L. & Worley, P.F. Synaptic activation causes the mRNA for the IEG Arc to localize selectively near activated postsynaptic sites on dendrites. *Neuron* **21**, 741–751 (1998).
- Gregory, R.I. *et al.* The Microprocessor complex mediates the genesis of microRNAs. *Nature* **432**, 235–240 (2004).
- Meister, G. *et al.* Identification of novel argonaute-associated proteins. *Curr. Biol.* **15**, 2149–2155 (2005).
- Tay, Y., Rinn, J. & Pandolfi, P.P. The multilayered complexity of ceRNA crosstalk and competition. *Nature* **505**, 344–352 (2014).
- Fone, K.C. & Porkess, M.V. Behavioural and neurochemical effects of post-weaning social isolation in rodents—relevance to developmental neuropsychiatric disorders. *Neurosci. Biobehav. Rev.* **32**, 1087–1102 (2008).
- Tay, Y. *et al.* Coding-independent regulation of the tumor suppressor PTEN by competing endogenous mRNAs. *Cell* **147**, 344–357 (2011).
- Denzler, R., Agarwal, V., Stefano, J., Bartel, D.P. & Stoffel, M. Assessing the ceRNA Hypothesis with Quantitative Measurements of miRNA and Target Abundance. *Mol. Cell* **54**, 766–776 (2014).
- Bosson, A.D., Zamudio, J.R. & Sharp, P.A. Endogenous miRNA and target concentrations determine susceptibility to potential ceRNA competition. *Mol. Cell* **56**, 347–359 (2014).
- Mukaetova-Ladinska, E.B., Arnold, H., Jaros, E., Perry, R. & Perry, E. Depletion of MAP2 expression and laminar cytoarchitectonic changes in dorsolateral prefrontal cortex in adult autistic individuals. *Neuropathol. Appl. Neurobiol.* **30**, 615–623 (2004).
- Raymond, G.V., Bauman, M.L. & Kemper, T.L. Hippocampus in autism: a Golgi analysis. *Acta Neuropathol.* **91**, 117–119 (1996).
- Penzes, P., Cahill, M.E., Jones, K.A., VanLeeuwen, J.E. & Woolfrey, K.M. Dendritic spine pathology in neuropsychiatric disorders. *Nat. Neurosci.* **14**, 285–293 (2011).
- Hutsler, J.J. & Zhang, H. Increased dendritic spine densities on cortical projection neurons in autism spectrum disorders. *Brain Res.* **1309**, 83–94 (2010).
- Sanders, S.J. *et al.* Multiple recurrent de novo CNVs, including duplications of the 7q11.23 Williams syndrome region, are strongly associated with autism. *Neuron* **70**, 863–885 (2011).

ONLINE METHODS

Animal experiments. All animal experiments were performed in accordance with the animal protection law of Germany and were approved by the local authorities responsible for Universities of Heidelberg and Marburg. For juvenile social isolation, rats were weaned on P21 and subsequently housed in isolation for 4 weeks. Otherwise, rodents were housed under standard cage conditions with food and water *ad libitum* and maintained on a 12 h/12 h light/dark cycle. The miR379–410 conditional knockout allele was generated at Taconic Artemis (Cologne, Germany) according to the strategy presented. At P21, the mice were genotyped with the Kapa mouse Genotyping kit (Kapa Biosystems) and the brains extracted and analyzed by real-time PCR or Hoechst staining.

Novel object recognition. The novel object recognition test was conducted during the light cycle in an open field, using methods previously described⁴⁰. Briefly, rats (P91 ± 6) were first habituated to the open field (60 × 60 × 60 cm; no objects present) by placing them in the box for 20 min. Then, 24 h after the habituation session, the novel object recognition test was conducted, which consisted of three phases: acquisition trial, inter-trial interval and recognition trial. In the acquisition trial, each rat was allowed to freely explore the open field containing two identical sample objects for 5 min. The objects were placed in one of the back corners of the box, with the objects situated 15 cm away from the walls. As objects, either two silver iron cylinders (5 cm in diameter, 8 cm high) or two red metal cubes (5 × 5 × 8 cm) were used in a counterbalanced manner. After the acquisition trial, the rats were returned to their home cages for 30 min, the inter-trial interval. During that time, one clean familiar object and one clean novel object were placed in the open field, where the two identical objects had been located during in the acquisition trial. After the inter-trial interval, each rat was returned to the open field for a 5-min recognition trial, during which time it was allowed to freely explore the familiar object and the novel object. Object investigation was defined as time spent sniffing the object when the nose was oriented toward the object and the nose-object distance was 5 cm or less. Recognition memory was defined as spending significantly more time sniffing the novel object than the familiar object. The memory index was calculated as follows: (Exploration time novel object)/(Exploration time novel object + Exploration time familiar object). Testing was performed under white light of approximately 5 lx. For behavioral analyses, a digital camera was mounted 1.5 m above the floor of the box. All rats were handled for 3 consecutive days in a standardized manner (5 min/d).

DNA constructs. The mouse Ube3a1 and Ube3a2 cDNAs, including coding and UTR sequences, were retrieved from pCMV6 vectors (Origene), cloned, and further subcloned into pGFP-C1 vectors (Clontech). For Ube3a1-fs, a frameshift mutation was inserted into the Ube3a ORF using site-directed mutagenesis (QuickChange). The rat Ube3a1 3' UTR was PCR amplified from P15 forebrain synaptosome cDNA and cloned into pGL3 (Promega) to obtain Ube3a-luc. Limk1-luc and Limk1-m134-luc have been described¹⁷. shRNA sequences were designed using the Dharmacon siRNA online design center and cloned into pSuper (Oligoengine) for transfections or pAM/U6-shRNA eGFP-CBA-hrGFP for infections.

Cell culture, transfection, stimulation and virus infection of primary neurons. Primary cultures of Sprague–Dawley rat (Charles River Laboratories, Sulzfeld, Germany) embryonic hippocampal and cortical neurons (embryonic day 18) were obtained and maintained as described previously¹⁷. Compartmentalized neuron cultures were obtained by plating dissociated hippocampal neurons onto 1- μ m-pore and 30-mm-diameter polyethylene terephthalate (PET) membrane filter inserts (Millipore) that were matrix-coated with poly-L-lysine (Sigma-Aldrich) and laminin (BD Biosciences) on both sides⁴¹. These neurons were treated with 10 μ M 5-fluoro-2'-deoxyuridine from DIV 3 to prevent glial cell proliferation. Neuronal transfections were performed with Lipofectamine 2000 (Invitrogen). A total of 1 μ g DNA per well of a 24-well plate was mixed with a 1:50 dilution of Lipofectamine 2000 in Neurobasal medium, incubated at 20–26 °C for 20 min and then further diluted 1:5 in Neurobasal medium. Neurons were incubated with the transfection mix for 2 h. Primary neurons were infected with rAAV by directly applying the virus in the culture medium. For a 24-well plate, 800,000 neurons per well were spotted with 1.5 μ L 670,000 IFU/ μ L rAAV and incubated for 7 d to obtain maximal expression. For stimulation experiments, cells were treated with either human BDNF (Peprotech, 40 ng/mL) or KCl (Sigma, 16 mM) for the time indicated. HEK293 cells were cultured in MEM medium

(Invitrogen) supplied with 10% (vol/vol) FBS, 1 mM glutamine, 100 units/ml penicillin and 100 μ g/ml streptomycin. HEK293 cells were transfected using the calcium phosphate method. A final CaCl₂ concentration of 0.1 M was used with an incubation time of 6 h.

Quantitative real-time PCR. RNA was purified using Trifast (Peqlab) or the mir-Vana miRNA Isolation Kit (Ambion) and treated with TURBO DNase (Ambion) to remove genomic DNA. Quantitative real-time PCR was performed with a StepOnePlus Real Time PCR System (Applied Biosystems) using iTaq SybrGreen Supermix with ROX (BIO-RAD). Primer sequences are provided below.

Preparation of infectious rAAV. Infectious rAAV was obtained as described previously⁴². Briefly, HEK293 cells were co-transfected 1:1:1 with pAAV-6P-SEWB⁴³ or AAV-6P-SEWB derivatives with helper plasmids (pDP1 and pDP2) using 13 μ g of each plasmid per 15-cm cell culture dish. After 3 d, cells were harvested for virus purification. Cells were resuspended in PO buffer (20 mM Tris, 150 mM NaCl, pH 8.0), lysed by three freeze-thaw cycles and centrifuged to remove cell debris. rAAV was further purified using the iodixanol density step gradient method⁴⁴. Viral titer was assessed by infecting primary cortical neurons with dilutions of the virus and estimating the viral IFU/ μ L using a confocal microscope. All viruses used were diluted so as to have approximately the same IFU/ μ L.

Nucleofection of primary neurons. Primary cortical neurons of rat embryos (E18) were nucleofected using the 4D-Nucleofector kit (Lonza), the P3 Primary Cell solution and program DC-104, according to the manufacturer's instructions.

Intraventricular injection of rAAV. P0 C57BL/6 mice (Charles River Laboratories, Sulzfeld, Germany) were cryoanesthetized and injected with 2 μ L purified rAAV stock into each lateral ventricle (2 mm ventral to the lambda, ± 0.7 mm from the midline, depth 1.8 mm) using a 10- μ L Hamilton syringe. Individual experiments were performed on pups from the same litters, which were previously tattooed on the footpads to identify the groups injected with rAAVs carrying different pAAV-6P-SEWB derivatives. The pups were grouped randomly and the examiner blinded to the conditions until after analysis. Several litters were then pooled to form the final data groups. Following injection, the pups were placed on a 37 °C warming pad and returned to the mother after regaining normal activity and color.

Immunocytochemistry. For immunostaining, hippocampal neurons were fixed for 20 min at 20–26 °C in paraformaldehyde/sucrose, rinsed in PBS and sequentially incubated with primary antibodies and Alexa-conjugated secondary antibodies, both diluted in 0.02% (wt/vol) gelatin–0.5% (vol/vol) Triton X-100–PBS. Four washes with Neurobasal medium were followed by fixation for 15 min in 4% (wt/vol) paraformaldehyde/sucrose. Imaging of GFP fluorescence from GFP-expressing cells was done without antibody amplification. After fixation, coverslips were mounted on microscope slides using AquaPoly/mount (Polysciences Inc.).

Image analysis. All image analysis was performed with the investigator blinded to the experimental conditions.

Dendritic complexity. Images from primary neuron cultures were obtained with a confocal laser scanning microscope (Zeiss LSM5 Pascal) using a 20 \times objective with a resolution of 1,024 × 1,024 pixels, corresponding to an image size of 450 μ m × 450 μ m. Dendritic complexity of pyramidal neurons was assessed by Sholl analysis as previously described¹⁶. Briefly, 10–15 concentric circles at increments of 20 μ m were superimposed on the pictures, centered on the soma. To obtain a Sholl profile of the dendritic arbor, the number of intersection with each circle was counted. A total of at least ten neurons were analyzed in each independent experiment, and averages were calculated on the basis of the values from at least three independent experiments. Images from mouse brain slices were taken with a confocal laser scanning microscope (Leica SP5) using a 40 \times objective at a resolution of 1,024 × 1,024 pixels, corresponding to an image size of 387.5 × 387.5 μ m; the pinhole was set to 1.2 Airy units and the interval to 1.19 μ m.

Dendritic spines. For the analysis of dendritic spines, z-stacks (seven consecutive 0.49-nm optical sections per stack) of images from dissociated primary hippocampal neurons were taken (Zeiss LSM5 Pascal) with a 63 \times objective

at $1,024 \times 1,024$ pixels, with a zoom factor of 1.7 for an image size of $144.7 \mu\text{m} \times 144.7 \mu\text{m}$. Spine volumes were subsequently analyzed with ImageJ software as described¹⁷. For each independent experiment, 12 neurons for condition were selected.

Electrophysiology. Miniature excitatory postsynaptic currents (mEPSCs) were recorded in whole-cell voltage-clamp mode using an EPC-10 patch-clamp amplifier and PATCHMASTER software (HEKA Elektronik, Lambrecht, Germany). Dissociated hippocampal neurons were transfected with the indicated shRNA expression vectors on DIV 12–13 and mEPSCs were measured on DIV 18–21. Cells were recorded from three independent experiments (control shRNA: $n = 15$ neurons in total; Ube3a1 shRNA: $n = 12$ neurons in total). For recordings, neurons were perfused at 20–26 °C with a bath solution containing (in mM) 140 NaCl, 2.8 KCl, 2 CaCl₂, 1 MgCl₂, 10 glucose and 10 HEPES (pH 7.3 with NaOH, 300–310 mOsm) with bicuculline (20 μM) and tetrodotoxin (1 μM). Patch pipettes contained (in mM) 120 potassium gluconate, 15 KCl, 5 NaCl, 10 HEPES, 2 MgCl₂, 10 EGTA, 4 Mg-ATP and 0.1 Na-GTP (pH 7.3 with KOH, 290–300 mOsm) and had resistances of 4–5.5 M Ω . Neurons were held at -70 mV and data were acquired for total of 15 min at a sampling rate of 20 kHz and filtered at 3 kHz. Series resistance was monitored every 5 min and cells with uncompensated series resistance of <21 M Ω were accepted. Offline analysis of mEPSCs was done with the Mini Analysis software (Synaptosoft Inc.) for 100–300 s from the last 5 min of current recordings (threshold: -5 pA, filter: 2 kHz), with the investigator blinded to the experimental conditions.

Luciferase reporter assay. Primary neurons were transfected in duplicate with 50 ng of pGL3-Ube3a1 or pGL4-PEST-Creb1 or 75 ng pGL4-PEST-Limk1 firefly reporter constructs and equal amounts of empty *Renilla* luciferase reporter as a transfection control. pGL3-Ube3a1 was transfected alone or with 30 nM of the appropriate pLNA (Exiqon) or 10 nM miRNA mimic (miR-134: IDT; other miRNAs: Ambion). pGL4-PEST-Limk1 or pGL4-PEST-Creb1 was transfected alone or with 5 ng of the relevant pSuper shRNA construct. Luciferase assays were performed using the Dual-Luciferase reporter assay system (Promega) on the GloMax R96 Microplate Luminometer (Promega).

Western blotting. Western blotting was performed as described previously⁴⁵. The following primary antibodies were used: mouse anti-Ube3a (aa501-712, Becton Dickinson, 1:1,000 dilution), rabbit anti-Pum2 (1:4,000 dilution, Novus Biologicals), rabbit anti-tubulin (1:7,500 dilution, Cell Signaling), mouse anti-Creb1 (1:1,000 dilution, Cell Signaling), rabbit anti-GFP (1:5,000 dilution, Life Technologies), mouse anti-Limk1 (1:200 dilution, BD Transduction Laboratories). Primary antibodies were recognized by either a horseradish peroxidase (HRP)-conjugated goat anti-rabbit antibody (1:20,000; Calbiochem) or an HRP-conjugated rabbit anti-mouse antibody (1:20,000; Calbiochem). Secondary antibodies were detected by enhanced chemiluminescence with the ECL Plus Western Blotting Detection System (GE Healthcare).

High-resolution fluorescence in situ hybridization (FISH). Dissociated hippocampal neurons were co-transfected at DIV 14 with 200 ng pGL4-Ube3a1 and 100 ng *Discosoma sp.* red fluorescent protein (DsRed) plasmid and fixed at DIV 19 using 4% (wt/vol) paraformaldehyde/4% (wt/vol) sucrose/PBS for 30 min at 20–26 °C. FISH was performed using the QuantiGene (QG) ViewRNA kit (Affymetrix) according to the manufacturer's protocol (with slight modifications) using probes directed against the Ube3a1 3' UTR, Ube3a2 3' UTR and Camk2a (positive control). A probe directed against the bacterial transcript DapB served as negative control. To preserve dendrite morphology, protease was either omitted (no-protease condition) or used at a dilution of 1:10,000 for 1 min (protease condition). After completion of the FISH protocol, cells were washed with PBS, preblocked in gelatin detergent buffer and processed for MAP2 immunostaining as described above. For z -stack images, five consecutive optical sections were taken at 0.4- μm intervals with a resolution of $1,024 \times 1,024$ pixels on a Leica SP5 confocal microscope using a 63 \times objective and a 3 \times digital zoom.

Synaptosome preparation. Synaptosomes were prepared from P15 Sprague-Dawley rat pups as previously described⁴⁶.

RNAseq analysis of rat hippocampal neurons. Reads were mapped to rn5 using STAR (version 2.4.0g1)⁴⁷ with the following flags:

```
STAR --readFilesIn FASTQ --genomeDir RN5 --outFilterType BySJout --outFilterMultimapNmax 2 --outFilterMismatchNmax 3 --outSAMstrandField intronMotif --outFilterIntronMotifs RemoveNoncanonical --outSAMtype BAM SortedByCoordinate --sjdbGTFfile ENSEMBL.genemodels.rn5.gtf
```

On the basis of a high sequence duplication level, we removed the PCR duplicates using Picard (version 1.105) with the following flags:

```
java -jar MarkDuplicates.jar INPUT=IN.BAM OUTPUT=OUT.BAM METRICS_FILE=STATS.TXT REMOVE_DUPLICATES=true
```

The resulting bam files were merged to one file per species using Samtools⁴⁸ and IGV-snapshots⁴⁹ were taken at the *Ube3a* genomic location (rn5:chr1:117746227–117843011).

Absolute quantification of mRNA. Standard curves were obtained from serial dilutions (100-fold) of plasmid DNA (stock 1 ng/ μl) containing the sequence of the gene of interest. The following plasmids were used: pGL4-Ube3a1, pcDNA.3-Limk1, Pum2-YFP. A slope of the standard curve was calculated by regression analysis and subsequently used for the calculation of RNA molecules/ng total RNA equivalent.

Statistics. *P*-values were calculated with Student's *t*-test (two-tailed, type 2) for one-way comparisons and with ANOVA followed by *post hoc* test (Student's *t*-test, two-tailed, type 2) for multi-way comparisons.

Power analysis (G-power) was performed to calculate required sample size. For most experiments, effect size was sufficiently high to use $n = 3$. Otherwise (Figs. 2g,h, 5g and 6a,b,d,f,g), larger sample sizes were used. The result of the power analysis was specifically reported for Figure 6d,g (see figure legend). The experiments were not done with the experimental conditions blinded to the investigator, with the exception for the analysis of microscopy data and patch-clamp recordings.

In the animal studies, the animals were assigned to the various groups randomly. In imaging studies, cell selection was performed randomly, excluding unhealthy cells and cells not easily identified as pyramidal neurons. Data were collected and processed randomly.

Data distributions were assumed to be normal, but this was not formally tested unless otherwise stated.

A **Supplementary Methods Checklist** is available.

Oligonucleotide sequences. Real-time qRT-PCR:

```
Gapdh fw: GCCTTCTCTGTGACAAAGTGGAA
Gapdh rev: CCGTGGGTAGAGTCATACCTGGAA
Ube3a1 fw: GGACCTGGCATCACCCATCA
Ube3a1 rev: ATTCCATTGAGGCTTTCCTATT
Ube3a2/3 fw: TTATTACTGCTTGAGGTTGAGCCTT
Ube3a2/3 rev: AAGATTACATGGTCTACAAATG
Rnu6 fw: CTCGCTTCGGCAGCACA
Rnu6 rev: AACGCTTACGAATTTGCGT
Creb1 fw: TCAGCCGGGTACTACCATTG
Creb1 rev: TTCAGCAGGCTGTGTAGGAA
Arc fw: TGGAGCACGTACGGAGGAC
Arc rev: CTCTCGCTCCACCTGCTTG
H1f0 fw: ACGGACCACCCCAAGTATTCAG
H1f0 rev: GGCCTTCTACCCACCTTGTA
Pre-miR-134 fw: TGTGACTGGTTGACCAGAGGG
Pre-miR-134 rev: GGTGACTAGGTGGCCACAG
Limk1 fw: CCTCCGAGTGGTTTGTGCGA
Limk1 rev: CAACACCTCCCCATGGATG
Fmr1 fw: CAAAGCGAGCCACATGTTA
Fmr1 rev: GGCAAGCTGCCTTGAACCTT
shRNA (targeting sequence):
Control shRNA: AAACCTTGTGGCTCCTTAGG
Ube3a1 shRNA: CATGCAGTCTAATGCTTTA
Ube3a2/3 shRNA: AGGGATAATTTGATGGTAA
Ube3a coding sequence shRNA: AGAAGAACTACAGAGTAT
Drosha shRNA: CAACATAGACTACACGATT
Tnrc6c shRNA: GGTTC AAGCACAGCTTTTG
```

Mutagenesis primers:

Ube3a1 shRNA-resistant fw: TTCCAATTTTCATGCAGTCTAACGCGTAA
TTTCATGAATTAATG

Ube3a1 shRNA-resistant rev: CATTTAATTCATGAAATTACGCGTTAGA
CTGCATGAAAATTGGAA

Genotyping primers:

A: 169–379lox-fw: GCCACTGCTTACTCTCATCTGC

B: 170–379lox-rev: CCGTATTATCCCATCAAGTAGC

C: 171–410lox-fw: CCAGATGTGCAATGGATGG

D: 173–410lox-rev: AAAGAGAGGTGACCATGCACTG

Antibodies. Mouse anti-Ube3a monoclonal antibody, BD Transduction Laboratories 611416

Chicken anti-GFP polyclonal antibody, Abcam 13970

Mouse anti- β -actin monoclonal antibody, clone AC-15, Sigma Aldrich A5441

Rabbit anti-tubulin monoclonal antibody, Cell Signaling 2125

Rabbit anti-GFP monoclonal antibody, Life Technologies G10362

Rabbit anti-Pumilio 2 polyclonal antibody, Novus Biological NB100-387

Mouse anti-CREB monoclonal antibody, Cell Signaling 9104

Mouse anti-LIMK1 monoclonal antibody, clone 42/LIMK1, aa.232–333, BD Transduction Laboratories 611749

Mouse anti-MAP2 monoclonal antibody, Sigma M9942

Rabbit anti-GFAP polyclonal antibody, DAKO Z033401

Rabbit anti-mouse IgG–HRP, Merck-Millipore 402335

Goat anti-rabbit IgG–HRP, Merck-Millipore 401315

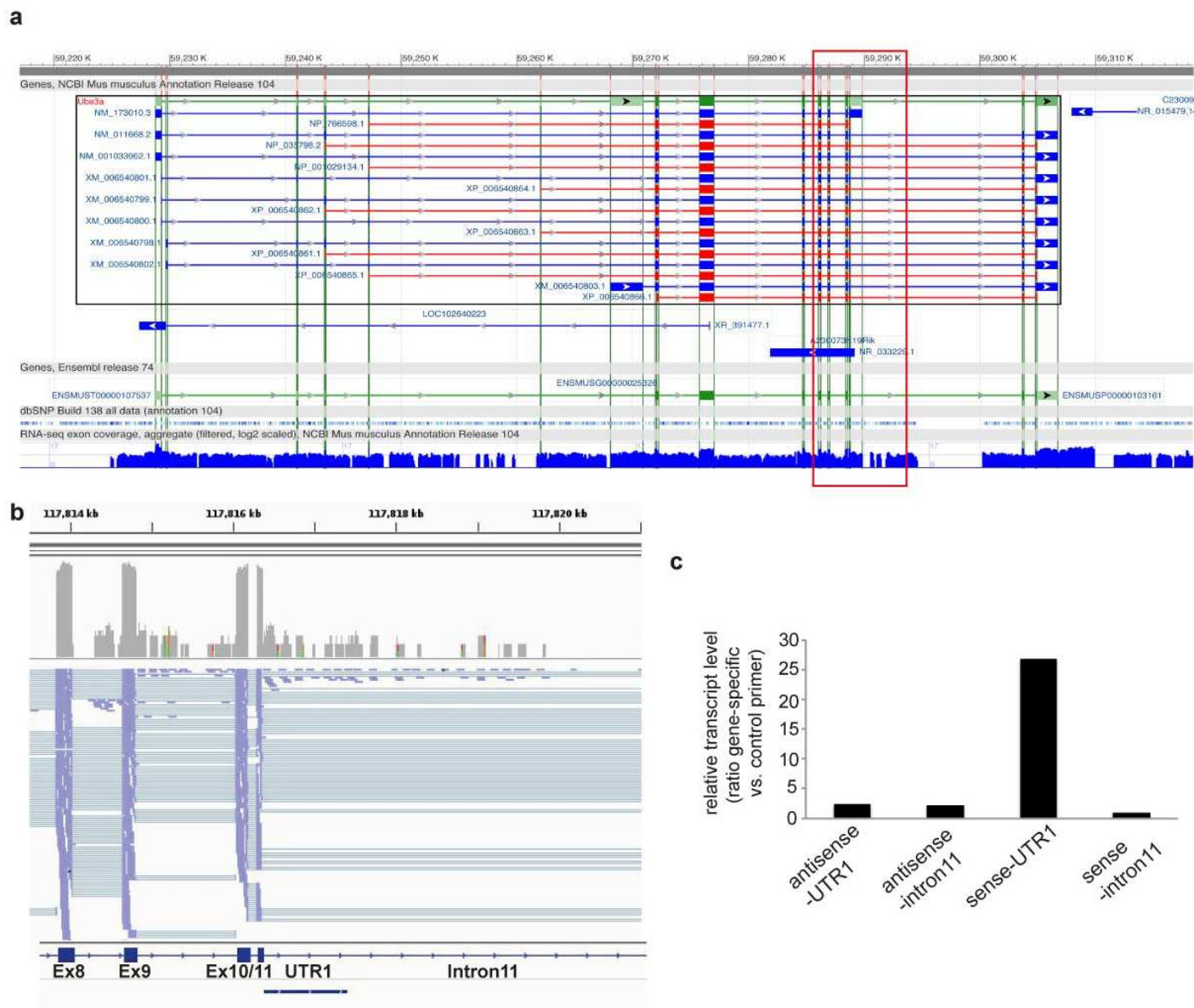
Donkey anti-mouse IgG–Alexa Fluor 546, Life Technologies A10036

Donkey anti-rabbit IgG (H+L)–Alexa Fluor 488, Life Technologies A-21206

Donkey anti-mouse IgG (H+L)–Alexa Fluor 647, Life Technologies A-31571.

40. Bevins, R.A. & Besheer, J. Object recognition in rats and mice: a one-trial non-matching-to-sample learning task to study 'recognition memory'. *Nat. Protoc.* **1**, 1306–1311 (2006).
41. Poon, M.M., Choi, S.H., Jamieson, C.A., Geschwind, D.H. & Martin, K.C. Identification of process-localized mRNAs from cultured rodent hippocampal neurons. *J. Neurosci.* **26**, 13390–13399 (2006).
42. Christensen, M., Larsen, L.A., Kauppinen, S. & Schratt, G. Recombinant adeno-associated virus-mediated microRNA delivery into the postnatal mouse brain reveals a role for miR-134 in dendritogenesis *in vivo*. *Front. Neural Circuits* **3**, 16 (2010).
43. Shevtsova, Z., Malik, J.M., Michel, U., Bahr, M. & Kugler, S. Promoters and serotypes: targeting of adeno-associated virus vectors for gene transfer in the rat central nervous system *in vitro* and *in vivo*. *Exp. Physiol.* **90**, 53–59 (2005).
44. Zolotukhin, S. *et al.* Recombinant adeno-associated virus purification using novel methods improves infectious titer and yield. *Gene Ther.* **6**, 973–985 (1999).
45. Siegel, G. *et al.* A functional screen implicates microRNA-138-dependent regulation of the depalmitoylation enzyme APT1 in dendritic spine morphogenesis. *Nat. Cell Biol.* **11**, 705–716 (2009).
46. Schratt, G.M., Nigh, E.A., Chen, W.G., Hu, L. & Greenberg, M.E. BDNF regulates the translation of a select group of mRNAs by a mammalian target of rapamycin-phosphatidylinositol 3-kinase-dependent pathway during neuronal development. *J. Neurosci.* **24**, 7366–7377 (2004).
47. Dobin, A. *et al.* STAR: ultrafast universal RNA-seq aligner. *Bioinformatics* **29**, 15–21 (2013).
48. Li, H. *et al.* The Sequence Alignment/Map format and SAMtools. *Bioinformatics* **25**, 2078–2079 (2009).
49. Thorvaldsdóttir, H., Robinson, J.T. & Mesirov, J.P. Integrative Genomics Viewer (IGV): high-performance genomics data visualization and exploration. *Brief. Bioinform.* **14**, 178–192 (2013).

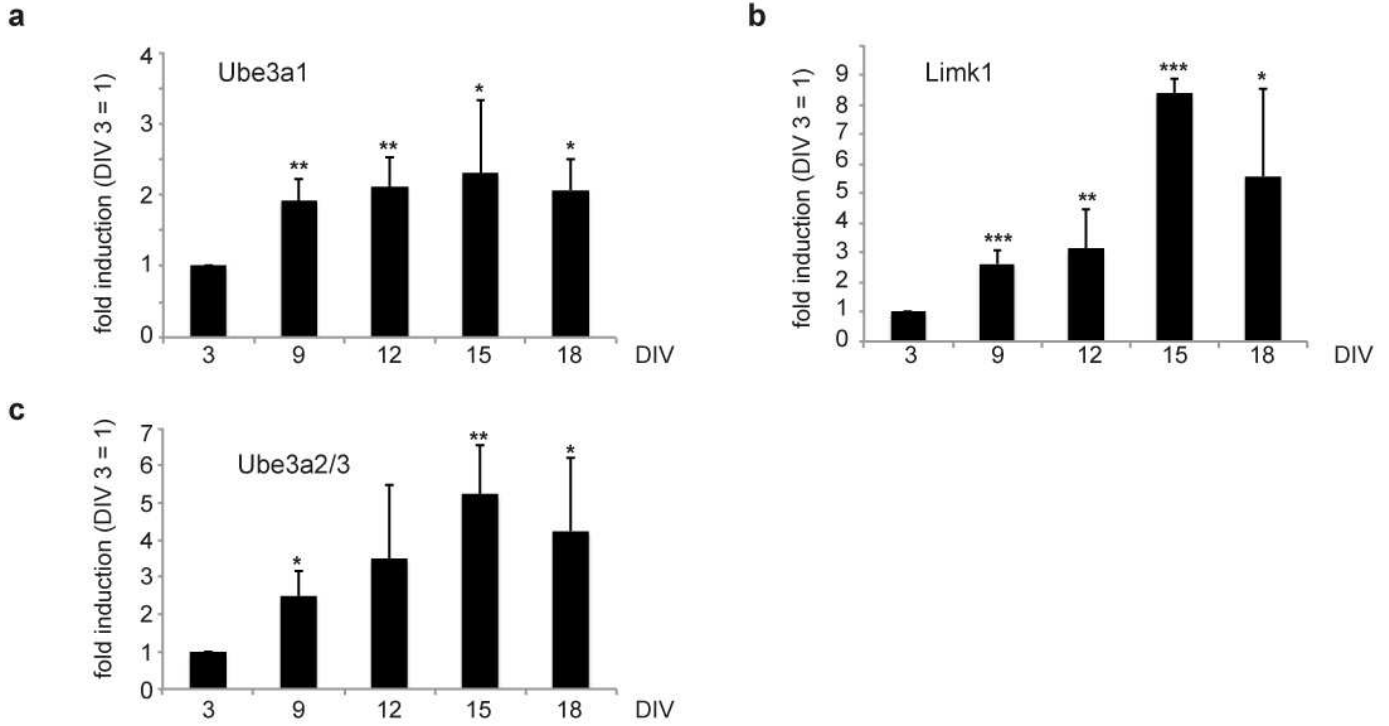
Supplementary figures



Supplementary Figure 1

Ube3a1 RNA expression analysis by RNA sequencing.

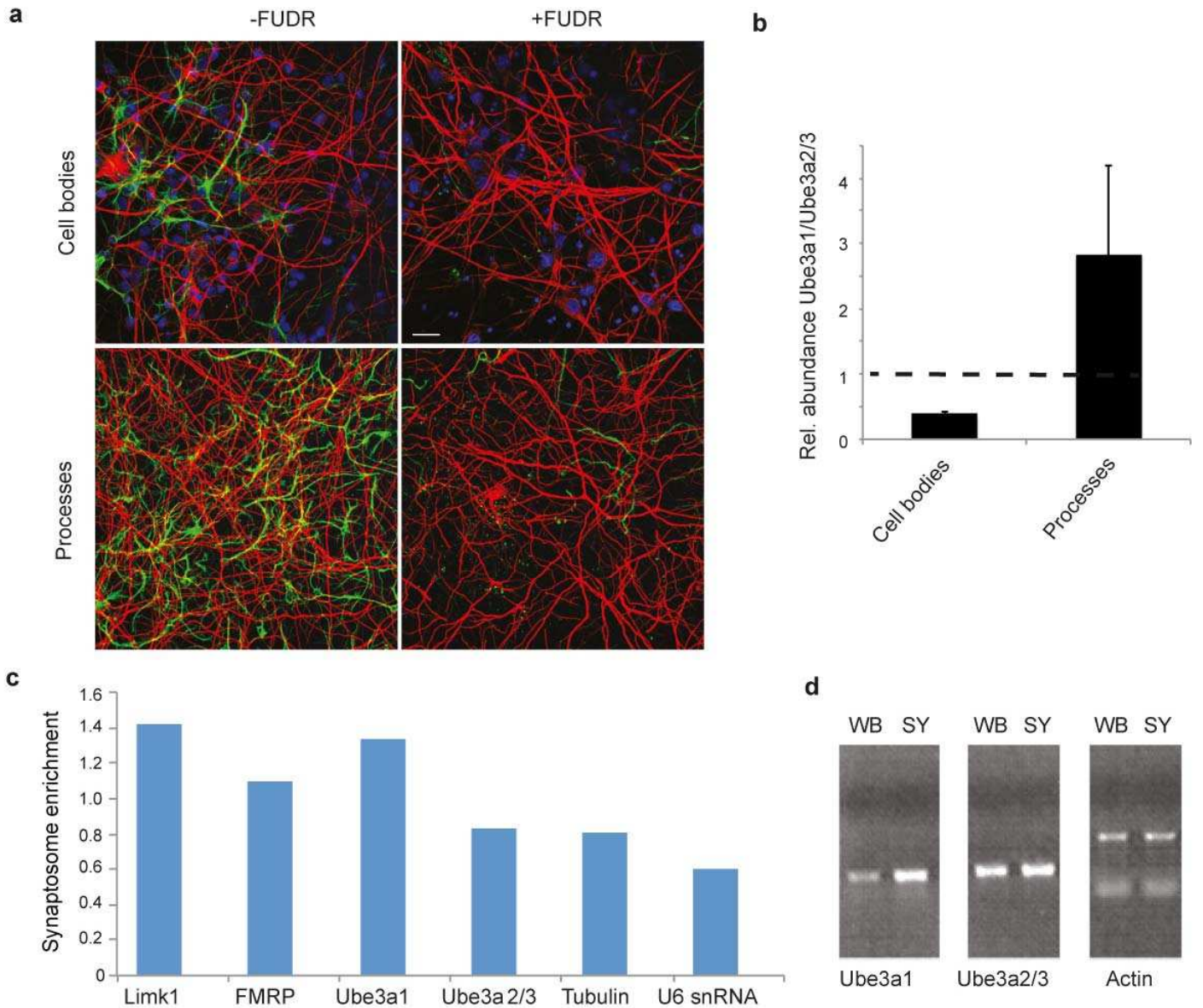
a) Genomic view (UCSC genome browser) of the murine *Ube3a* locus including alternative *Ube3a* transcripts. The region surrounding the *Ube3a* 3'UTR is boxed. Note the presence of sequence reads in the aggregate RNA-seq exon coverage panel at the genomic location of the *Ube3a* 3'UTR. b) Representation of sequence reads at the location of the *Ube3a* 3'UTR (boxed region in a) from rat hippocampal neurons according to ribo-minus RNA sequencing. The position of *Ube3a* exons 9-11, intron 11 and the UTR1 is indicated. c) Strand-specific qPCR analysis of 3'UTR1 or intron11 containing transcripts in either antisense (as) or sense orientation.



Supplementary Figure 2

Developmental expression of Ube3a1 RNA.

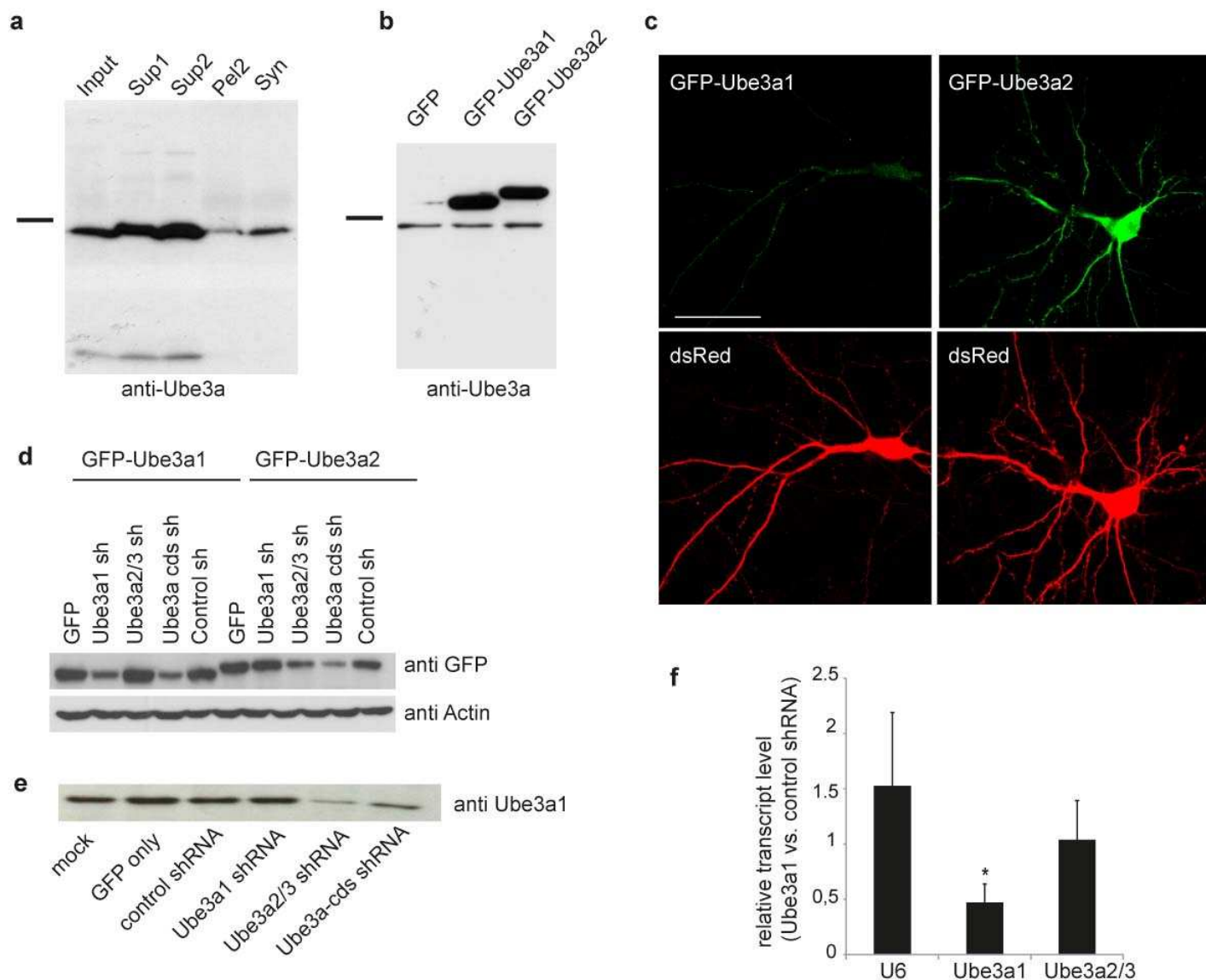
qPCR analysis of Ube3a1 RNA (a), Limk1 mRNA (b) Ube3a2/3 mRNA (c) expression from developing primary rat hippocampal neurons. Values are presented relative to expression at 3 DIV. N=3-5. *p<0.05, **p<0.01, ***p<0.001 (T-test).



Supplementary Figure 3

Subcellular expression of Ube3a1 RNA

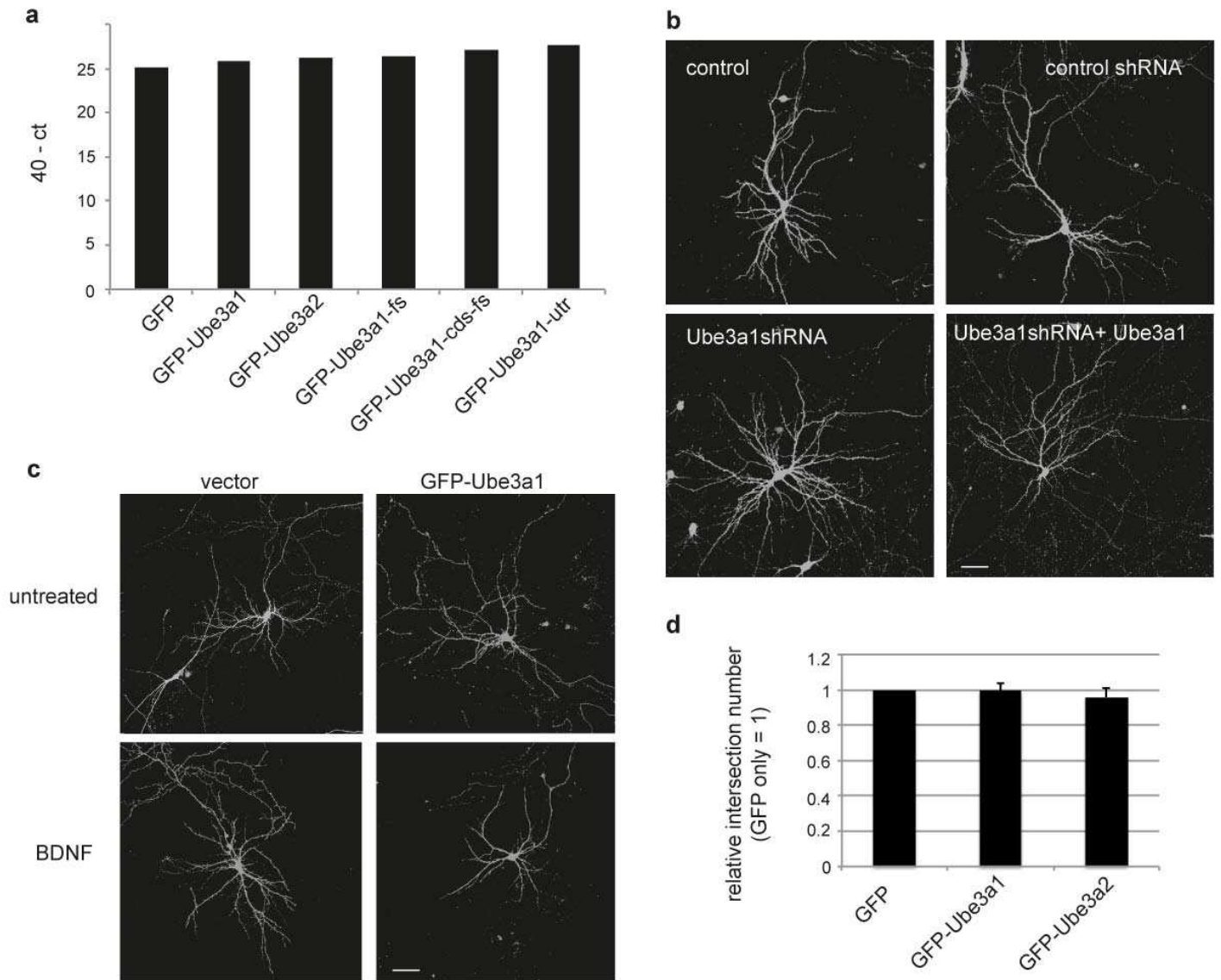
a) Representative immunofluorescence analysis of cell body (upper panel) or process (lower panel) compartments from standard (left panel) or FUDR-treated (right panel) compartmentalized hippocampal neuron cultures, stained with anti-GFAP (green), anti-MAP2 (red) or Hoechst (blue). Scale bar = 50 μ m. b) qPCR analysis of Ube3a1 and Ube3a2/3 with RNA from cell bodies and processes of compartmentalized hippocampal neuron cultures. Bar graphs represent the average ratio of Ube3a1 to Ube3a2/3 RNA levels from three independent preparations \pm SD. c) qPCR analysis of indicated RNAs in rat P15 forebrain synaptosomes. Values are presented relative to a whole forebrain control sample. d) Conventional RT-PCR analysis of P15 whole rat forebrain (WB) and synaptosomes (SY) with primers directed against the indicated transcripts.



Supplementary Figure 4

Ube3a protein expression and knockdown validation.

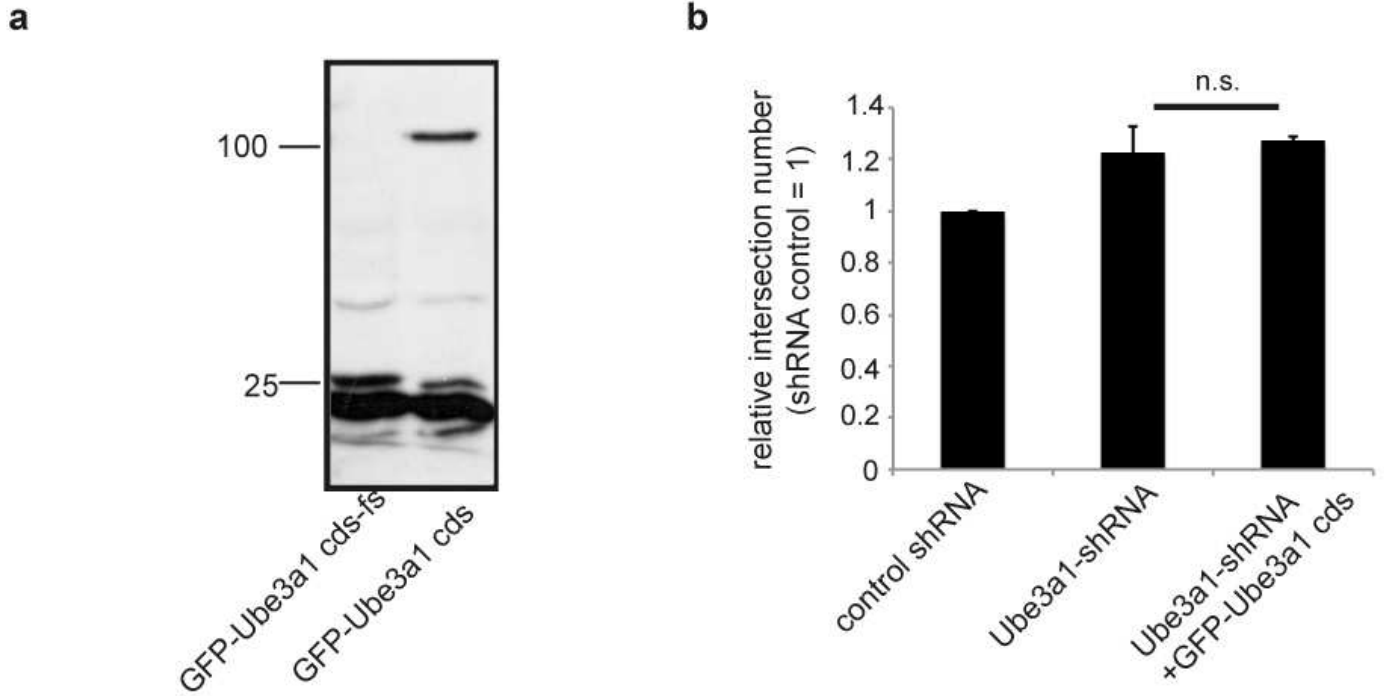
a) Different fractions from a rat P15 forebrain synaptosome preparation were used for Western blotting with a monoclonal mouse anti-Ube3a antibody (Becton Dickinson) which recognizes aa. 501-712 of mouse Ube3a. Marker lane indicates 100 kD. Sup: supernatant; Pel: pellet; Syn: synaptosomes. b) HEK293 cells were transfected with the indicated constructs and analyzed for the expression of GFP-Ube3a-fusion proteins by Western blotting using the anti-Ube3a antibody described in a). c) Primary rat hippocampal neurons (13-18 DIV) were co-transfected with *GFP-Ube3a*-fusion constructs and dsRed and analyzed by confocal microscopy. Scale bar = 50 μ m. d) HEK293 cells were co-transfected with GFP-Ube3a-fusion and indicated shRNA constructs. Expression was assessed by Western blotting using an anti-GFP antibody and an anti-Actin antibody as a loading control. e) Primary rat hippocampal neurons (10-18 DIV) were infected with rAAV expressing the indicated shRNA constructs. Expression of endogenous Ube3a protein was measured by Western blotting using an anti-Ube3a antibody that recognizes the common Ube3a N-terminus. anti- β -actin Western served as a loading control. f) qRT-PCR analysis of indicated RNAs from hippocampal neurons infected with rAAV-Ube3a1-shRNA or rAAV-control-shRNA. Values were normalized to Gapdh expression and are presented as the ratio of Ube3a1 vs. control shRNA infected neurons \pm SD. N=4 (ANOVA $p=0.015323$; * $p<0.05$ (post-hoc T-test)).



Supplementary Figure 5

Regulation of dendritogenesis by GFP-Ube3a1 and GFP-Ube3a2.

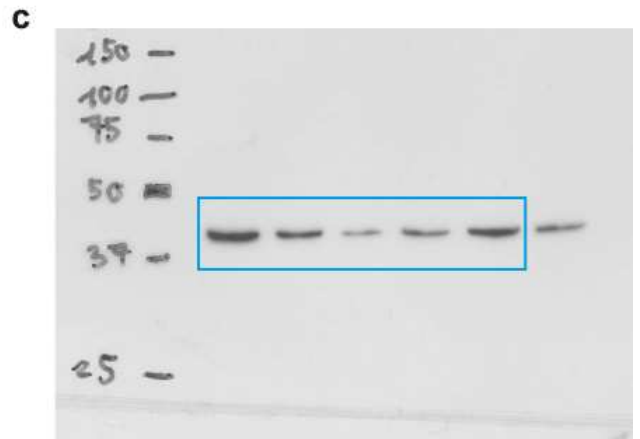
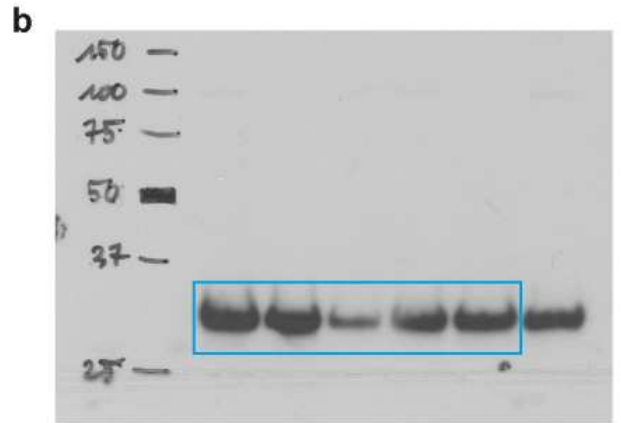
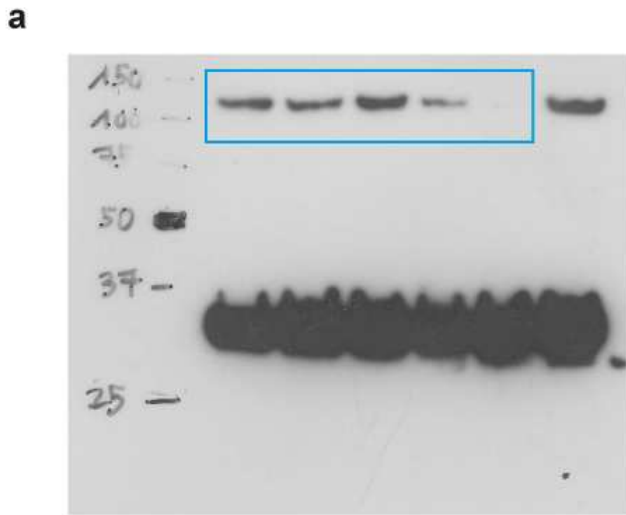
a) qPCR analysis of GFP RNA expression in primary cortical neurons that had been nucleofected with the indicated GFP-Ube3a-fusion constructs. Values are presented as 40-ct and are representative for multiple independent experiments. b) Representative images of primary hippocampal neurons (DIV 13 - 18) transfected with the indicated shRNA and *Ube3a1* expression constructs. c) Representative images of primary hippocampal neurons (DIV 7 - 10) transfected with the indicated expression vectors and treated with BDNF (40 ng/ml) for 48 hours prior to fixation. Scale bar = 50 μ m. d) Quantification of dendrite complexity in neurons transfected with the indicated GFP expression plasmids. Values are presented relative to GFP-only transfected neurons. n=3.



Supplementary Figure 6

The Ube3a1 coding sequence (cds) is not involved in dendritogenesis.

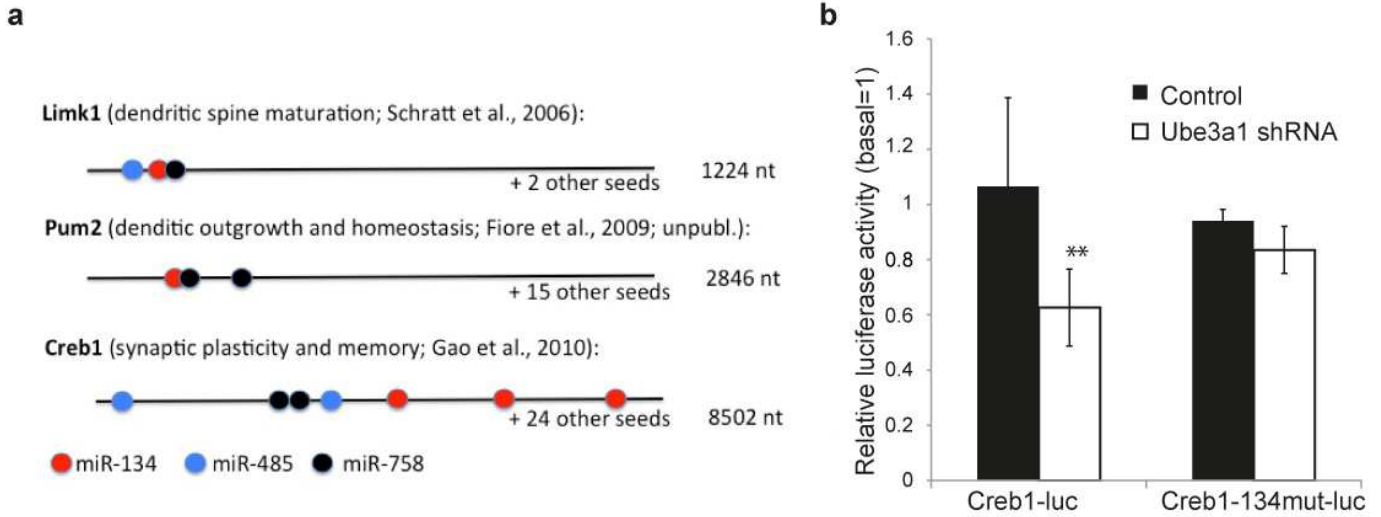
a) anti-GFP Western blot with lysates from HEK293 cells transfected with the indicated *GFP-Ube3a*-fusion constructs. b) Quantification of dendrite complexity in neurons transfected with the indicated shRNA and *Ube3a1* expression constructs. Values are presented relative to control shRNA transfected neurons. N=3. n.s.: not significant.



Supplementary Figure 7

Full-length blots related to **Figure 4a**.

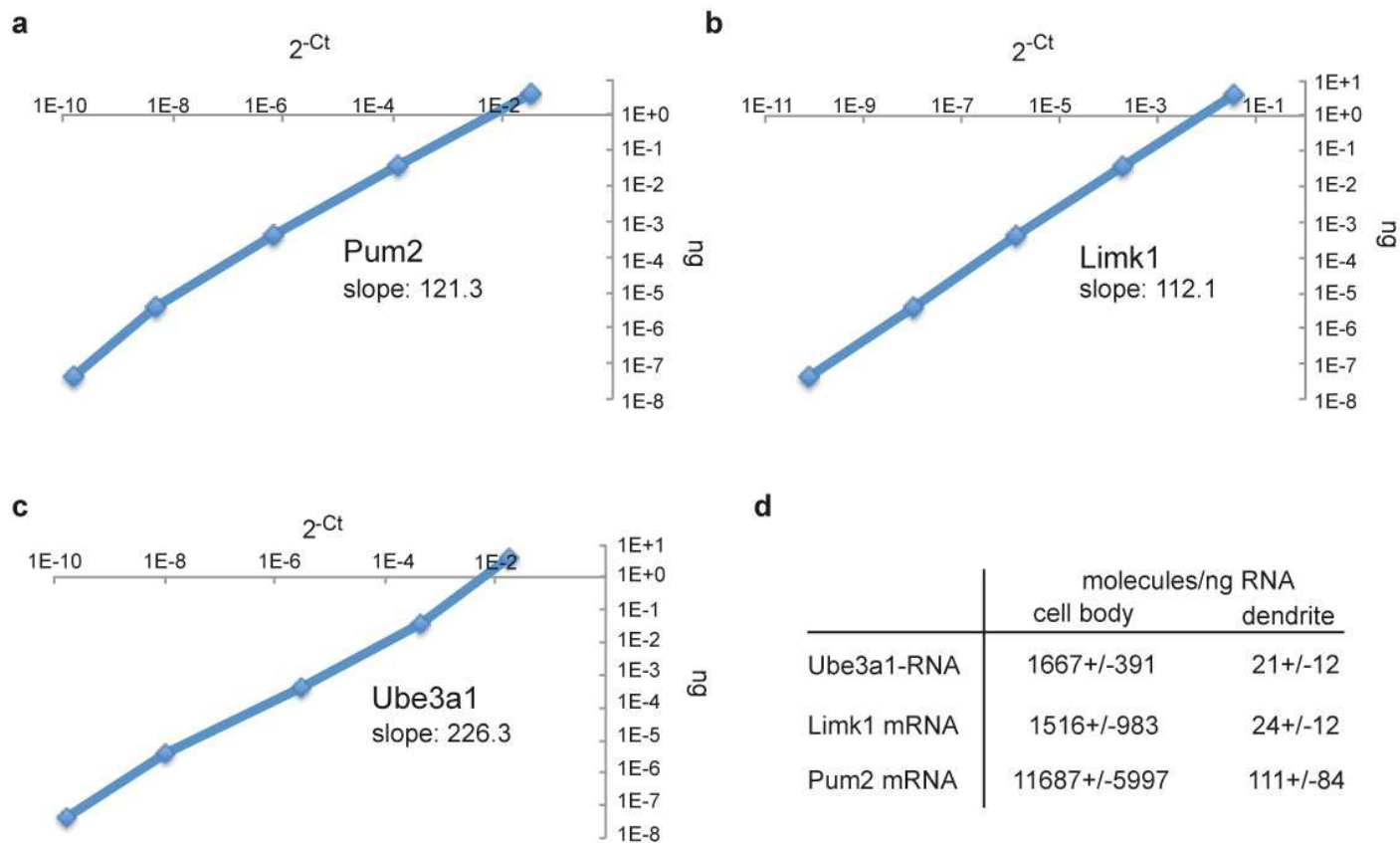
a) GFP-Drosha. b) GFP. c) beta-Actin. Boxes indicate regions of the blot presented in Fig. 4a. Additional band in a) represents overexposed GFP signal.



Supplementary Figure 8

Ube3a1 ceRNA function.

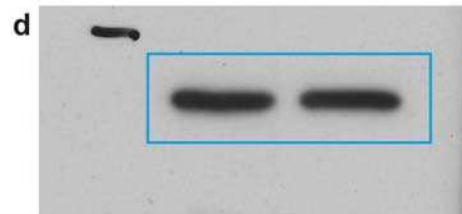
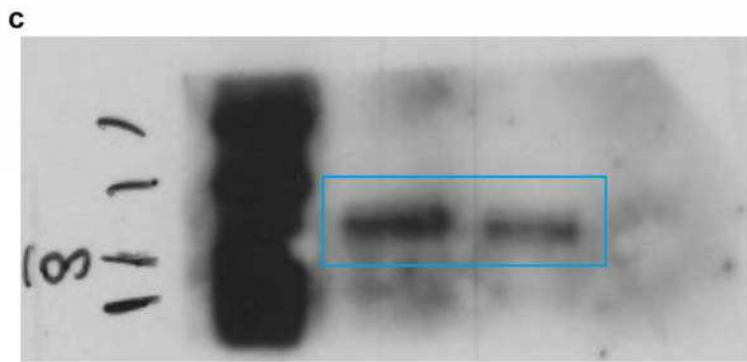
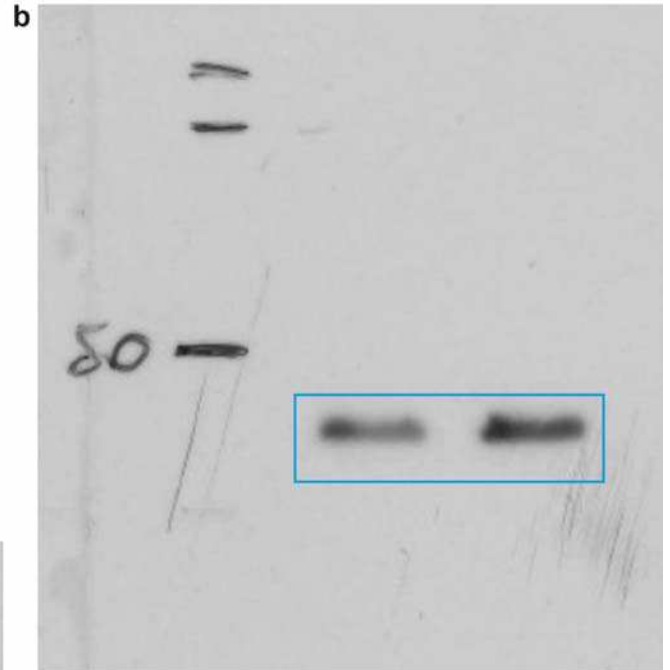
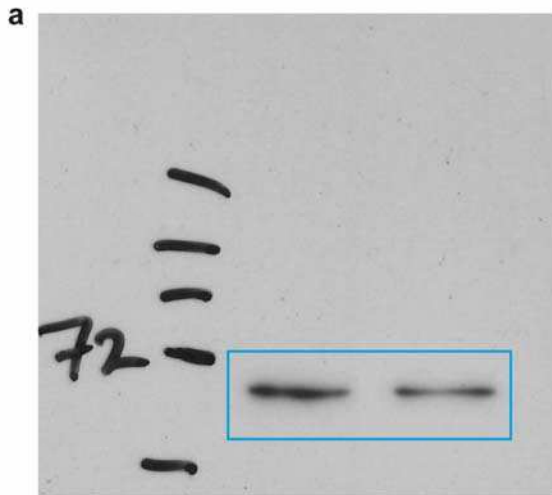
a) Schematic representation of rat 3'UTRs for known miR-134 target mRNAs. Putative binding sites predicted by TargetScan (www.targetscan.org) for miR-134, miR-485 and miR-758 are marked by colored circles. The total number of additional miR379-410 seed matches is indicated. UTRs are not drawn to scale. b) Luciferase assay in primary hippocampal neurons co-transfected with *Creb1-luc* reporters and indicated shRNAs. Values are relative to reporter expression under basal conditions. N=7 (*Creb1-luc*). N=4 (*Creb1-m134-luc*). **p<0.01 (T-test).



Supplementary Figure 9

Quantitative PCR of miR-134 target mRNAs in neuronal cell bodies and dendrites.

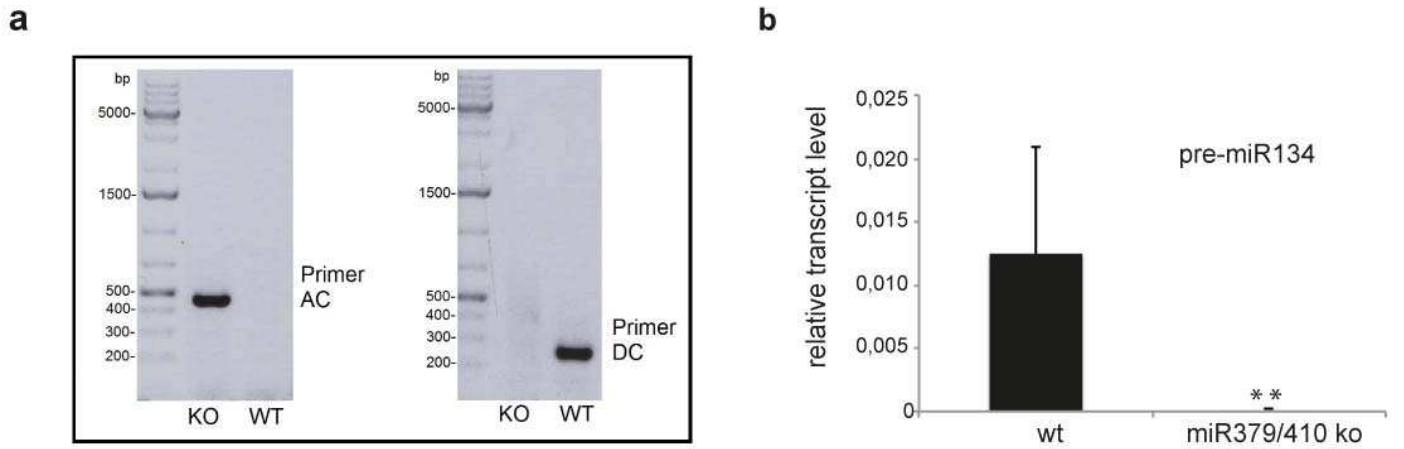
a-c) Standard curves with indicated amounts of plasmids containing *Pum2* (a), *Limk1* (b) and *Ube3a1* (c) sequence. The slope of a regression curve based on measured Ct-values is indicated in each diagram. d) Calculated RNA molecules per ng total RNA isolated from either the cell body or dendrite compartment of FUDR-treated hippocampal neurons (DIV 18) cultured on filter insets. Results from three independent experiments \pm SD are shown.



Supplementary Figure 10

Full-length blots related to **Figure 5f**.

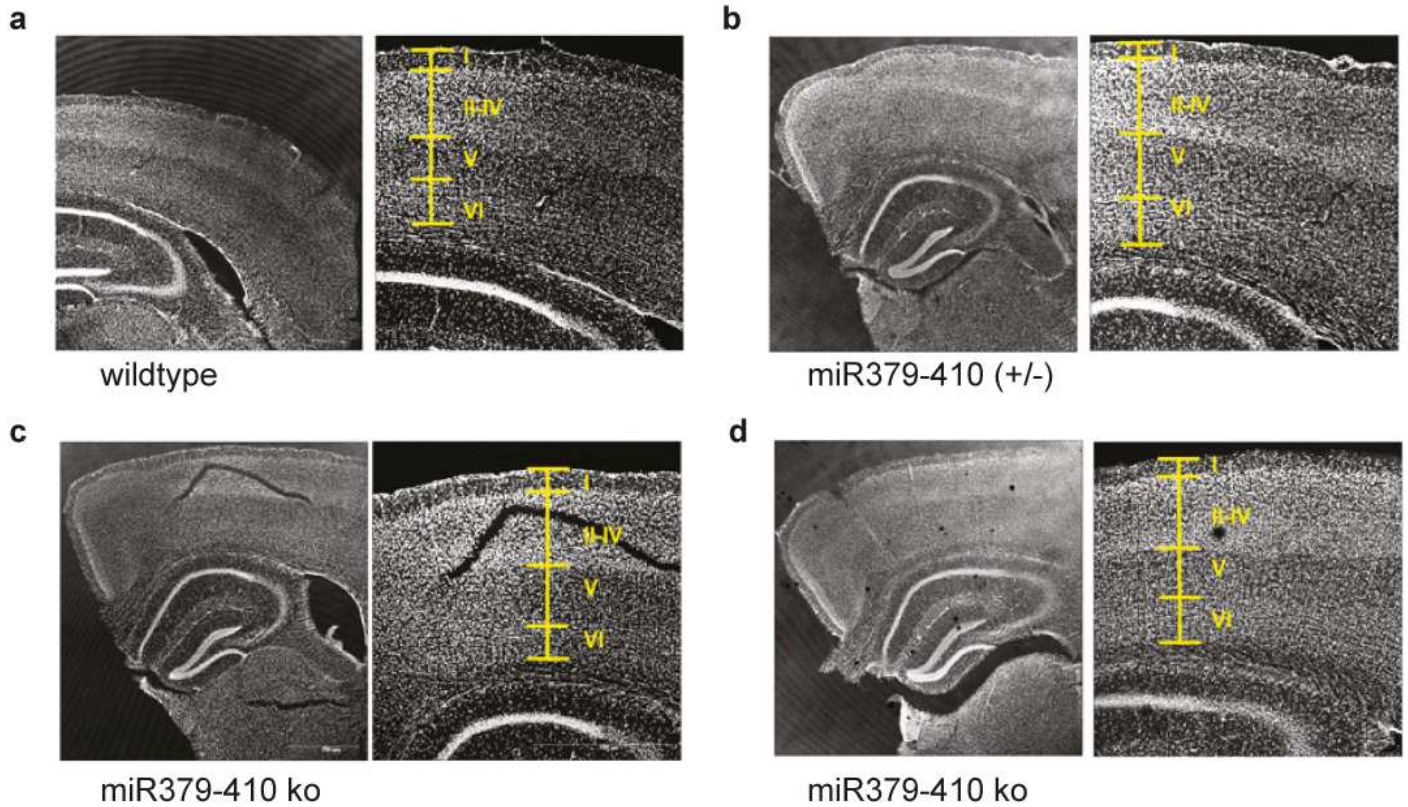
a) Limk1. b) Creb1. c) Pum2. d) Tubulin. Boxes indicate regions of blot presented in Fig. 5f. Membranes were cut after blotting to simultaneously probe for proteins running at different molecular weights.



Supplementary Figure 11

Genotyping and validation of *miR379-410*^{-/-} mice.

a) Genotyping PCR of *miR379/410*^{-/-} (KO) and wild-type (WT) mice using the indicated primer pairs. b) qPCR analysis of pre-miR-134 expression in wild-type (wt; n=7) and *miR379/410*^{-/-} mice (ko; n=7). **p<0.01.

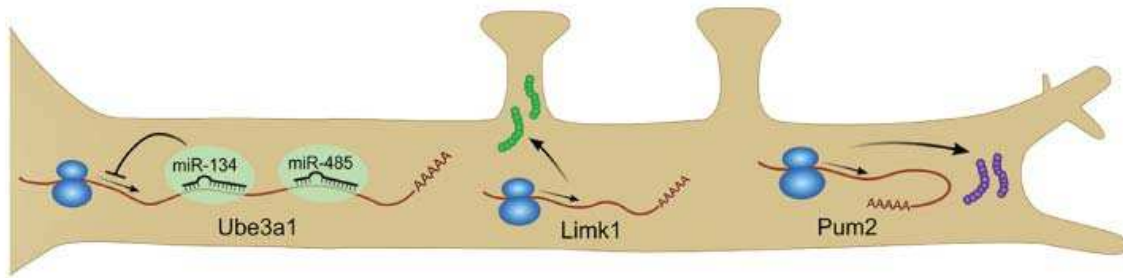


Supplementary Figure 12

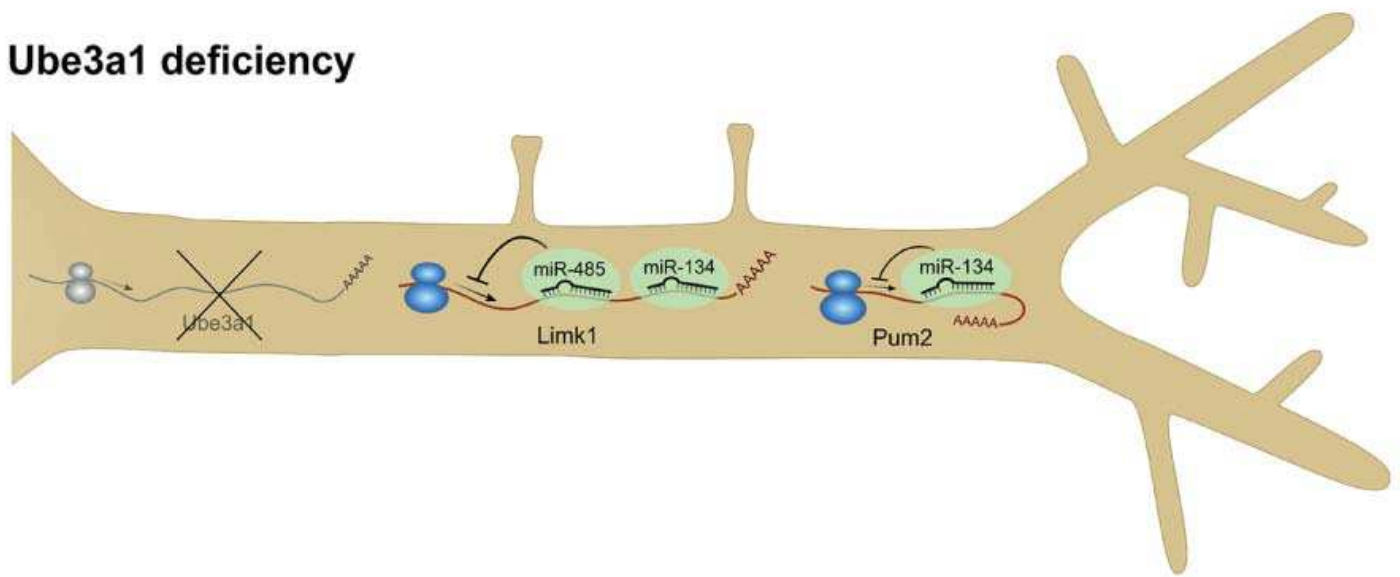
Normal cortical layering in *miR379-410*^{-/-} (ko) mice.

Coronal brain sections (80 μm, single hemisphere) of 8-weeks old wildtype (a), *miR379-410*^{+/-} (b) or *miR379-410*^{-/-} (ko; c, d) mice stained with nuclear Hoechst dye. The positions of cortical layers I-VI are indicated in the higher magnification images (right panels). No differences were observed in the general organization of the cerebral cortex or hippocampus.

normal Ube3a1 expression



Ube3a1 deficiency



Supplementary Figure 13

Model for the ceRNA function of Ube3a1 during dendritic development.

During normal activity-dependent neuronal development, Ube3a1 RNA levels steadily increase, resulting in the sequestration of dendritic miRNAs from the miR379-410 cluster, including miR-134 and miR-485. This releases protein-coding targets of these miRNAs, such as Limk1 and Pum2 mRNA, from translational repression, thereby leading to enhanced local synthesis of Limk1 and Pum2, which in turn promotes spine growth and inhibits dendrite elaboration, respectively. In conditions of Ube3a1 RNA deficiency, spine growth is suppressed whereas the brake on dendrite elaboration is loosened.

Table 1: MMU Ube3a1 3'UTR (mm10, chr.7:59288785-59289818)

GTGTTTAATTCTTAAAAAGGAAGATTTTATTCATCAAACATGTAGATGTGTGCTTT
 TG**TGTCCT**GTATCTGTAGGTACTGGTTACCA**AACAAG**TAAGCTCAAAAATAGACC
 TGTATTAATATTTCCAATTTTCATGCAGTCTAATGCTTTATTTTCATGAATTAATGA
 TTTAAGTCTCATATTT**TCTCAACC**CTTTGCCTTATTTTTGGTCATGTGTAAGATGG
 CACATTATTTAGTCTTTAAGATACTTGGGAAGAACCATGTATACTAGTGATTCTGA
 ACAATTCTTAGGACAGTATTACCACTAACATCGTTCTCTAGTCAAATGCCCTTATT
TCTACTTCTGTAATATGCTACT**TATCCA**ATTCTGAAAGATCTTTCCCCCATCTTCT
AATGTGACTGATCAAAATGCAGAGTAGTCTTTTTGGCATCCA**CTATGAT**GTCATA
 GGTATTTAAACAGTTATCTTTTTGTAGATCACTTGAGCTATAAGACTCAAATATGT
 TAACAATAGAATGAATATTAAGTGTGTCTAGTAATGATACATTATCATTG**TTATATT**
TATATTACAGTATTACTTTATTCATTTAAGTTTGTAGAAGATTACTCTTGCTTTGCC
 CTTTTTTTTTAAATAGAAAAGCAAATATGTTATTTATTCAGCTTTTAGGTAATTTAAA
 TAACAAAATTCAGAGTAAAGCAAACAAAACCATAACATGTCA**TATGAT**ATATCA
 TTTCTAAGCACAATGGCAATTATTAATGAATATAAAAATTTATCATTTCATATTTGCT
 TCTAACACC**AGTCACAA**AAGTG**GCAACCATTATAT**TGCTGCTCAGTTTTAAAGGT
 AATTCATAACAGGGATAAACATGGTAATACAGAAGCCTTAATGGGAATATCCTAG
TATTATCTCTACAATATGGCAAAA**TAATGTT**TTAGATTGAT**TATGATTAATGT**ATG
 CATTGAT**TATTAT**CCT**TTTGTT**ATTGGCAATAGAATTATCATGACAGTGGGGCT
 GTTACA**AATAAAG**TTTTTCATTCTTA

miRNA	SEED Sequence on DNA	Start
>mmu-miR-1197-3p.MIMAT0005858	TGTCCT	59
>mmu-miR-544-5p.MIMAT0017282	AACAAG	88
>mmu-miR-539-5p.MIMAT0003169	TTTCTC	183
>mmu-miR-758-5p.MIMAT0017235	TCAACC	187
>mmu-miR-1197-5p.MIMAT0017331	TCAACC	187
>mmu-miR-411-5p.MIMAT0004747	TCTACT	337
>mmu-miR-376b-5p.MIMAT0003388	TATCCA	358
>mmu-miR-376c-5p.MIMAT0005295	TATCCA	358
>mmu-miR-323-3p.MIMAT0000551	TAATGT	392
>mmu-miR-376b-3p.MIMAT0001092	CTATGA	435
>mmu-miR-154-3p.MIMAT0004537	TATGAT	436
>mmu-miR-410-3p.MIMAT0001091	TTATAT	554
>mmu-miR-410-3p.MIMAT0001091	TTATAT	560
>mmu-miR-154-3p.MIMAT0004537	TATGAT	719
>mmu-miR-134-5p.MIMAT0000146	AGTCAC	797
>mmu-miR-758-3p.MIMAT0003889	TCACAA	799
>mmu-miR-496a-5p.MIMAT0017244	GCAACC	810
>mmu-miR-453-3p.MIMAT0004870	GCAACC	810
>mmu-miR-380-5p.MIMAT0000744	CAACCA	811
>mmu-miR-410-3p.MIMAT0001091	TTATAT	817
>mmu-miR-369-3p.MIMAT0003186	TATTAT	898
>mmu-miR-323-3p.MIMAT0000551	TAATGT	922
>mmu-miR-543-3p.MIMAT0003168	AATGTT	923
>mmu-miR-154-3p.MIMAT0004537	TATGAT	939
>mmu-miR-323-3p.MIMAT0000551	TAATGT	945
>mmu-miR-369-3p.MIMAT0003186	TATTAT	963
>mmu-miR-495-3p.MIMAT0003456	TTTGTT	972

* putative polyA sites in bold

Table 2: RNO Ube3a1 3'UTR (rn6, chr.1, 116660510-116661593)

GTGAGGTGTTAATTCTTAAAAAGGAAGACTTTTCATCAAAGAAGTGCATGTGTG
 CTTTTGTGCATGTATCTGTTGGTACTGGTTACCGAACAAAGTAAGCTCAAAGTA
 GGCTCGTATTAATATACTAATTTTCATGCAGTCTAATGCTTTATTTTCATGAATTA
AATGATTTATGTCTCCTAT**TTTCTC**TTGCCTTTGGTTTATTTTTGGTAATATATAAA
 TGGTAGATTATTTAGTCTTTAAGATACTTGGGAAGAACCATGTGTACTTG**TGATT**
CTGAACAGTTCTTGGGACAGTA**TTACCA**CTAATATTGTTCTCTAGTCAAATGCC
 TTGTTT**TCTACT**TCTCTGTAATATGCTAC**TATCCA**ACTCTGAAAGATCTTTTTCCC
 TTGTCTTATAATCTGAATGGTCAAATGCCCTTTTGGCATCCACTGTGATGTCAG
 GGGCATTTAATCAG**ATATTT**TTCTGGAAGATCGTTTGAGCTATAAGACTCAAGTA
 TGTGGACAATAGAATGAATATTA**ACTATGT**CTAGT**AATGAT**AA**TTACCATTATAT**
TTATATCATAG**TATTATTTTATTAT**TCATTT**CAGTTT**GTAGAGACTACTCTTGCTTT
 GCACTTT**CTAATACCAGTCACAAAGGTGT****TTTCTC**ATGGCAGCC**ATTATAT**TGCT
 GTTCATTTTTCTTTTTTTCTTTTTGAGTGAATAGAAGGAACATATACTTAATTTT
 TT**TTTGTT**TTTTTTCTTGGATATTTTATGTAT**TTACAT**TTCAA**ATGTTATCCA**CTTCC
 CCCACTCTCCCACTCCATCC**CTGTTTCTATGA**GGATACTTTCACTCTCACC
 CATCCACTCCATCCTCAGGGACCTGGCATCACC**CTACAT**TGGGGAAACAAGCC
 GCTGCTCAGTTTGTAAAGT**TGATTC**ATAACAGGGAT**CAACAT**GGTAATAGGAAAG
CCTCAATGGGAATATCCTAGCATTATCTCTACAATATGGCAAAGTAATTTTTAGA
TTAATGTATGCGATTTGCTTATTTATTCTCTTATTATTGGCAATAGGATTATCATG
 AGATTAGAGCTATTA**AAAATAAA**ATTTT

miRNA	SEED Sequence on DNA	Start	Norm. Read count
>rno-miR-382-3p.MIMAT0003202	AATGAT	166	27168
>rno-miR-539-5p.MIMAT0003176	TTTCTC	185	1241
>rno-miR-377-3p.MIMAT0003123	TGATTC	273	1099
>rno-miR-1193-5p.MIMAT0017858	TTACCA	300	n.d.
>rno-miR-411-5p.MIMAT0005312	TCTACT	339	29353
>rno-miR-376b-5p.MIMAT0003195	TATCCA	362	1504
>rno-miR-376c-5p.MIMAT0017219	TATCCA	362	n.d.
>rno-miR-376c-3p.MIMAT0003194	CTATGT	523	1455
>rno-miR-382-3p.MIMAT0003202	AATGAT	534	27168
>rno-miR-1193-5p.MIMAT0017858	TTACCA	543	n.d.
>rno-miR-410-3p.MIMAT0005311	TTATAT	549	50701
>rno-miR-410-3p.MIMAT0005311	TTATAT	555	50701
>rno-miR-369-3p.MIMAT0003207	TATTAT	566	21740
>rno-miR-369-3p.MIMAT0003207	TATTAT	574	21740
>rno-miR-496-3p.MIMAT0012860	TAATAC	620	3812
>rno-miR-134-5p.MIMAT0000840	AGTCAC	627	26284
>rno-miR-758-3p.MIMAT0005335	TCACAA	629	2259
>rno-miR-539-5p.MIMAT0003176	TTTCTC	641	1241
>rno-miR-410-3p.MIMAT0005311	TTATAT	657	50701
>rno-miR-495-3p.MIMAT0005320	TTTGTT	726	14109
>rno-miR-411-3p.MIMAT0017304	TTACAT	756	10822
>rno-miR-543-3p.MIMAT0003175	AATGTT	766	8416
>rno-miR-376b-5p.MIMAT0003195	TATCCA	771	1504
>rno-miR-376c-5p.MIMAT0017219	TATCCA	771	n.d.
>rno-miR-494-3p.MIMAT0003193	TGTTTC	807	2868
>rno-miR-376b-3p.MIMAT0003196	CTATGA	812	22584
>rno-miR-380-3p.MIMAT0017302	CTACAT	870	10219
>rno-miR-377-3p.MIMAT0003123	TGATTC	908	1099
>rno-miR-409a-3p.MIMAT0003205	CAACAT	925	3358
>rno-miR-485-5p.MIMAT0003203	AGCCTC	942	5037
>rno-miR-323-3p.MIMAT0000550	TAATGT	1001	41164

* putative polyA site in bold

Table 3: HSA Ube3a-005 3'UTR (hg38, chr.15, 25353033-25354353)

GGTGAGGTA CT TAGTTCTTCAGAGGAAGATTTGATTCACCAAAGGG**GTGTGT**GA
TTTTGCTTCAGACCTTTATCTCTAGGTAATAATTCCCAAATAAGCAA**CTCACAA**
TTGTCATCTATATACTTAGAT**TTGTAT**TTG**TAATAT**AATCACCATTTTTTCGAGCTAA
TCTTGTGATTTATTTTCATGAATGAAGTGTG**TTATAT**ATAAGTCTCATGTAATCTC
CTGCATTTGGCGTATGGATTATCTAGTATTCCTCACTGGTTAGAGTATGCTTACT
GCTGGTTAGAAGATAATTAATAAAGGCTACCATGTCTGCAATTTTCTTTCTTTT
GAACTCTGCATTTGTGAACTG**TTACAT**GGCTTCCAGGATCAAGCACTTTTTGAG
TGAATGGTAGTCTTTTATTTAATTCTTAAGAT**TAATAT**GTCCAGATACATACTAGT
ATTTCCATTTTACACCCTAAAAACTAAGCCCTGAATTCTCACAGAAAGATGTAG
AGTTCCAGTTCTATCTGCTTTAAGCAAATGCCCTTACTACT**TCTACTGTCTAC**
TTCTGTGTA CT ACATCATCCAATTCTGAA**AGACAT**AGGCTTCC**CCATCC**CCTGCT
AAGACTGGTTCAAGTGGCAGCTACTGATGGATTGGTGAGAAGGCATGCAAACAC
GTACCTTCTGGAAGTTGTCTCAAAGGCTATTGCTCTAAGACTCAAGTATATAA
ACACTAGAATGAATATCAACTCTATCTAGCA**AATAAATGTT**ATTT**TTATATTA**CAGT
TGACCCTTGAACAACACAGCTGTGAACTTCATGGGCCCTCTGACATGCAGATTT
TT**TTTCTC**AACTAAGAGCAGATTCAGTGGGACTCAGAACCTGCATATCAGAGGG
CTGACTTTCATACATGCCAGTTTCACAGGGCCA**ACTGCAGAA**CTTGAGCGTGCA
TGGATTTTGGTATACACACGTGGTCTGGAACCAATCCCTGTCACATATACCAA
GGGATGGCTGTATGTTACT**TTATAT**TC**ATTTGTT**CTGTTATTTTATAAGGTTGTT
GTCGTGGTATGTGGGAATTCACCAGTATTTCTTCTTTCTGGTGCACCGTTGGTCA
TTTCTGGCAGCAGTGGTGAATGTATTTACTCTTAGCAACCTCTGTGCTGCTACCT
GTTCTGAGTTTCAAAGGTGATTC**ATTA**AGGGTTGGGATAACATGGTGATAGGA
AAAACCCCTCATC**AGTCACAA**GGAGTATAACAGCAATATCTCTG**TAATAT**GAT
TGATCATAGATATAATTTCTAGTAGGAAAAAAGTCATATCTTG

miRNA	SEED Sequence on DNA	Start
>hsa-miR-329-3p. MI0001725	GTGTGT	47
>hsa-miR-758-3p. MI0003757	TCACAA	104
>hsa-miR-381-3p. MI0000789	TTGTAT	132
>hsa-miR-656-3p. MI0003678	TAATAT	141
>hsa-miR-410-3p. MI0002465	TTATAT	199
>hsa-miR-411-3p. MI0003675	TTACAT	356
>hsa-miR-379-3p. MI0000787	TTACAT	356
>hsa-miR-656-3p. MI0003678	TAATAT	422
>hsa-miR-411-5p. MI0003675	TCTACT	544
>hsa-miR-411-5p. MI0003675	TCTACT	551
>hsa-miR-654-3p. MI0003676	AGACAT	585
>hsa-miR-1193 MI0014205	CCATCC	599
>hsa-miR-543 MI0005565	AATGTT	754
>hsa-miR-410-3p. MI0002465	TTATAT	764
>hsa-miR-889-3p. MI0005540	ATATTA	766
>hsa-miR-539-5p. MI0003514	TTTCTC	832
>hsa-miR-544a. MI0003515	GCAGAA	920
>hsa-miR-410-3p. MI0002465	TTATAT	1011
>hsa-miR-495-3p. MI0003135	TTTGTT	1020
>hsa-miR-134-5p. MI0000474	AGTCAC	1227
>hsa-miR-758-3p. MI0003757	TCACAA	1229
>hsa-miR-656-3p. MI0003678	TAATAT	1258

* putative polyA sites in bold

7-Appendix

7.1- Curriculum Vitae

Name: **Jeremy**

Middle Name : **Matthias**

Surname : **Valluy**

Date of Birth: 27.06.1984

Nationality: French

Marital status: Married

Institute address:

Institut für Physiologische Chemie,
Biochemisch Pharmakologisches
Centrum (BPC)
Philipps-Universität Marburg
Karl-von-Frisch-Str. 1 (1.OG)
35032 Marburg
Germany

Home address (Germany):

Leopold-Lucas-Strasse 73a
35037 Marburg
Germany
Tel.: +49173-5923586
E-mail: jeremy.valluy@gmail.com

Education

Dec 2009- June 2015

PhD in Pr. Gerhard **Schratt**'s lab, first in Ruprecht-Karls-University Heidelberg, and then in Philipps-University Marburg (Germany). *Study of the post-transcriptional regulation of neuronal development.*

2009

Master's degree in Cellular Biology -University Joseph Fourier – Grenoble (France), Mention Bien : *Principal courses attended: neurobiology, neurophysiology, high-throughput biology, biology of aging, epigenetics*

- 2008** First year of Master's degree on an exchange programme -Georg August Universität Göttingen (Germany) ; *principal courses attended: animal physiology, developmental biology, neurobiology, behavioral biology*
- 2007** **B.Sc. in Biology** - University Joseph Fourier - *principal courses attended: cell biology, neurobiology, molecular biology*
- 2004** University Joseph Fourier - **PCEM1** (*First year of Medical School*): *Passed but not admitted in the competitive examination (numerus clausus)*
- 2002** Charles Baudelaire High School- French scientific **Baccalaureate** *Major: Physics/Chemistry, International option in English, passed with distinction-mention Bien.*
- 1995-99** Yew Chung International School Shanghai: Junior High School *Courses taught in English and Chinese, students treated as native speakers*

Publications

A coding-independent function of an alternative Ube3a transcript during neuronal development.

Nature Neuroscience, 2015, ISSN: 1097-6256

Valluy J, Bicker S, Aksoy-Aksel A, Lackinger M, Sumer S, Fiore R, Wüst T, Seffer D, Metge F, Dieterich C, Wöhr M, Schwarting R, Schratt G.

Meetings

2014-Marburg Faculty of Medicine- PhD competition (Talk) : second place.

2013-GRC dendrites : Molecules, structure and function- Les Diablerets, Switzerland- work presented during poster session.

2012-FENS- Barcelona- work presented during poster session.

7.2- list of academic teachers

The following non exhaustive list represents my academic teachers in Grenoble (France), and Germany (Internships in bold).

Heidelberg and Marburg

Schratt

Göttingen

Heinrich

Treue

Grenoble

Albrieux

Andrieux

Block

Bonaz

Boucher

Cretin

Fraboulet

Giroud

Hans

Hemming

Kay

Markowicz

Mercier

Nonchev

Rousseau

Ruigrok

Sadoul

Schneider

Torch

Viallet

Vourc'h

7.3- Acknowledgements

I am grateful to those who have accompanied me and guided me through the long, and sometimes difficult, journey through research, publication and graduation.

My first thanks go to my supervisor, Prof. Dr. Gerhard Schratt, for believing in me and giving me the opportunity to research non-coding RNAs with him. Through his guidance and support I was able to grow as a scientist and learn a craft of which one can be proud. Any and all shortcomings in this process are my own. His enthusiasm was especially determinant during the publication process, and we owe the positive response of the publisher entirely to him.

I am grateful for the work environment setup by the whole team, who through change and difficulty could always adapt to give the best of themselves, and allow me to do my thing. I especially extend a heartfelt thank you to the technical personnel, Tatjana Wüst, Gertraud Jarosch, Renate Gondrum, Eva Becker, Karlheinz Burk, Heinrich Kaiser, Ute Beck and Bettina Kowalski.

I could not have done it without the moral and scientific support of Dr. Roberto Fiore, who knew when to be supportive and when not to withhold critique. I hope to have been worthy of his sharp mind and friendship.

I also abused the kindness and knowledge of Dr. Sharof Khudayberdiev who provided unending support and guidance.

I was privileged to work with Ayla Aksoy Aksel, Anna Antoniou, Kerstin Weiss, Silvia Bicker, Marek Rajman, Federico Zampa, Julianne Thümmeler, Martin Lackinger, Reuben Saba, Gabrielle Siegel and Peter Störchel, who also kindly helped me with the translation of the summary of the thesis.

I fulfilled my teaching duties under the guidance of Christian Wrocklage, Bernd Kösters, Birgit Rost and Cecillia Patrascan. I can never thank them enough.

I would also like to thank all my co-authors on the publication . Their work made it what it is.

Finally, I thank my parents, who never fail to support me when I need it, and my wife, Laetitia, who stood by me during the whole adventure in Germany, and surprisingly, continues to do so. Watching her take a risk dropping everything and following me here, and develop so beautifully is both delightful and humbling. May I always have the strength to support her and provide her the happiness she deserves.

7.4- Eine ehrenwörtliche Erklärung

Ich erkläre ehrenwörtlich, dass ich die dem Fachbereich Medizin Marburg zur Promotionsprüfung eingereichte Arbeit mit dem Titel “ **Regulation of microRNA function in rodent hippocampal neurons by an alternative Ube3a transcript** ” im Institut für Physiologische Chemie unter

Leitung von Prof. Dr. Gerhard Schratt ohne sonstige Hilfe selbst durchgeführt und bei der

Abfassung der Arbeit keine anderen als die in der Dissertation aufgeführten Hilfsmittel benutzt habe. Ich habe bisher an keinem in- oder ausländischen Medizinischen

Fachbereich ein Gesuch um Zulassung zur Promotion eingereicht, noch die vorliegende oder andere Arbeit als Dissertation vorgelegt.

Vorliegende Arbeit wurde in folgenden Publikationsorganen veröffentlicht.

"A coding-independent function of an alternative Ube3a transcript during neuronal development. "

Nature Neuroscience, 2015, ISSN: 1097-6256

Valluy J, Bicker S, Aksoy-Aksel A, Lackinger M, Sumer S, Fiore R, Wüst T, Seffer D, Metge F, Dieterich C, Wöhr M, Schwarting R, Schratt G.

Marburg, den _____
